



Rosenfeldt, Mathias Tillmann (2013) *p53 and the role of autophagy in pancreatic cancer development*. PhD thesis.

<http://theses.gla.ac.uk/4961/>

Copyright and moral rights for this work are retained by the author

A copy can be downloaded for personal non-commercial research or study, without prior permission or charge

This work cannot be reproduced or quoted extensively from without first obtaining permission in writing from the author

The content must not be changed in any way or sold commercially in any format or medium without the formal permission of the author

When referring to this work, full bibliographic details including the author, title, awarding institution and date of the thesis must be given

Glasgow Theses Service

<http://theses.gla.ac.uk/>

theses@gl.a.ac.uk

p53 and the role of autophagy in pancreatic cancer development

Mathias Tillmann Rosenfeldt

A thesis submitted to the University of Glasgow for the degree of Doctor of Philosophy

August 2013

Beatson Institute for Cancer Research
Garscube Estate
Switchback Road
Glasgow, G61 1BD

© Mathias Rosenfeldt, August 2013

Abstract

Autophagy is an intracellular catabolic process that involves the sequestration of proteins and whole organelles into specialized cargo vesicles (autophagosomes) and their delivery to lysosomes with subsequent degradation. Autophagy is active at low levels at any time in virtually all cells and can be induced upon a variety of different stimuli. The core function of autophagy is the degradation and recycling of intracellular material. However, how this impacts on cellular survival likely depends on the biological context.

The role of autophagy in cancer is very complex and incompletely understood. It is therefore very surprising that few studies exist that employ genetically modified mouse models of human cancer to examine the role of autophagy in this context. This is even more true when considering, that pharmacological inhibition of autophagy is currently being used in several clinical trials to treat cancer of various origins. The goal of this study was to examine the role of autophagy in a mouse model of pancreatic cancer. To achieve this several mouse strains were crossed: a) Pdx1-Cre LSLKRasG12D/wt mice that develop Pancreatic Ductal Adenocarcinoma (PDAC) similar to humans initiated by oncogenic Ras and b) Atg5flox/flox or Atg7flox/flox mice that permit Cre-induced deletion of either one of the essential autophagy regulating genes 5 and 7 (Atg5, Atg7). Offspring allowed us to examine the role of autophagy in pancreatic function.

Loss of autophagy in the pancreas leads to exocrine and endocrine tissue destruction and reduces survival in approx. 60% of animals. The early death in autophagy-deficient mice can be delayed by additional deletion of p53; the mortality rate however remains unchanged. Moribund mice show a diabetic phenotype with elevated blood glucose and fructosamine levels. In the absence of oncogenic Ras autophagy deletion does not lead to cancer formation or occurrence of pre-malignant lesions in mice aged up to 700d.

In mice that express oncogenic Ras in the pancreas (Pdx1-CreKRasG12D/wt) additional, genetic deletion of autophagy leads to accumulation of pre-malignant Pancreatic Intraepithelial Neoplasias (PanINs) that unlike their autophagy proficient counterparts never progress to cancer. In this genetic context autophagy therefore serves as a tumour promotor. In stark contrast in mice expressing oncogenic Ras and lacking both copies of p53 (Pdx1-KRasG12D/wt p53^{-/-}) inhibition of autophagy, either genetically by deletion of Atg5, Atg7 or pharmacologically by chloroquine, tumour onset is accelerated. Therefore in a p53-deficient situation autophagy is now a tumour suppressor. Tumours that developed from a p53-proficient background have increased autophagy compared to tumours that developed from a p53-null background. Furthermore p53^{-/-} Atg7^{-/-} tumours have increased glycolysis *in vitro* and *in vivo* and enhanced intracellular metabolites of the anabolic Pentose Phosphate Pathway (PPP) compared to p53^{-/-} Atg7^{+/+} tumours.

In summary it is the p53 status that determines the role of autophagy in PDAC development. In tumours developing from a p53-proficient background loss of autophagy completely prevents cancer development; whereas in tumours arising from p53-deficient tissue loss of autophagy accelerates tumour formation.

Table of Contents

Abstract	2
Table of Contents	3
List of Figures	6
Accompanying Material.....	8
Acknowledgement.....	9
Author's Declaration.....	10
Introduction.....	11
1.1 Autophagy	12
1.1.1 Autophagy: Vesicle formation	13
1.1.2 Autophagy: Molecular basis of vesicle formation	14
1.1.3 The autophagy machinery	14
1.1.4 Origin of the phagophore/isolation membrane	17
1.2 Cellular respiration serves energy production and anabolism.....	20
1.2.1 Glycolysis.....	20
1.2.2 Citric Acid Cycle.....	21
1.2.3 Oxidative phosphorylation	21
1.2.4 Pentose Phosphate Pathway	21
1.3 Connections between autophagy and (glucose) metabolism.....	22
1.4 P53 control of autophagy and metabolism	24
1.4.1 P53 and the regulation of autophagy and metabolism	25
1.5 Autophagy and cancer	26
1.6 The Pancreas.....	30
1.6.1 The Exocrine Pancreas	30
1.6.2 The Endocrine Pancreas	31
1.7 Pancreatic Cancer	32
1.7.1 Exocrine Pancreatic Cancer	33
1.7.1.1 Development of Pancreatic Ductal Adenocarcinoma (PDAC).....	33
1.7.1.2 Rare forms of Exocrine Pancreatic Cancer.....	36
1.7.2 Endocrine Pancreatic Cancer	36
2 Materials and Methods.....	37
2.1 Animal experiments	37
2.2 Mouse models.....	37
2.2.1 Pdx1-Cre mouse	38
2.2.2 LSL-KRasG12D mouse	39
2.2.3 Atg7flox/flox mouse	39
2.2.4 Atg5flox/flox mouse	40

2.2.5	P53flox/flox mouse	40
2.3	Materials	40
2.4	Genotyping	40
2.5	Tissue harvest	41
2.6	Immunohistochemistry	41
2.6.1	Quantification of histology data.....	42
2.6.2	Quantification of PanINs.....	42
2.6.3	Quantification of p53 and caspase-3 levels.....	42
2.6.4	Senescence-associated- β -galactosidase (Sa- β -Gal) staining	42
2.7	Blood biochemical analysis.....	43
2.8	Analysis of fecal elastase	43
2.9	Cell culture	44
2.9.1	Generation of cell lines	44
2.10	Immunofluorescence.....	45
2.11	Protein Analysis	45
2.11.1	Protein Extraction.....	45
2.11.2	Protein separation / Polyacrylamide Gel Electrophoresis (SDS-PAGE)	46
2.11.3	Protein Immobilisation.....	46
2.11.4	Protein detection.....	47
2.12	Autophagic Flux analysis.....	47
2.13	Metabolic analysis	48
2.13.1	Oxygen Consumption Rate (OCR) & Extracellular Acidification Rate (ECAR) 48	
2.13.2	Massspectrometry of metabolic intermediates.....	48
2.13.3	FDG-PET/CT	49
2.14	Statistics	50
3	Results	51
3.1	Effects of genetic deletion of autophagy in the pancreas	51
3.1.1	Pdx1-Cre efficiently recombines the Atg7flox/flox and Atg5flox/flox alleles 51	
3.1.2	Genetic ablation of autophagy in the pancreas reduces survival	54
3.1.3	Pancreas specific deletion of autophagy causes destruction of endocrine and exocrine tissue.....	57
3.1.4	Genetic ablation of autophagy in the pancreas does not lead to cancer.....	60
3.1.5	Conclusions: autophagy-deletion in the pancreas	70
3.2	Effects of autophagy deletion in the pancreas in the presence of oncogenic KRasG12D	71
3.2.1	Genetic ablation of autophagy in the pancreas in mice expressing oncogenic KRas reduces survival.....	71
3.2.2	Pancreas specific deletion of autophagy leads to enhanced PanIN formation in mice expressing oncogenic KRas	73

3.2.3	Autophagy-deficient PanINs activate a cell death program.....	79
3.2.4	Genetic ablation of autophagy blocks development of pancreatic cancer	82
3.2.5	Genetic ablation of autophagy in the pancreas in mice expressing oncogenic KRas causes endocrine but not exocrine dysfunction.....	86
3.3	P53-modulates the effects of autophagy on pancreatic cancer development	88
3.3.1	Simultaneous, genetic deletion of p53 and autophagy in pancreata expressing oncogenic KRas permits and accelerates tumour development.....	88
3.3.2	Pharmacological inhibition of autophagy in Pdx1-Cre KRasG12D/wt p53 ^{-/-} mice accelerates tumour development	99
3.3.3	Conclusion: Autophagy deletion in the pancreas expressing oncogenic KRas	104
3.4	Characterization of ATG7 proficient and deficient pancreatic tumours	105
3.4.1	Loss of p53 reduces autophagy in pancreatic tumours	105
3.4.2	Atg7 deficiency increases glycolysis and anabolism in p53 ^{-/-} tumours <i>in vitro</i>	110
3.4.3	Atg7 deficient tumours have increased glucose uptake compared to Atg7 proficient tumours <i>in vivo</i>	115
3.4.4	Conclusion: Role of autophagy in p53-deficient tumours	119
4	Discussion	120

List of Figures

Figure 1: Core autophagic machinery.....	16
Figure 2: Autophagy.....	19
Figure 3: Histological characterization of Pdx1-Cre Atg7 ^{-/-} pancreata.....	52
Figure 4: Loss of Atg5 in the pancreas mimics the phenotype of Atg7-loss.....	53
Figure 5: Loss of Atg7 in the pancreas increases mortality.....	55
Figure 6: Loss of Atg5 in the pancreas increases mortality.....	56
Figure 7: Effects of loss of autophagy on pancreatic acinar tissue over time.....	61
Figure 8: Effects of loss of autophagy on pancreatic endocrine tissue (islets) over time....	62
Figure 9: Quantification of p53 accumulation and caspase-3 activation in Atg7 ^{-/-} acinar tissue over time.....	63
Figure 10: Effects of Atg5 deletion on exocrine and endocrine pancreatic tissue.....	64
Figure 11: Additional deletion of p53 ^{-/-} in PDX-Cre Atg7 ^{-/-} animals delays early death..	65
Figure 12: The absence of p53 in Pdx1-Cre Atg7 ^{-/-} mice abrogates exocrine caspase-3 activation but does not prevent exocrine and endocrine tissue destruction.....	66
Figure 13: Biochemical profiling of Pdx1-Cre Atg7 ^{+/+} and Pdx1-Cre Atg7 ^{-/-} mice.....	67
Figure 14: Biochemical profile of Pdx1-Cre Atg5 ^{+/+} compared to Pdx1-Cre Atg5 ^{-/-} mice.....	68
Figure 15: Loss of p53 in the pancreas does not affect survival or pancreatic function.....	69
Figure 16: Overall survival of Pdx1-Cre KRasG12D/wt mice with (red) and without (blue) additional deletion of Atg7.....	72
Figure 17: Effect of PDX-Cre mediated Atg7-loss in the pancreas of mice expressing mutant KRasG12D.....	76
Figure 18: Loss of Atg5 in the pancreas of PDX-Cre KRasG12D/wt mice mimics the phenotype of Atg7-loss in pancreata expressing mutant KRasG12D.....	77
Figure 19: Comparison of total PanIN numbers in Pdx1-Cre KRasG12D/wt mice that are either Atg7 ^{-/-} (red) or Atg7 ^{+/+} (blue) over time.....	78
Figure 20: Atg7-deficient PanINs show markers of senescence and activate a cell death program.....	80
Figure 21: Quantification of p53 and caspase-3 activation in PanINs.....	81
Figure 22: Tumour free survival of Pdx1-Cre KRasG12D/wt Atg7 ^{+/+} compared to Pdx1-Cre KRasG12D/wt Atg7 ^{+/+} mice.....	83
Figure 23: PanIN grading in Pdx1-Cre KRasG12D/wt Atg7 ^{+/+} and Pdx1-Cre KRasG12D/wt Atg7 ^{-/-} mice.....	84
Figure 24: Tumour free survival of Pdx1-Cre KRasG12D/wt Atg5 ^{+/+} compared to Pdx1-Cre KRasG12D/wt Atg5 ^{-/-} mice.....	85
Figure 25: Biochemical profiling of Pdx1-Cre KRasG12D/wt mice with and without genetic deletion of Atg7.....	87
Figure 26: Tumour free survival of Pdx1-Cre KRasG12D/wt p53 ^{-/-} Atg7 ^{+/+} vs mice Pdx1-Cre KRasG12D/wt p53 ^{-/-} Atg7 ^{-/-}	91
Figure 27: PDACs from Pdx1-Cre KRasG12D/wt p53 ^{-/-} Atg7 ^{-/-} mice are autophagy deficient.....	92
Figure 28: Early tumour onset in Pdx1-Cre KRasG12D/wt p53 ^{-/-} mice, when Atg7 is deleted.....	93
Figure 29: Representative H&E images reflecting the different tumour onset in Pdx1-Cre KRasG12D/wt p53 ^{-/-} Atg7 ^{+/+} and Pdx1-Cre KRasG12D/wt p53 ^{-/-} Atg7 ^{-/-} mice.....	94
Figure 30: Comparison of PanIN numbers in 21d old Pdx1-Cre KRasG12D/wt p53 ^{-/-} mice Atg7 ^{+/+} and Pdx1-Cre KRasG12D/wt p53 ^{-/-} Atg7 ^{-/-}	95
Figure 31: Biochemical profiling of tumour-bearing, moribund Pdx1-Cre KRasG12D/wt p53 ^{-/-} mice +/- Atg7.....	96

Figure 32: Tumour free survival of Pdx1-Cre KRasG12D/wt p53 ^{-/-} Atg5 ^{+/+} vs Pdx1-Cre KRasG12D/wt p53 ^{-/-} Atg5 ^{-/-} mice.....	97
Figure 33: PDACs from Pdx1-Cre KRasG12D/wt p53 ^{-/-} Atg5 ^{-/-} mice are autophagy deficient.....	98
Figure 34: Chloroquine (CQ) treatment accelerates tumour onset in Pdx1-Cre KRasG12D/wt p53 ^{-/-} mice.	101
Figure 35: H&E sections of tumours from Pdx1-Cre KRasG12D/wt p53 ^{-/-} mice +/- CQ treatment.....	102
Figure 36: Chloroquine treatment does not affect pancreatic morphology and function in Pdx1-Cre KRasG12D/wt p53 ^{+/+} mice.	103
Figure 37: Increased LC3-puncta accumulation in PDACs from Pdx1-Cre KRasG12D/wt p53 ^{+/+} compared to Pdx1-Cre KRasG12D/wt p53 ^{-/-} mice.....	107
Figure 38: Autophagic flux is increased in cell lines generated from PDACs that developed in Pdx1-Cre KRasG12D/wt p53 ^{+/+} vs Pdx1-Cre KRasG12D/wt p53 ^{-/-} mice.....	108
Figure 39: Metabolic profiling of Pdx1-Cre KRasG12D/wt p53 ^{-/-} Atg7 ^{+/+} and Pdx1-Cre KRasG12D/wt p53 ^{-/-} Atg7 ^{-/-} tumour cells.	112
Figure 40: LCMS analysis of exometabolites and endometabolites in autophagy proficient and deficient tumour cells.	113
Figure 41: ATG7-deficiency does not reduce intracellular TCA-cycle intermediates or Acetyl-CoA levels.	114
Figure 42: ¹⁸ F-FDG PET/CT imaging of autophagy proficient and autophagy deficient tumour in vivo.	117
Figure 43: 2-DG uptake and phosphorylation in Atg7 ^{-/-} and Atg7 ^{+/+} tumour cell lines.	118

Accompanying Material

Chapters 1.1.2 - 1.1.4 including Figure 1 and Figure 2 are taken from a review that I wrote myself [161]. Likewise the figures in the review article were created by me. Permission to reuse this material has been granted by the publisher (Oxford University Press) and copies of the permission can be found in the appendix.

Acknowledgement

I am indebted to Kevin Ryan for entrusting me to work on the project and for his excellent guidance throughout my PhD. I am furthermore grateful to Owen Sansom for teaching me how to work with animals and for his constant advice on mouse colony management and experiments. Rachel Ridgway and Jennifer Morton were indispensable for mouse experiments and advice. Agata Mrowinska and Prof Kurt Anderson made the in vivo imaging possible. A “big-time” thank you goes to Eyal Gottlieb, Chrisitan Frezza, Leon Zheng, Gillian McKay for help, work and advice on metabolic experiments. I am grateful to Colin Nixon and his team for always having the masses of IHC-stains back “yesterday” and their excellent quality of work. Beatson Biological Services (“The Mouse House”) made it possible to manage so many mice and took the bulk load of routine mouse work on their shoulders. All Beatson Services were extremely helpful and importantly saved a lot of time. Thanks to all my colleagues in the “Cell Death Laboratory” for their constant help and advice. Finally I cannot thank Jim O’ Prey enough. Without his constant help, patience and advice throughout the years this would not have been possible.

I thank Cancer Research UK for funding this research and would like to extend my gratefulness to all fundraisers and donors, who make the inspiring work of this charity possible.

Author's Declaration

I declare that I am the sole author of this thesis and the work presented here is entirely my own unless stated otherwise. This thesis does not include work that has been submitted for consideration for any other degree or qualification.

Introduction

Cells rely on energy and building blocks to maintain their normal function and to proliferate. Amongst the most important mechanisms to sustain sufficient supply of ATP and biosynthetic precursors are cellular respiration and autophagy. In cancer cells these processes are frequently altered and it is conceivable that specific metabolic traits of cancer might be exploitable for treatment. While for example it is generally accepted that certain cancer cells derive significantly more energy from glycolysis than non-malignant cells even under normoxia (Warburg effect) [48] it is unclear how autophagy impacts on cancer. Published literature implies that autophagy is critically required for tumour cell survival at least in a subset of tumours. Based on this assumption several clinical trials are underway testing the impact of pharmacological autophagy-inhibition on different malignancies including pancreatic cancer and breast cancer (<http://clinicaltrials.gov/>, search terms: cancer + chloroquine). Strikingly, pre-clinical studies in mice to verify the impact of autophagy on cancer are scarce.

To provide much needed *in vivo* data about the role of autophagy in cancer I examined the role of autophagy during pancreatic cancer development by using a genetically modified mouse model of Pancreatic Ductal Adenocarcinoma (PDAC) interbred with conditionally autophagy-defective mice.

A mouse model of pancreatic ductal adenocarcinoma (Pdx1-Cre KRasG12D) cancer was chosen for several reasons: a) the mouse model closely recapitulates the multi-step carcinogenesis that is known from human PDAC [67], b) oncogenic KRas has been reported to impact on autophagy [160] and c) senescence is a proven tumour barrier in PDAC development and autophagy has been implicated in the senescence process [192].

My data shows that in pancreatic tumours arising from p53-proficient cells autophagy is required for tumour formation and genetic ablation of autophagy completely blocks tumour development. Therefore in this situation autophagy is as a tumour promoter. In tumours that grow in the absence of p53 autophagy conversely acts as a tumour suppressor, and genetic or pharmacological ablation of autophagy accelerates tumour onset. Autophagy-deficient tumours have discernible metabolic differences compared to autophagy-proficient tumours both *in vitro* and *in vivo*. In conclusion the p53 status determines the role of

autophagy in pancreatic cancer development and loss of p53 switches autophagy from being a tumour promoter to being a tumour suppressor.

Before presenting the results of my work key processes required to understand the work will be explained.

1.1 Autophagy

The term autophagy subsumes three distinct processes that all describe lysosomal degradation of cytoplasmic material but differ in the route of cargo delivery to the lysosome: microautophagy, chaperone-mediated autophagy and macroautophagy. The term microautophagy is reserved for the direct engulfment of cytoplasmic material by lysosomes. Likewise chaperone-mediated autophagy is a form of direct lysosomal entrapment but in contrast to microautophagy only protein/chaperone complexes, i. e. only a subset of proteins containing an identifier motif are engulfed by lysosomes [194]. Macroautophagy is the most widely studied form of autophagy and is unique amongst all forms of autophagy in so far as it exclusively involves the formation of specialized cargo vesicles, called autophagosomes. Macroautophagy describes a process that leads to sequestration of intracellular material including macromolecules and whole organelles in aforementioned autophagosomes, which then fuse with lysosomes to allow degradation of their content [161]. My work solely focuses on macroautophagy which is hereafter referred to as autophagy for simplicity.

Turnover of cytoplasmic content is the core function of autophagy and likely happens at any given moment in every cell at low, basal levels. Autophagy is adaptive and dynamic and can be rapidly induced by different stresses such as nutrient deprivation, hypoxia and activated oncogenes [160], [126], [7]. Depending on the stimulus and cellular context, autophagy breaks down different substrates, serves diverse purposes and can lead to different cellular outcomes [30], [166], [163]. It is therefore not surprising that autophagy is involved in a variety of different physiological and pathological processes, including inflammation, development, energy homeostasis, cancer, cell survival and cell death [110], [108]. Autophagy is believed to be primarily cytoprotective, possibly by providing energy and biosynthetic precursors for metabolic pathways from the breakdown of macromolecules when external nutrients are sparse and by limiting cellular stress through

clearance of damaged proteins and organelles. However, autophagy is also contributing to cell death, albeit probably not being a cell death program per se [127], [99], [98]. Surprisingly, on a molecular level it is an epigenetic, nuclear feature that appears to make the life or death decision for autophagy. Fuellgrabe and colleagues found that post translational acetylation of histone H4 at lysine 16 determines the outcome of autophagy. Acetylation (H4K19ac) promotes cell death, whereas deacetylation by the histone acetyltransferase hMOF supports cell survival [38]. A long standing question in autophagy research is: How does autophagy contribute to cancer development? This is an unresolved problem of high importance because clinical trials are currently underway, that target autophagy to treat cancer. On this note and on the fact that existing data supports both tumour promoting and tumour suppressive functions of autophagy, it is very surprising that *in vivo* data addressing this question is very limited. The conceptual ideas how autophagy might influence tumourigenesis will be discussed in a separate chapter.

1.1.1 Autophagy: Vesicle formation

Autophagy is regulated by a number of genes called AuTophagy-related genes (ATGs), whose combined action leads to the formation of the earliest, detectable morphological structure of autophagy: the phagophore, also called the isolation membrane. The phagophore is a double membrane construct that engulfs intracellular material and elongates to finally form the closed, double-membrane-bound hallmark vesicle of autophagy: the autophagosome. In a process termed “maturation” autophagosomes then fuse with lysosomes, to form autolysosomes. Autolysosomes are single-membrane-bound degradative vesicles that contain digestive enzymes, most notably cathepsins, to break down macromolecules [161]. In a process termed autophagic lysosome reformation (ALR) functional lysosomes are regenerated from autolysosomes [193] (compare Figure 2).

1.1.2 Autophagy: Molecular basis of vesicle formation

Chapters 1.1.2 to 1.1.4 including Figure 1 and Figure 2 are taken with permission (see appendix) from a review that I wrote myself, including the preparation of figures [161].

Autophagy is activated in response to a whole host of stimuli including nutrient depletion, hypoxia and activated oncogenes. The majority of pro-autophagic events converge on the serine/threonine protein kinase mTOR (MTOR, mammalian/mechanistic target of rapamycin) [44], [81], [141]. Another important, nutrient-sensitive entry route to ATG signalling is the class III phosphatidylinositol 3-kinase complex (PI3K-III) consisting of hVps34 (PIK3C3, the orthologue of yeast Vps34), Beclin 1 (yeast Atg6) and p150/hVps35 (PIK3R4; yeast Vps15) [141], [42]. Many of the aforementioned ATGs are restricted to a certain type of autophagy (see above). The ‘core’ autophagic machinery encompasses only those ATGs that are necessary for autophagosome formation in all subtypes and these can be divided into several distinct groups: (i) the unc-51-like kinase 1/2 (ULK1/2) complex (ii) the multi-spanning membrane protein Atg9, (iii) the PI3K-III complex and (iv) the ubiquitin-like ATG12 and microtubule-associated protein 1 light chain 3 alpha (MAP1LC3A) conjugation systems. The following sections detail how these proteins regulate the various stages of the autophagy process.

1.1.3 The autophagy machinery

Initiation and nucleation are terms used to describe the events that lead to the formation of the initial autophagic structure: the phagophore or isolation membrane. mTOR forms the catalytic subunit of two different protein complexes: mTORC1 and mTORC2. The former contains mTOR and RAPTOR (regulatory-associated protein of MTOR), whereas mTORC2 contains among others, mTOR and RICTOR (rapamycin-insensitive companion of MTOR) (11). In nutrient-rich states, mTORC1 but not mTORC2 forms a complex with ULK1/2 (orthologues of yeast Atg1), mAtg13, FIP200 (RB1CC1; mammalian orthologue of Atg17) and the newly identified ATG101, as a result of interaction between RAPTOR

and ULK1 [81], [69], [143]. mTOR phosphorylates ULK1 and Atg13 and thereby keeps the kinase activity of ULK1 in check. Upon treatment with rapamycin or in fasting conditions, mTORC1 breaks free from the ULK complex and the inhibitory phosphorylation of ULK1 is lost. ULK1 then autophosphorylates and activates Atg13 and FIP200. The activated ULK complex localizes to the developing phagophore. The relationship between mTOR and activation of the ULK complex is shown in Figure 1. Startlingly, the inverse relationship between mTOR activity and autophagy is not universal, as autophagy induced by 6-thioguanine has been reported to require activation and not inhibition of mTOR [196]. There are two mammalian orthologues of Atg9: ATG9L1 (mAtg9) is ubiquitously expressed, whereas expression of ATG9L2 is restricted to the placenta and pituitary gland. The exact function of mAtg9 currently remains elusive but it is required for LC3 lipidation and knockout mice die after birth as do Atg5- and Atg7-knockout animals [186], [101], [96]. Phosphatidylinositol 3-phosphate (PtdIns(3)P) is a prerequisite for the nucleation process. It is produced by the PI3K-III-hVps34 complex when bound to its core partners Beclin 1 and p150/hVps35 [42]. The complex is found on the phagophore and thought to facilitate recruitment of other ATGs to the developing vesicle. Importantly, autophagy can be positively and negatively modulated at the level of the Beclin 1-hVps34-p150/hVps35 complex depending on additional, regulatory binding partners of Beclin 1 (Figure 1) [160], [42]. ATG14/BARKOR (Beclin 1-associated autophagy-related key regulator), UVRAG (protein product of the ultraviolet radiation resistance gene) and activating molecule in Beclin 1-regulated autophagy are pro-autophagic regulators of the PI3K-III complex. Simultaneous binding of both UVRAG and RUBICON (RUN domain and cysteine-rich domain containing) inhibits the autophagy-promoting activity of the complex [76], [174], [200], [37], [114]. Elongation and closure describe the development of the characteristic double-membrane-bound autophagosome from its precursor structure and require two ubiquitin-like conjugation systems. The ubiquitin-like ATG12 is conjugated to ATG5 via the E1-like protein ATG7 and the E2-like ATG10. ATG16 then enters the complex and directs the large (L), newly formed ATG16L (ATG12-ATG5-ATG16) complex to the isolation membrane. The Atg16L complex is required for autophagosome formation, guides LC3 to the phagophore and promotes lipidation of LC3 (Figure 1) [41], [59], [170]. The ubiquitin-like yeast protein Atg8 has several orthologues in mammalian cells: MAP1LC3 (LC3), GABARAPL2 (GATE16), GABARAP and GABARAPL1 (ATG8L). LC3 is the most thoroughly investigated of these proteins and its modification during autophagy is exploited as a marker for autophagy [94], [83]. Newly synthesized LC3 is immediately cleaved at its C-terminal end by the

protease Atg4 into the cytoplasmic form LC3-I. If autophagy is active, LC3-I is then conjugated to phosphatidylethanolamine via ATG7 and the E2-like ATG3 [84]. In its conjugated form, LC3 is called LC3-II and is recruited via its lipid moiety to the inner and outer surfaces of the autophagosomal membrane, i.e. unlike LC3-I, LC3-II is not freely dispersed in the cytoplasm (Figure 1). The exact order of Atg activation is not clear and there is intensive crosstalk between the different Atg systems. However, it is generally accepted that the ULK1 kinase complex and the PI3K-III complex act upstream of the ubiquitination systems [172].

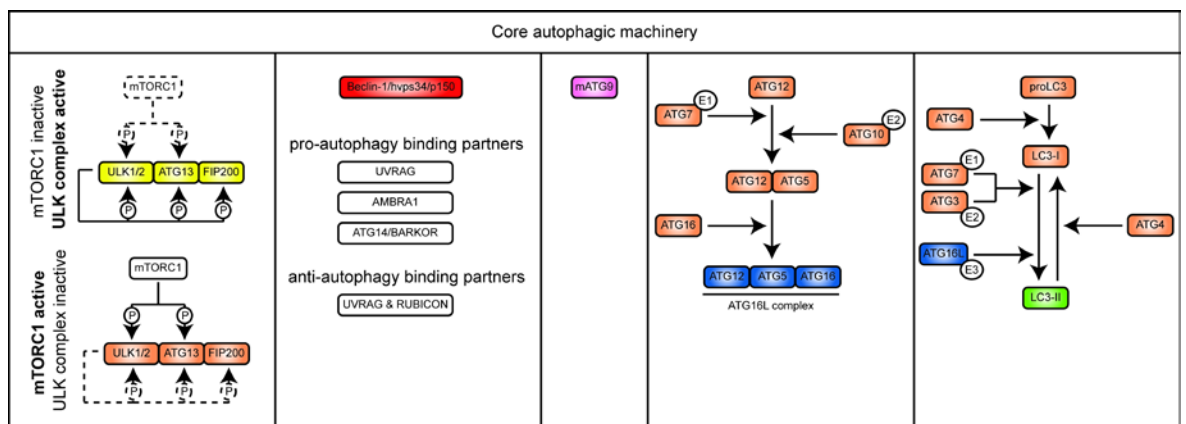


Figure 1: Core autophagic machinery.

Autophagic core machinery. The ULK kinase complex, the PI3K-III complex, mAtg9 and the two ubiquitination systems are indispensable for autophagy. Members of the core machinery are shown in coloured boxes. Modulators that are not part of the core machinery are shown in white boxes. For details, see text.

The maturation process encompasses the fusion of autophagosomes with lysosomes to form autolysosomes. Autolysosomes are singlemembrane-bound, acidic vesicles comprised of the outer membrane of autophagosomes and the lysosome that degrade the autophagosomal cargo via acidic hydrolases provided by the lysosome. The process is less well understood but involves the action of lysosomal proteins, such as lysosomal-associated membrane protein 1/2 (LAMP1/2) and also again, Beclin 1 [157], [160]. Work by Yu et al. [193] has recently shed light on the ultimate fate of autolysosomes. During autophagy-initiation mTOR is inhibited but becomes reactivated at later stages as a result of the release of cellular constituents into the cytoplasm following the breakdown of

macromolecules within autolysosomes. Increased mTOR activity then inhibits autophagy and leads to the formation of proto-lysosomal extensions (LAMP1+, LC3-) from autolysosomes (LAMP1+, LC3+) [172]. Ultimately, these proto-lysosomal extensions detach from the autolysosome and mature into functional lysosomes. Inhibition of mTOR, or (auto-)lysosomal function, prevents autophagic lysosome reformation (Figure 2). Autophagy is therefore controlled by a negative feedback mechanism that is regulated by mTOR [193], [172]. Until recently, it was believed that the two ubiquitination systems are indispensable for autophagy. However, Nishida et al. [148] introduced the term ‘alternative macroautophagy’ to describe a degradative process in response to starvation and etoposide treatment that involves autophagosome-like structures that are not decorated by LC3-II. Strikingly, this process is independent of both ATG5 and ATG7 but critically relies on ULK1 and Beclin 1. Double-membrane bound vesicles that included cytoplasmic material were generated in a RAB9 (RAB9A, member RAS oncogene family)-dependent fashion by the fusion of isolation membranes and vesicles derived from the trans-Golgi and late endosomes [148]. Since this process occurs without involvement of crucial regulators for ‘conventional’ or ‘canonical’ autophagy, it is debated whether this phenomenon is something altogether different from autophagy [95].

1.1.4 Origin of the phagophore/isolation membrane

The first detectable structure during autophagy in mammalian cells is the isolation membrane or phagophore. Considerable insight has been gained in the last 2 years in relation to its sites of origin. Current consensus favours that in mammalian cells, the isolation membrane develops from at least three different, preformed sources: the endoplasmic reticulum (ER), the plasma membrane and mitochondria [5], [57], [178], [156]. Axe et al. [5] proposed that the phagophore is derived from so-called omegasomes (cup-shaped protrusions from the ER). Moreover, it has recently been confirmed that isolation membranes are physically connected to the ER and are cradled by two ER membranes, which is reminiscent of the omegasome [64], [191]. Upon starvation, the hVps34 kinase is recruited via ATG14L to the ER, where it creates a local increase in PtdIns(3)P, that is essential for autophagosome development [137]. Proteins that specifically recognize PtdIns(3)P are then recruited to the omegasome/cradle, WD repeat domain, phosphoinositide interacting 2 and ZFYVE1, zinc finger, FYVE domain containing 1, the latter of which can be used to pinpoint the location of the

omegasome/cradle [178], [153]. The phagophore extends from the PtdIns(3)P-rich region and is cradled by two ER membranes [139]. Small sections of ER are encapsulated within autophagosomes by this mechanism. The ULK complex and LC3 localize to the omegasome, as well as the ATG16L complex via ATG16 [139] (Figure 2). ATG16L1 has also been reported to be associated with the plasma membrane [156]. This association was mediated by an interaction between ATG16L1 and the heavy chain of clathrin and it is believed that this interaction is required for the formation of early autophagosome precursors (Figure 2). Inhibition of clathrin-mediated internalization reduces the formation of these pre-autophagosomal structures as well as mature autophagosomes [156]. It was proposed by the authors of this study that due to the size of the plasma membrane, this source of autophagosomes may be particularly important during intense autophagic activity [156]. A switch may therefore occur from sources of membrane utilized under basal conditions to the plasma membrane under stressed conditions in order to perhaps maintain intracellular organelle integrity. Mitochondria have also recently been proposed as an alternative route of phagophore generation [57]. Under starving conditions, ATG5 and LC3 localize to the outer membrane of mitochondria, which serves as a cornerstone for phagophore development. Mitofusin 2 connects mitochondria to the ER and thereby enables transfer of phosphatidylserine from the ER to mitochondria, which seems to be essential for autophagosome generation. In mitochondria, phosphatidylserine then gets processed to phosphatidylethanolamine, which becomes an essential component of the developing autophagosome as described previously [84]. Figure 2 illustrates the development and recycling of autolysosomes from early precursors and the involvement of the core autophagic machinery in each step. It seems appropriate to underline that the proposed models of autophagosome generation are not mutually exclusive and probably coexist. It is possible that depending on cellular context and activating triggers, one or all routes are initiated. However, in mammalian cells, each model points away from the assembly model (where phagophores develop *de novo*), unlike in yeast where the phagophore develops from a phagophore assembly site [147].

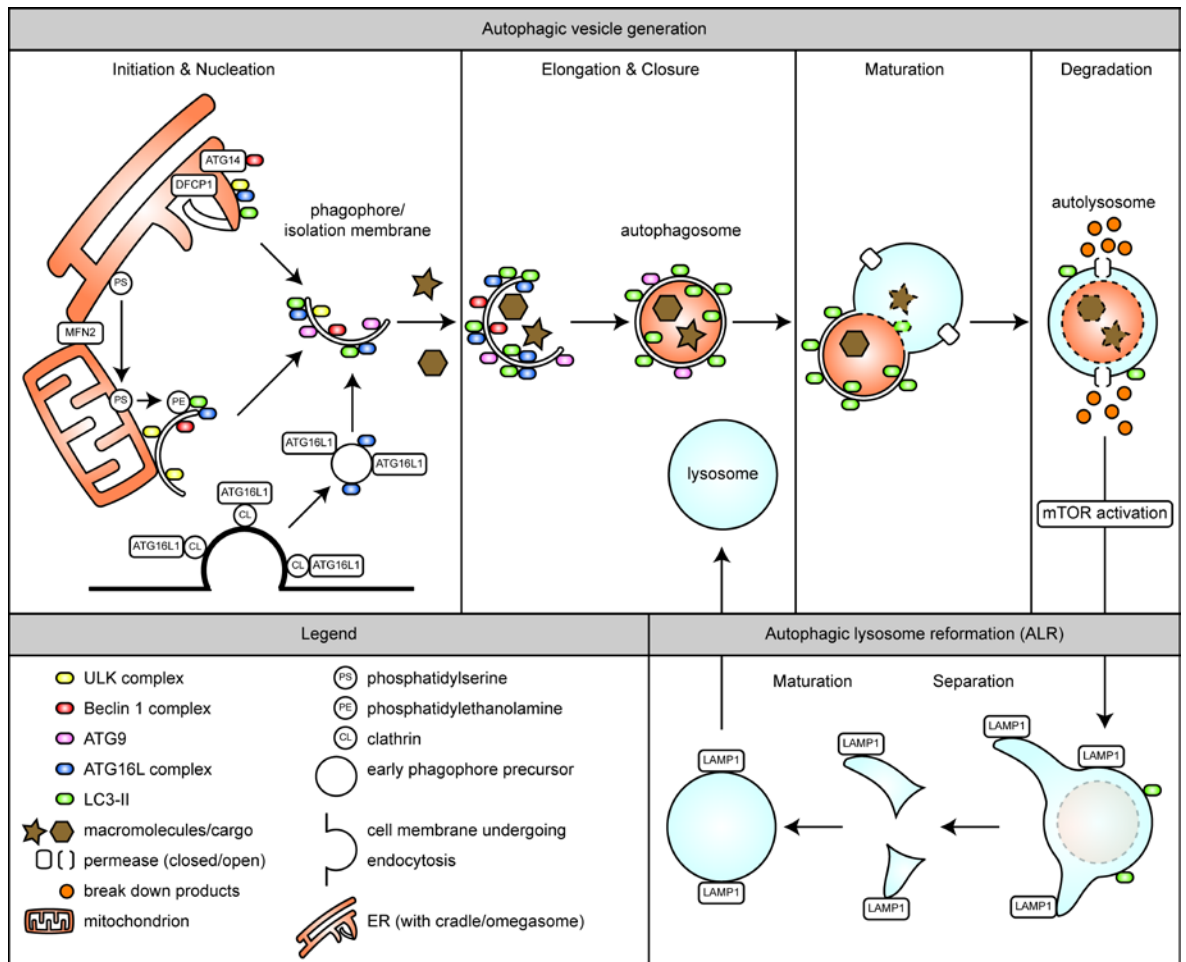


Figure 2: Autophagy.

Autophagic vesicle generation and recycling. The first steps of autophagosome formation are initiation and nucleation. The earliest detectable autophagic structure is the double-membrane-bound phagophore/isolation membrane that evolves from the ER, mitochondria or the plasma membrane following activation of the ULK1 and Beclin 1 complexes (initiation/nucleation). Subsequently, the ATG16L complex, LC3-II and mAtg9 are recruited to the developing isolation membrane. The membranous structure evolves (elongation) and encapsulates macromolecules to become the closed hallmark structure of autophagy, the autophagosome. After fusion with a lysosome (maturation), the intravesicular constituents of the autophagosome get degraded and released into the cytosol, thereby creating a local rise in nutrient availability. This leads to reactivation of mTOR and regeneration of a mature lysosome from autolysosomes in a process called autophagic lysosome regeneration. Members of the core autophagic machinery that are involved in each step and can be found on the corresponding structure/vesicle are shown in coloured boxes. For details, see text.

1.2 Cellular respiration serves energy production and anabolism

Cellular respiration is an umbrella term for a number of intracellular, metabolic processes that convert nutrients into energy and also produce a diverse range of intermediates to fuel and maintain cell metabolism. Important corner stones of cellular respiration are glycolysis, the citric acid cycle and oxidative phosphorylation.

1.2.1 Glycolysis

Glycolysis is the process of glucose breakdown into pyruvate with a net gain of two molecules of the central energy carrier ATP (adenosine triphosphate) and two molecules of the reducing agent NADH (reduced form of nicotinamide-adenine dinucleotide). Glycolysis is a cytosolic process and does not require oxygen. Hence the frequently used term “aerobic glycolysis” only means “glycolysis in the presence of oxygen”. This is to emphasize the fact that under certain conditions cells, especially cancer cells prefer to catabolize glucose to pyruvate (with subsequent fermentation to lactate) even in the presence of oxygen instead of completely breaking it down in mitochondria via the citric acid cycle and oxidative phosphorylation (OXPHOS) (see below) at a net gain of 31 molecules of ATP. ATP production through glycolysis is approx. 18-times less efficient than ATP production from complete oxidation but this is compensated by a greatly increased reaction speed [61], [48].

Glycolysis adapts to extra- and intracellular conditions and the flux through the glycolytic pathway can be regulated by changes in the enzymatic activity of three key enzymes: hexokinase, phosphofructokinase and pyruvate kinase [21], [1], [187], [123], [48]. Glycolysis is not to be misunderstood as a purely catabolic process to generate energy. Its metabolites are important pre-cursors for a host of anabolic process such as the Pentose Phosphate Pathway, gluconeogenesis and triglyceride synthesis (Galuzzi 2012). In summary, glycolysis is both a catabolic process to generate energy and a supplier for anabolic pathways to supply building blocks for cell growth and cellular homeostasis.

1.2.2 Citric Acid Cycle

The Citric Acid Cycle, also called the TriCarboxylic Acid (TCA) cycle or Krebs cycle, is arguably the central metabolic node in all cells that contain mitochondria. In a series of mitochondrial reactions acetyl-coenzyme A (acetyl-CoA) from various sources is oxidized to oxaloacetate and NADH and FADH₂ (reduced form of flavin adenine dinucleotide) are produced. In a process called oxidative phosphorylation (OXPHOS) ATP is then produced from NADH and FADH₂. Importantly intermediates of the TCA cycle can be siphoned off for anabolic processes such as gluconeogenesis, lipid metabolism and amino acid synthesis [187], [123], [48].

1.2.3 Oxidative phosphorylation

The process of oxidative phosphorylation (OXPHOS) is carried out by a set of mitochondrial protein complexes and enzymes and serves to produce ATP in the presence of oxygen. In a chain of redox reactions called the respiratory chain, reduced hydrogen carriers such as NADH and FADH₂ are oxidized and the released energy is conserved in the form of ATP. The majority of hydrogen carriers is derived from the TCA-cycle [187], [123], [48].

1.2.4 Pentose Phosphate Pathway

The Pentose Phosphate pathway (PPP) or hexose monophosphate shunt is a cytosolic, bi-phasic reaction and is a source of reducing power in the form of NADPH (to produce reduced glutathione). It also supports anabolic processes, such as fatty acid synthesis and nucleotide biosynthesis. Glucose is converted in a multi-step reaction to ribulose 5-phosphate in the first, oxidative and irreversible phase. Then in a set of reversible reactions, that are called the non-oxidative phase of the PPP, fructose 6-phosphate and glyceraldehyde 3-phosphate are generated. The first intermediate of the non-oxidative phase, ribose 5-phosphate, is a direct precursor of nucleotide biosynthesis. Fructose 6-phosphate can a) re-enter the PPP via conversion to glucose 6-phosphate to produce more NADPH and reduce oxidative damage or b) enter the glycolytic pathway to be converted to pyruvate to fuel fatty acid synthesis.

1.3 Connections between autophagy and (glucose) metabolism

Autophagy itself contributes to metabolic homeostasis but in reverse it is also regulated by the metabolic state of a cell [142], [31]. In the following key conductors that orchestrate autophagy and glucose utilizing pathways are exemplarily discussed: AMP-activated protein kinase (AMPK), glyceraldehyde 3-phosphate dehydrogenase (GAPDH) and TP53-induced glycolysis and apoptosis regulator (TIGAR).

The AMP-activated protein kinase (AMPK) is an important hub that synchronizes various metabolic pathways, including autophagy, to coordinate nutrient availability with energetic requirements and the demand for biosynthetic precursors [39], [74], [32]. AMPK primarily responds to the intracellular ATP/AMP ratio. A low ratio i. e., high levels of AMP as an indicator of a low-energy status, activate AMPK. By and large, AMPK induces catabolic pathways to provide cells with ATP and down-regulates anabolic processes [39].

AMPK can activate autophagy via several different approaches that target critical regulators of autophagy. AMPK suppresses mTORC1 via interaction with the TSC complex and Raptor [74]. Phosphorylation of TSC2 by AMPK leads to inactivation of Rheb and thereby alleviates the inhibitory effect of Rheb on mTORC1 [56], [32]. Inoki et al. have shown that AMPK can phosphorylate Raptor and thereby inactivate mTORC1 with subsequent activation of autophagy [75]. In glucose starved cells AMPK binds to and phosphorylates ULK1 on multiple sites to induce autophagy [32]. In order to prevent possibly detrimental and sustained autophagy ULK1 can phosphorylate and inactivate AMPK [111]. Kim and colleagues recently showed that AMPK also phosphorylates pro- and anti-autophagic class III phosphatidylinositol (PtdIns)-3 kinase, PIK3C3/VPS34 complexes [92]. In hypoglycaemia Atg14 which is only present in the pro-autophagic BECN1/VPS34 complex switches AMPK phosphorylation sites on VPS34 and also allows AMPK phosphorylation of BECN1. This results in enhanced autophagy [91]. AMPK mediated phosphorylation with subsequent stabilisation and accumulation of the cyclin-

dependent kinase inhibitor p27/kip1 protects cells from metabolic stress by induction of autophagy [115].

Besides its influence on direct regulators of autophagy AMPK also closely regulates other metabolic processes such as glucose- and lipid metabolism as well as OXPHOS. AMPK has been shown to stimulate glucose uptake and glycolysis by increasing the activity of the glucose transporter GLUT1 [39] and by increasing the expression of GLUT4 and its translocation to the plasma membrane [39]. In another example that links AMPK, glycolysis and autophagy directly, Ferraro and colleagues showed that in apoptosome-deficient cells exposed to cytotoxic stress, sustained ATP production via glycolysis is dependent on autophagy [36]. Furthermore, pharmacological inhibition of glycolysis via 2-deoxyglucose leads to induction of reactive oxygen species (ROS) and AMPK dependent autophagy [184]. If cells cannot meet their metabolic needs from the breakdown of carbohydrates, especially glucose, then AMPK mediates a metabolic switch, allowing cells to generate energy primarily from lipids via enhanced mitochondrial fatty acid oxidation [74]. AMPK has also been shown to increase mitochondrial mass and mitochondrial oxidative capacity (OXPHOS) [39].

The glycolytic enzyme glyceraldehyde 3-phosphate dehydrogenase (GAPDH) directly connects glycolysis with a master regulator of autophagy: mammalian target of rapamycin (mTOR) [107]. Rheb (Ras homologue enriched in brain) binds and activates mTORC1 (mTOR complex 1) and thereby inhibits autophagy. During hypoglycaemia GAPDH increasingly binds to Rheb which leads to inhibition of mTORC1 signalling and subsequent activation of autophagy. Notably, GAPDH is essential for glucose-dependent Rheb-mediated regulation of mTORC1 activity. AMPK and TSC1 (hamartin, tuberous sclerosis 1 protein) are not required for this interaction [107]. GAPDH protects cells from caspase-independent cell death following mitochondrial outer-membrane permeabilization. This survival function not only involves but also depends on increased glycolysis and autophagy, possibly to clear damaged mitochondria. GAPDH fulfils a plethora of functions aside from its role in glucose metabolism. Nuclear GAPDH takes part in transcription, cell cycle regulation and even DNA repair. Upon induction of MOMP (mitochondrial outer membrane permeabilization) in cells that are protected from caspase-independent cell death, GAPDH translocates to the nucleus and enhances expression of Atg12. Expression of Atg12 but not Atg5 can substitute for GAPDH in terms of protection from caspase-independent cell death following MOMP [23].

TIGAR alleviates the activity of 6-phosphofructo-1-kinase (PFK-1) by reducing the levels of intracellular fructose-2,6-bisphosphate (Fru-2,6-P₂). Fru-2,6-P₂ enhances the affinity of the glycolytic enzyme PFK-1 for its substrate fructose 6-phosphate. As a result glycolysis is bypassed in favour of the Pentose Phosphate Pathway [9]. Loss of TIGAR has been shown to upregulate autophagy, possibly as a consequence of increased ROS production due to reduced flux through the PPP [8].

The aforementioned links between glucose metabolism and autophagy are not exclusive and other connections have been reported. For example glycogen autophagy, i. e., the sequestration and degradation of glycogen via autophagy to glucose especially in hepatocytes, compensates postnatal hypoglycaemia by feeding into the glycolysis and pentose phosphate pathway [97]. Furthermore mouse embryonic fibroblasts (MEFs) that express oncogenic HRasV12 have reduced glycolysis when autophagy is abrogated by genetic deletion of Atg5 compared to autophagy competent cells (HRasV12/wt ATG5^{-/-} MEFs vs HRasV12/wt ATG5^{+/+} MEFs) [119].

In summary autophagy and glucose utilizing metabolic pathways share common regulators and are connected to collectively meet the energetic and biosynthetic requirements of a cell.

1.4 P53 control of autophagy and metabolism

The transcription factor p53 is mutated or lost in approx. 50% of all human cancers [58]. It regulates a plethora of cellular processes amongst which are failsafe programs like apoptosis and senescence to block cellular transformation. During the process of becoming malignant, cells encounter a variety of stresses such as genotoxic damage, oncogene activation and hypoxia that all activate p53 to facilitate cell death or to inhibit cell proliferation (and allow for recovery from the insult) [182]. Recent years saw an increased focus on metabolic regulation of cancer cells and sparked the hope that potential differences can be exploited for tumour therapy. Important metabolic processes such as glycolysis and autophagy are also regulated by p53 and these interactions are increasingly becoming a focus of p53-related research [48].

1.4.1 P53 and the regulation of autophagy and metabolism

Autophagy is clearly regulated by p53 but it is difficult to ascertain the net effect of p53 on autophagy as it seems to be context dependent, i. e., does p53 induce or inhibit autophagy [160] [109]. In the absence of cellular stress basal levels of cytoplasmic but not nuclear p53 inhibit autophagy [176]. In contrast, it has also been shown that p53 induces autophagy. Activated p53 accumulates in the nucleus to initiate transcription of its target genes. Amongst these are several isoforms of the autophagy-inducer DRAM1 (damage-regulated-autophagy modulator 1) [26], [124] as well as Sestrin1 [14] and Sestrin2 [14], [128]. In response to genotoxic stress Sestrins activate AMPK to inhibit mTORC1 possibly via TSC2 and activate autophagy [39]. TSC1 which inhibits RHEB and therefore leads to inhibition of mTORC1 and subsequent activation autophagy is a direct transcriptional target of p53 [31]. In summary the regulation of autophagy by p53 is complex with the emerging pattern that the subcellular localization of p53 is a determining factor for p53 to induce or inhibit autophagy. Almost certainly context specific aspects are likewise important and also impact on the role of p53-induced autophagy as either pro-survival or pro-death [109].

As mentioned before metabolic regulation by p53 extends beyond the control of autophagy. In the presence of oxygen most normal cells generate ATP from OXPHOS, unlike tumour cells that have frequent mutations in p53 and a higher propensity to derive ATP from “aerobic glycolysis” [48]. Thus it does not really come as a surprise that p53 mostly promotes OXPHOS and hinders glycolysis. P53 is important to sustain mitochondrial DNA and mass [100], [104] and controls the transcription of important regulators of OXPHOS like cytochrome c oxidase 2 (SCO2) [136], subunit I of cytochrome c oxidase and p52R2, a subunit of ribo-nucleotide reductase [48]. With regards to orchestrating glycolysis p53 has been shown to repress the transcription of glucose transporters directly (GLUT1, GLUT4) [167] or indirectly via inhibition of NF-κB (GLUT3) [88]. TIGAR is a direct target of p53 and diverts glucose utilization towards the pentose phosphate pathway and away from glycolysis [9]. Complicating factors are that p53 has also been described to induce glycolytic enzymes hexokinase-2 [135] and the muscle-specific phosphoglycerate mutase [164]. Importantly p53 promotes the antioxidant defence directly through regulation of TIGAR, sestrins and p53INP1 as well as indirectly through stabilization of the transcription factor Nrf2 (that induced a variety of “anti-oxidant” genes) by p21 [48].

1.5 Autophagy and cancer

In cancer cells failsafe mechanisms like cell death and senescence that normally prevent chronic and unrestricted growth are overruled by genetic mutations and epigenetic alterations. In 2000 Hanahan and Weinberg defined the core hallmarks of cancer: self-sufficiency in growth signals, insensitivity to anti-growth signals, tissue invasion & metastasis, limitless replicative potential, sustained angiogenesis and evasion of cell death [60]. Eleven years later the same authors classified reprogrammed cellular metabolism as an emerging hallmark of cancer to complement the original core traits of malignancy [61].

Undoubtedly the most common metabolic abnormality in cancer cells is the Warburg effect, i. e., the preferred production of lactate from glucose even in the presence of normal oxygen levels [185]. In contrast, under normoxia most normal cells feed the majority of glucose into the mitochondrial TCA-cycle and use OXPHOS for ATP generation. Notwithstanding they have the ability to shift towards glucose fermentation under hypoxia. Glucose fermentation comes at the cost of an approx. 18 fold less net gain of ATP when compared to full mitochondrial oxidation. This is compensated by an increased glucose uptake in cancer cells and is believed to provide additional benefits for neoplastic cells [48]. A) Glucose metabolites can be siphoned into biosynthetic pathways such as the PPP to provide biomass required for new cells. B) Lactate production leads to extracellular acidification, which harms normal cells but not cancer cells [47]. C) It is also postulated that increased aerobic glucose fermentation reduces oxidative stress “during the phases of the cell cycle where maximally enhanced biosynthesis and cell division do occur” [13]. As detailed before autophagy itself is a metabolic process and tightly interwoven with glucose metabolism. A large number of publications link autophagy and cancer but a unifying theme, i. e. when and how autophagy promotes or suppresses cancer has not yet emerged [4], [132].

Inactivation or deletion of certain autophagy genes has been reported to increase the predisposition to tumour development [155], [195], [131], [175]. Mono-allelic loss of BECN1 (the gene encoding the essential autophagy gene Beclin 1) is frequently observed in human breast, ovarian and prostate cancer [116]. Likewise BECN1 heterozygosity in mice increases the propensity for cancer development [155]. Mice that are deficient in Atg4C have an increased susceptibility to develop fibrosarcomas, but only after subjection to a chemical carcinogenesis protocol [131]. In humans frame shift mutations of ATG2B,

ATG5 and ATG12 have been found in gastric and colorectal cancers [85]. Liver specific deletion of Atg7 or Atg5 in mice leads to growth of benign liver adenomas [175].

One could easily assume now that impaired autophagy facilitates tumour development. However, it is not so easy because the exact opposite has also been shown.

Myc-driven murine lymphomas utilize autophagy as a survival mechanism. In reverse inhibition of autophagy enhanced therapeutic outcome in the same study [3]. Autophagy allows ovarian cancer cells to enter a state of reversible dormancy in conditions that they could not survive when autophagy was pharmacologically inhibited [122].

It is not unlikely that the desire to classify autophagy dogmatically either as pro tumorigenic or tumour suppressive can in reality not be fulfilled due to the complex involvement of autophagy in processes that influence tumour development and therapy: cell death, senescence, oxidative stress, inflammation, immunity and metabolism [61], [160], [161]. How autophagy modulates the decision between cell death and cell survival is context dependent [71], [99]. Two examples are the connection between autophagy and anoikis on the one hand and between autophagy and necrosis on the other hand. Anoikis is a form of cell death that occurs when cells detach from their surrounding extracellular matrix. Autophagy protects from anoikis [43] and thereby possibly facilitates metastatic spread. In this context it is conceivable that inhibition of autophagy might be beneficial for therapy.

Cancer cells frequently endure metabolic stress in poorly vascularized tumour regions and apoptotic cell death is commonly disabled. In this scenario inhibition of autophagy leads to necrotic cell death and concomitant release of pro-inflammatory cytokines which ultimately promote mutational events and therefore tumour growth [27]. Furthermore, chemo- and radiotherapy have both been shown to induce autophagy with context dependent life- or death roles for autophagy [160], [161], [2].

Senescence is a clinically relevant tumour barrier and considered to be a sustained cell arrest that is reinforced by a characteristic secretion of immune modulatory cytokines. Impaired autophagy delays the onset of senescence and modifies the secretory phenotype which might affect the clearance of senescent cells [192].

Damaged organelles, especially mitochondria, are a source of oxidative stress. Damaged proteins, if not cleared, are akin to non-inheritable mutation. Autophagy ensures quality control and thereby removes the aforementioned threats to preserve cellular integrity and genomic stability [86], [134]. Here it clearly would be problematic to inhibit autophagy in tumour therapy. And indeed it has been shown that inhibition of autophagy increases oxidative stress with subsequent activation of the DNA damage response and promotion of genetic instability. As a result tumour formation is promoted [86].

Chronic inflammation is recognized as a risk factor for cancer development [24]. As already mentioned impaired autophagy can cause necrotic death and thereby create a pro-inflammatory environment. Furthermore impaired autophagy has also been implicated in a variety of inflammatory processes that are independent of necrotic cell death and could potentially precede the occurrence of cancer, e. g., inflammatory bowel disease [15], [165], [16], [117] and pancreatitis [129].

Inhibition of autophagy potentially limits immune recognition of cancer cells through impairment of antigen presentation [113] and T-cell function [154].

The connection between autophagy and glucose metabolism was detailed before (see 1.3). Autophagy furthermore controls lipid metabolism with potential implications for cancer biology. Impaired autophagy leads to reduced breakdown of triglycerides and possibly as a result impaired β -oxidation [173]. Thus the supply of acetyl-CoA for the TCA cycle is reduced and the production of energy and biosynthetic precursors is impaired. Recent work suggested that tumours driven by oncogenic Ras require autophagy to sustain OXPHOS. Inhibition of autophagy decreased metabolic intermediates of the TCA cycle (citrate and isocitrate) and therefore supposedly the supply chain of hydrogen carriers for mitochondrial OXPHOS is disrupted. It was concluded that autophagy is critically required for tumour survival in tumours driven by oncogenic Ras [189], [54], [55].

In summary it is unclear when and how autophagy impacts on tumour development, partly because of its involvement in a plethora of different processes which have important ramifications for cancer. When reduced to its currently known core function, autophagy is a catabolic process that clears cytoplasmic material and supplies raw material for energy-producing and anabolic pathways. Depending on the cellular requirements dictated by extra (e. g. hypoxia) and intracellular cues (e. g. oncogene activation) it might be that either a genome destabilizing situation is favourable for tumours (i. e. lack of autophagy)

or a situation in which autophagy supports growth through increased provision for anabolic pathways is beneficial for cancer growth. In the first instance, inhibition of autophagy might not be desirable as it would further increase the mutational capacity. In the latter instance impairment of autophagy could shut down the supply for anabolic pathways and thereby aid tumour therapy.

The goal of my thesis is to examine the role of autophagy in cancer development *in vivo*. Despite having some very limited *in vivo* evidence (see beginning of this section) studies that examine the role of genetic and or pharmacological inactivation of autophagy in an oncogene-driven mouse model of cancer are sparse. We chose pancreatic cancer as our model system for several reasons: a) the murine model closely resembles the human disease, b) pancreatic cancer usually develops from a set of premalignant lesions that are senescent, c) the KRas oncogene is mutated not only in pancreatic cancer but many other human cancers and has been shown to influence autophagy, and d) there was considerable experience with the mouse model in the institute.

The following sections will introduce the pancreas and its physiological functions as well as give an overview about pancreatic cancer.

1.6 The Pancreas

The pancreas is a vital, bi-functional, abdominal gland and is anatomically divided into the head that is in close proximity to the duodenum, the body part and extending to the left side of the body in direct neighbourhood to the spleen is the tail. The human pancreas has a diameter of approx. 1.5x3.5x2.5cm (LxHxW) and weighs approx. 60-80g in adults. Its two main functions are: a) production of digestive enzymes in exocrine cells and b) production of hormones in endocrine cells, most notably insulin and glucagon in the islets of Langerhans to maintain glucose homeostasis [6], [150], [152], [181], (www.pancreaticcancer.org.uk, <http://www.cancerresearchuk.org/cancer-help/type/pancreatic-cancer/>).

1.6.1 The Exocrine Pancreas

Every day the exocrine pancreas produces approx. 1-2l pancreatic juice that helps to neutralize and process acidic chyme (pre-digested food from the stomach). The secretion consists of an aqueous bicarbonate component and an enzymatic component. Pancreatic enzymes are produced in acinar cells and secreted into the acinar lumen that is connected to a drainage system formed by ductal cells (see below). Pancreatic enzymes are important for the digestion of proteins (proteolytic enzymes such as trypsinogen, chymotrypsinogen), lipids (lipolytic enzymes such as lipase, phospholipase A, cholesterol esterase) and carbohydrates (amylolytic enzymes such as amylase). Importantly, autodigestion is prevented by two mechanisms: a) enzymes are produced and secreted as inactive precursors (zymogens) and b) protease-inhibitors found in acinar cells and pancreatic juice inhibit premature stimulation. Pancreatic enzymes are activated in the intestine by reaction with bile salts and duodenal enzymes.

Ductal cells form a complex drainage system for the pancreatic juice and finally discharge into the main pancreatic duct. They secrete large quantities of bicarbonate into the pancreatic juice which is therefore alkaline in nature. The main pancreatic duct fuses with the common bile duct and drains into the duodenum.

Pancreatic secretion is in under nervous and hormonal control. The parasympathetic nervous system, as well as hormones that are secreted from the duodenum (secretin, cholecystokinin) and from the stomach (gastrin) stimulate secretion. In contrast certain

hormones released from the islets of Langerhans (glucagon, somatostatin) inhibit the production of pancreatic juice (<http://www.cancerresearchuk.org/cancer-help/type/pancreatic-cancer/>, www.pancreaticcancer.org.uk).

1.6.2 The Endocrine Pancreas

The endocrine part of the pancreas accounts for only 2% of total organ weight and can be easily distinguished in haematoxylin and eosin (H&E) stained histological sections as bright red islets scattered throughout exocrine parenchyma that stains dark red. These regions are highly vascularized and are called the islets of Langerhans. Unlike pancreatic enzymes the hormones are directly secreted into the blood from at least 5 different cell types found in islets: α -cells produce glucagon, β -cells are the majority of islet cells and produce insulin and amylin, δ -cells produce somatostatin, γ -cells (=PP cells) produce pancreatic polypeptide and ϵ -cells produce ghrelin. Insulin is the most important hormone to regulate glucose homeostasis (<http://www.cancerresearchuk.org/cancer-help/type/pancreatic-cancer/>, www.pancreaticcancer.org.uk).

1.7 Pancreatic Cancer

In the UK nearly 9000 patients are newly diagnosed with pancreatic cancer every year (www.pancreaticcancer.org.uk). The clinical signs of pancreatic cancer depend on the type of cancer (see below) and are largely not specific, especially in the case of Pancreatic Ductal Adenocarcinoma which accounts for 85% of all cases. Symptoms include: abdominal pain, jaundice, weight loss, altered stool, nausea, fever and sometimes diabetes. The genesis of pancreatic cancer is complex and multifactorial. However, it is believed that the most prevailing risk factors are cigarette smoking in up to 20% [11] and family history in 7-10% of all cases [152]. Other contributing factors include chronic pancreatitis, male sex, advanced age, obesity and diabetes mellitus [181]. The 5-year survival rate is only 3% and the median survival after initial diagnosis is 6 month. There are three main reasons for the dismal prognosis of pancreatic cancer: a) the tumour only becomes clinically symptomatic at late stages when curative treatment attempts are no longer an option, b) tests that allow reliable detection of early stages are not available and c) pancreatic cancer is largely resistant to radio- and chemotherapy [181], [6], [17], [150].

Despite significant scientific advancements the only curative therapy still today is a surgical procedure pioneered in 1935 by Allen Oldman Whipple and colleagues called pancreatoduodenectomy or Whipple procedure. This is the surgical removal of the distal stomach, the duodenum, the gallbladder with the common duct and the head region of the pancreas. Still even after surgery with curative intent the 5-year survival rate does not exceed 20%. Neoadjuvant or adjuvant radiotherapy and/or chemotherapy do not provide remarkable survival benefits [6], [150].

Every cell of pancreatic origin can progress to cancer. Hence different types of pancreatic cancer exist. They are separated into exocrine tumours arising from exocrine cells and endocrine tumours that develop from hormone producing cells. This strict differentiation is complicated by the fact that trans-differentiation from endocrine to exocrine tissue and vice versa has been described [201]. Tumours can develop in any part of the pancreas but form most frequently in the head region (65%) and less frequently in the body and tail region of the organ.

1.7.1 Exocrine Pancreatic Cancer

Exocrine pancreatic cancer is the most common (95%) of all malignancies originating from pancreatic tissue. Pancreatic ductal adenocarcinoma accounts for the vast majority (90%) of exocrine tumours.

1.7.1.1 Development of Pancreatic Ductal Adenocarcinoma (PDAC)

It is believed that the majority of pancreatic ductal adenocarcinomas emanate from non-malignant precursor lesions called Pancreatic Intraepithelial Neoplasias (PanINs) and only in rare cases does it evolve from mucinous cystic neoplasms (MCN) or intraductal papillary neoplasms (IPMN) [181] [70]. PanINs are duct-like structures and can be divided into grades 1A, 1B, 2 and 3 depending on the degree of their cytogenetic abnormalities (compare Figure 17). Whereas nuclear abnormalities are lacking in PanIN1A/B they are increasingly present in PanIN2 and PanIN3. PanIN1 and PanIN2 are also classified as low-grade and PanIN3 as high grade. Terhune et al. estimated the likelihood of a PanIN lesion to progress to invasive PDAC at 1% [177].

Oncogenic KRas mutations are considered to be one of the earliest mutational events in pancreatic cancer development and have been found in 36% of PanIN1, 44% of PanIN2, 87% of PanIN3 [112] and in nearly all cases of invasive cancer [29]. KRas is a small GTPase that hydrolyzes guanosine triphosphate (GTP) to guanosine diphosphate (GDP). It transmits extracellular signals from growth factors and cytokines to activate multiple downstream pathways that are involved in different processes such as cell death and proliferation. It is activated by extracellular cues including growth factors and inflammatory cytokines “which indirectly interact with guanine nucleotide exchange factors (GEFs)” [29]. GEFs bind to KRas and facilitate the normally very slow dissociation of inhibitory GDP from KRas to allow GTP binding to and activation of Ras. GTPase-Activating proteins (GAPs) have the opposite function and terminate Ras signalling. GAPs enhance the conversion of GTP to GDP by Ras-proteins and thereby turn Ras signalling off [87]. Amino acid substitution at position 12 in KRAS, from a glycine (G) to an aspartic acid (D) (KRasG12D) is the most common mutation in the KRas proto-oncogene in pancreatic cancer. Oncogenic KRas has a significantly impaired ability to enter the OFF state and as a result proliferative extracellular signals are transmitted longer than intended [73], or KRas acts independent from extracellular influences and is considered to be

constitutively active [29]. KRas regulation is influenced by other factors such as subcellular localization and therefore GDP/GTP binding is not always the sole determinant of Ras-activity. Many healthy people harbour oncogenic KRas mutations in the pancreas but only a minority develops cancer [121], [149]. Merely a fraction of cells that express oncogenic KRas in genetically modified mouse models of cancer progresses to become invasive cancer [50]. This is in part attributed to the fact that most KRasG12D-expressing cells disappear from the pancreas and only a small proportion remains to form PanINs [145]. Furthermore, mounting evidence indicates that reaching certain threshold levels of oncogenic Ras activation as well as the time of KRas activation are critical determinants in a cells response to Ras signalling [73], [29], [180]. In conclusion the mere presence of oncogenic KRas is not sufficient for transformation of otherwise normal cells and additional factors are required to tear down the barrier to tumour formation.

In line with this is the observation that, during progression from low grade to high grade, PanINs accumulate additional mutations and are increasingly dysplastic. Although it should not be interpreted as a scheduled timeline it is believed that telomere shortening and acquisition of oncogenic KRas are the earliest events in pancreatic neoplasia. In later stages tumour suppressors such as p16/CDKN2A (usually in PanIN2), SMAD4, BRCA2 and TP53 (in PanIN3) are inactivated [181], [70]. Loss of other tumour suppressors such as PTEN [66], or altered microRNA expression and epigenetic changes have also been reported amongst other factors to contribute to PDAC development [181]. In conclusion, only the combined effects of an initiating mutation together with the acquisition of additional lesions are sufficient to bypass tumour barriers, importantly the disruption of the senescence barrier in PanINs, and allow the formation of invasive carcinoma.

A striking, histological feature of pancreatic ductal adenocarcinoma is desmoplasia, i. e., tumour associated growth of fibrous and connective tissue plus an overabundance of inflammatory immune cells [53]. Especially inflammation has been shown to promote tumourigenesis *in vivo*. Adult pancreatic cells of the acinar/centroacinar lineage are resistant to transformation upon activation of oncogenic KRas. In contrast, in the same situation additional pharmacological induction of pancreatitis with the cholecystokinin analogue cerulein allows formation of PanIN and ultimately the development of invasive cancer [51], at least in part through abrogating the senescence barrier of PanINs [49]. Rhim and colleagues recently showed that pancreatic epithelial cells from PanINs can metastasize before the onset of invasive carcinoma and that the inflammatory stroma is critically required for this phenomenon [158]. And it is not to be forgotten that chronic

pancreatitis is a risk factor for the development of pancreatic carcinoma in humans and anti-inflammatory drugs have been shown to reduce the mortality in human PDAC [162].

In summary, pancreatic ductal adenocarcinoma accounts for the overwhelming majority of all pancreatic cancers and still today has a dismal prognosis. It develops from pre-cancerous lesions that harbour an initiating mutation, usually in the KRas protooncogene. Additional genetic or epigenetic events are required for the genesis of invasive carcinoma. The microenvironment, especially inflammation supports cancer development.

1.7.1.2 Rare forms of Exocrine Pancreatic Cancer

Exocrine pancreatic cancer other than PDAC is uncommon and encompasses the following malignancies:

Acinar Cell Carcinoma develops directly from acinar cells and is mainly found in older men.

Intraductal Papillary Mucinous Neoplasm (IMPN). IMPN are tumours that develop from cells lining the main pancreatic duct and its side branches. IMPN can be benign but are known to progress to invasive carcinoma.

Mucinous Cystic Neoplasm (MCN). Pre-dominantly women are affected by this tumour entity. MCN are rarely found in the pancreatic head region. They can reach diameters of several cm and produce mucins. Like IMPN MCNs can develop into carcinomas.

Extreme rarities amongst exocrine pancreatic tumours are Pancreatoblastomas, Serous Cystadenocarcinomas and Solid Pseudopapillary Neoplasms (www.pancreaticcancer.org.uk, <http://www.cancerresearchuk.org/cancer-help/type/pancreatic-cancer/>).

1.7.2 Endocrine Pancreatic Cancer

Endocrine tumours originate as their name suggests from endocrine pancreatic cells. They are also called Neuroendocrine Tumours (NETs) or Islet Cell Tumours. All endocrine tumours combined make less than 5% of all pancreatic tumours. According to the cell of origin they are called Glucagonomas (from α -cells), Insulinomas (from β -cells), Somatostatinomas (from δ -cells) and VIPomas. Their clinical appearance is usually dictated by the symptoms that the respective, excessive hormone levels produce, e. g., severe hypoglycaemias in insulinomas [20], [198].

2 Materials and Methods

2.1 Animal experiments

All mice were bred and housed in accordance with UK Home Office guidelines. Animal studies were done under the project license of Jennifer Morton (license number 60/4096) and my personal license (12198). Mice were housed under non-barrier conditions with a 12h lights on, 12h lights off cycle and fed standard chow (Harlan Laboratories) with free access to water.

For mouse husbandry the animals were at least 42d of age and pups were weaned between 21d and 28d of age.

Mice were either sacrificed with a schedule 1 method of the Animal Scientific Procedures Act (ASPA) at indicated time points or when they became clinically moribund and showed signs of disease such as: inappetence, weight loss, dehydration, abdominal swelling, piloerection, hunched appearance, altered breathing rate, polyuria or inertia.

Very rarely mice, especially of old age, developed lymphoma or sarcoma. Anal papillomas and intussusceptions (a condition in which a part of the intestine has invaginated into another section of intestine) were observed on occasion in mice expression oncogenic KRas. All of those events were extremely rare, in line with previous experience [145] and not attributable to changes in autophagy.

2.2 Mouse models

All animals in this study were of mixed background (C57BL6/Sv129).

By crossing the different mouse models detailed below it was possible to generate pancreas specific knockdown of autophagy in the presence or absence of mutant KRasG12D and or Trp53 and thereby examine the role of autophagy in pancreatic cancer development. It is important to be aware of the fact that all target genes were deleted and/or activated at the same time during embryonic development and therefore before tumours became manifest.

It clearly would also be desirable and informative to delete autophagy in pre-existing tumours but at the time of the study mouse models that would allow this were not available and this is therefore a worthy follow up question.

2.2.1 Pdx1-Cre mouse

During embryonic development the first discernible pancreatic progenitors arise in the dorsal and ventral endoderm at embryonic day 8 (E8.0) [45]. Pancreatic development amongst other factors critically depends on timely expression of key transcription factors in the pancreatic endoderm. Pancreatic and duodenal homeobox 1 (Pdx1) is the first important transcription factor to be identified during pancreatic development from E8.5 and is necessary for development past initial pancreatic bud formation. Pdx1 deficiency is lethal and leads to arrested growth of pancreatic primordia with resulting complete pancreatic agenesis at birth [80]. Initially Pdx1 expression is confined to endodermal regions destined to become the pancreas. However from E9.5 it is also expressed in cells that will develop into the posterior part of the stomach, the duodenum and the bile duct. During embryonic development Pdx1 is strongly expressed throughout all pancreatic cell lineages i. e, both the endocrine and exocrine pancreas and over time becomes gradually restricted to islet-cells. In adult animals pancreatic Pdx-1 expression is virtually confined to islet cells, with very sparse expression in the exocrine pancreas [45], [67], [80]. In line with its expression pattern in adult mice, conditional inactivation of Pdx1 leads to diabetes [80].

Maureen Gannon and Christopher Wright generated a Pdx1-Cre transgenic mouse that allows Pdx1 driven deletion of “floxed” genes. Cre-expression is mosaic in all areas where Pdx1 is normally expressed [45]. Considering the appearance of Pdx1 during embryonic development it is clear that the pancreas is only the major but not the exclusive organ for Pdx1 expression. Therefore potential phenotypes in Pdx1 Cre recombined mouse models could be attributable to extra-pancreatic effects. All mouse cohorts used in this study clearly developed a pancreatic pathology and potential extra-pancreatic phenotypes were clinically irrelevant.

2.2.2 LSL-KRasG12D mouse

The LSL-KRasG12D mouse was generated by Erica Jackson, Tyler Jacks and David Tuveson [77]. “A Lox-STOP-Lox construct was inserted into the the mouse genomic KRAS locus upstream of a modified exon 1 engineered to contain a G→A transition in codon 12. This mutation, commonly found in human PDA, results in a glycine to aspartic acid substitution in the expressed protein, compromising both its intrinsic and extrinsic GTPase activities and resulting in constitutive downstream signaling of Ras effector pathways”[67]. “Prior to breeding with Cre-expressing animals, LSL-KRAS G12D mice are functionally heterozygous for the wild-type allele (KRAS^{+/-}). Excision of the silencing cassette and subsequent recombination allows for expression of the mutant allele, resulting in a heterozygous mutant condition (KRAS^{+/G12D}).” [67]. When bred with Pdx-1 Cre transgenic mice (Pdx-1-Cre KRas^{+/G12D}) expression of the mutant allele is achieved and leads to progressive acquisition of pancreatic ductal lesions that recapitulate the full spectrum of human pancreatic intraepithelial neoplasias (PanINs) in virtually all mice. In approximately 1/3 of mice these develop into invasive PDAC [67].

2.2.3 Atg7flox/flox mouse

Mice that allow conditional Cre-mediated deletion of the essential autophagy gene Atg7 were created by Masaaki Komatsu and Tomoki Chiba [96]. A construct containing the fused cDNA of exon 14-17 replaced exon 14 which is essential for Atg7-mediated autophagy. This sequence was flanked by loxP sites (Atg7flox/flox). Uninduced mice express functional Atg7, have normal autophagy and do not have any pathological phenotype. After Cre-mediated induction the essential exon 14 (along with the fused cDNAs of subsequent exons) is excised, Atg7 is then no longer expressed and autophagy is completely blocked. Notably, embryonic, homozygous deletion of Atg7 achieved by crossing with oocyte specific Zp3-Cre leads to mice that are born without any overt abnormalities but succumb to death, like Atg5^{-/-} mice, within 24h after birth. It is believed that this neonatal lethality is the result of being cut off from the maternal circulation and an inability to compensate (with autophagy) for the initial decline in nutrient supply. Force feeding can partly overcome that phenomenon [101] [96]. When bred to Pdx1 Cre transgenic mice (Pdx1-Cre Atg7flox/flox) pancreas specific excision of Atg7 is achieved and thereby the problem of neonatal lethality is circumvented.

2.2.4 Atg5flox/flox mouse

The Atg5flox/flox mouse was made by Taichi Hara and Noboru Mizushima[62]. Here exon 3 is flanked by loxP sites and upon Cre-induced recombination it is excised rendering the affected tissue autophagy-incompetent. Mice carrying the floxed alleles are normal [62].

2.2.5 P53flox/flox mouse

Mice that allow conditional Cre-mediated deletion of p53 were generated by Jos Jonkers and Anton Berns [78]. By inserting LoxP sites into introns 1 and 10 of Trp53 it was ensured that Cre-mediated excision removes nearly all coding sequences of Trp53 and thus avoids the production of biologically active p53 polypeptides. After recombination mice possess a Trp53 Δ 2-10 allele and animals homozygous for the Trp53 Δ 2-10 mutation behaved like Trp53-knockout mice in terms of tumour-susceptibility. Non-recombined Trp53flox Δ 2-10/flox Δ 2-10 animals are normal [78].

2.3 Materials

All reagents were purchased from Sigma Aldrich (Sigma-Aldrich Company Ltd, Heatherhouse Industrial Estate, Irvine, Scotland) unless otherwise stated.

2.4 Genotyping

In line with standard procedure at the Beatson Institute genotyping was done from ear clippings by an external provider (Transnetyx Inc., Cordova, TN, USA, <http://www.transnetyx.com/>). The company determines the genotype of a mouse from ear clippings by using a proprietary method that is based on real-time PCR and DNA hybridisation.

2.5 Tissue harvest

Mice were humanely killed with a schedule 1 method of the animals scientific procedures act before tissue harvest. If blood samples were to be taken, then the mice were sacrificed by exposure to carbon dioxide in a rising concentration; otherwise the preferred method of killing was manual dislocation of the neck.

The pancreas was removed immediately after death and preserved in two different ways:

- a) Formalin fixation: the pancreas was placed for a minimum of 24h in an adequate volume (approx. 25ml) of 10% neutral buffered formalin (Leica Biosystems, Newcastle Upon Tyne, United Kingdom, catalogue number #3800600E) at room temperature.
- b) Cryopreservation: the tissue was placed in a plastic bag and immediately covered with dry ice to achieve rapid cryopreservation. Frozen tissue was then stored at -80°C .

2.6 Immunohistochemistry

Tissue embedding in wax and immunohistochemistry other than Sa- β -Gal staining were done by the Beatson Institute for Cancer Research Histology Service headed by Colin Nixon. All antibody stainings were done on $4\mu\text{m}$ thick sections. We devised a protocol for in situ visualization of autophagosomes in formalin fixed tissue and the detailed experimental procedures can be found in [159]. Specifics of individual antibodies are listed below and the staining procedure followed a protocol that I developed myself and is outlined in [159].

Antibody	Clone	Cat#	Dilution	Supplier
p21	M-19	sc-471	1:400	Santa Cruz Biotechnology
p53	CM5	VP-P956	1:200	Vector Laboratories
ATG7	H-300	sc-33211	1:50	Santa Cruz Biotechnology
LC3	5F10	0231-100	1:100	Nanotools
cleaved caspase 3	ASP175	9661	1:50	Cell Signaling Technology
SQSTM1/p62		BML-PW9860	1:1250	Biomol

2.6.1 Quantification of histology data

To objectify histological images, quantification was done where necessary as detailed below.

2.6.2 Quantification of PanINs

The number of PanIN's is expressed as PanIN/mm² tissue and was calculated as follows: The number of PanINs/section was counted on HE slides and then the area in mm² of the tissue section on the scanned slide was measured with ImageJ software. The PanIN count was then divided by the area to yield the numbers for the graph.

2.6.3 Quantification of p53 and caspase-3 levels

For each genotype and type point p53 and caspase-3 positive and negative cells were counted from on average >600 cells from Atg7-proficient and Atg7-deficient tissue per individual mouse (acinar tissue for Kraswt/wt mice and PanINs for KRasG12D/wt animals). The age and number of mice counted is stated in the figure legends.

2.6.4 Senescence-associated- β -galactosidase (Sa- β -Gal) staining

Staining was done on 10 μ m thick sections of cryopreserved tissue that were provided by the Beatson Institute for Cancer Research Histology Service. Tissue sections were fixed for 15min at room temperature in freshly prepared in fixative solution (2% paraformaldehyde and 0.25% glutaraldehyde in PBS), followed by three washing steps (PBS, 1mM MgCl₂, pH5.5). After the last wash step, the slides were immersed into freshly prepared staining solution (in PBS: 1mM MgCl₂, 5mM K₃Fe(CN)₆, 5mM K₄Fe(CN)₆, 1mg/ml X-Gal, pH5.5). The slides were incubated for 12-16h in the dark at 37°C in ambient atmosphere. After the staining, the slides were washed a minimum of three times in PBS and 3 times in 70% ETOH to remove residual salts and/or X-Gal crystals. Samples were then allowed to air dry at room temperature and then counter-stained with Safranin O. Images were taken using conventional bright field microscopy. Critical steps in the staining procedure are to

keep the samples moist at all times (from cryopreservation onwards) until the staining is finished, to properly adjust the pH and to include $MgCl_2$ as it is an important co-factor for the β -galactose reaction.

2.7 Blood biochemical analysis

Mice were killed by exposure to carbon dioxide in a rising concentration. Then blood was obtained by cardiac puncture and immediately transferred to lithium heparin polystyrene tubes (Teklab Ltd, Durham, United Kingdom). Plasma was separated from the cellular blood components by centrifugation at 1500g for 15min and stored at $-20^{\circ}C$ before further analysis. Biochemical analysis was done by the Veterinary Diagnostic Services Laboratory at Garscube Campus, University of Glasgow. Analysed parameters were a) for endocrine pancreatic function (glucose, fructosamine) and b) for exocrine pancreatic function (amylase, lipase, cholesterol, triglycerides).

2.8 Analysis of fecal elastase

Mice have a roughly ten bowel movements every hour [18]. Faecal pellets were secured from mice housed individually for approx. 10 min in a single cage before being culled. Faecal pellets were stored at $-20^{\circ}C$ before analysis.

30mg faecal matter was mixed with 500 μ l solubilisation buffer (0.1% Triton X-100, 0.5M NaCl, 0.1M $CaCl_2$). The faecal pellet was disrupted by sonication for 15min in a water bath (Diagenode Bioruptor XL, maximum setting H1, 30s on then 30s interval). After centrifugation at 12000g for 15min the supernatant was transferred to a fresh tube and used for further analysis. All steps were carried out at $4^{\circ}C$. 1ml elastase standards of different concentrations (100mU/ml to 1mU/ml) were prepared from a 1:20 Elastase stock solution (Elastase, Sigma E1250, 10mg at 4U/mg, 20U/ml) by dilution in solubilisation buffer. 100 μ l sample, standards and solubilisation buffer (=blanks) were pipetted into individual wells of Safire Black 96-well plates. 5 μ l of 0.2mM elastase substrate ((CBZ-Ala-Ala-Ala-Ala)₂-R110, Molecular Probes R6506, stock solution was 10mM in DMSO) was added to each well (10 μ M final concentration/well). Fluorescent emission as a readout of faecal

elastase activity was measured in 10min intervals for 90min in a Safire Fluorescent Plate Reader (excitation was at 498nm, emission at 521nm). The standard curve was then used to calculate the activity in mU/mg faecal matter. This protocol was adapted from [197].

2.9 Cell culture

For *in vitro* experiments primary pancreatic tumour cells from individual tumours were generated as described (2.9.1). The cells were cultured in Dulbecco' s Modified Eagle Medium (DMEM) supplemented with 2mM L-glutamine, 10% fetal bovine serum (FBS), 25U/ml penicillin and 25µg/ml streptomycin. Glucose concentrations are indicated in the results section and either 4.5g/l or 1g/l glucose were used. For maintenance the cells were kept in exponential growth phase and were routinely passaged 2/week. Cells were cultured in a humidified incubator at 37°C with 5% CO₂ and ambient O₂. From these stock cultures cells were taken for further experiments.

2.9.1 Generation of cell lines

Several cell lines were generated from tumours of individual mice and indicated genotypes. A tumour piece of approx. 3x3x3mm was minced with scalpels and re-suspended in 10ml DMEM supplemented with 2mM L-glutamine, 20% FBS, 25U/ml penicillin, 25µg/ml streptomycin and 200µg/ml gentamycin. The tumour suspension was then left undisturbed under standard cell culture conditions (see 2.9) for 72h to allow cell adhesion to the culture dish. Thereafter medium was changed regularly 2/week until cells reached confluence (approx. 2-3 weeks). Subsequently the cells were passaged to larger cell culture dishes. Cell lines were frozen in FBS + 10% DMSO in liquid nitrogen after initial expansion. Established stock cell lines were grown in DMEM supplemented with 2mM L-glutamine, 10% FBS, 25U/ml penicillin and 25µg/ml streptomycin. Early stocks of cells were used for experiments.

2.10 Immunofluorescence

Cells were seeded on glass cover slips at equal densities in DMEM 1g/L glucose and cultured in exponential growth phase for 24h prior to fixation. For fixation medium was removed and then ice-cold methanol was added for 15min. During the fixation process the cell culture plates were kept at -20°C. Thereafter all plates (containing the cover slips with adherent and fixed cells) were washed 3x in PBS. Then a blocking step for 1h in PBS with 3% BSA followed. For antigen visualization the coverslips were incubated “sunny side down” on a 25ul primary antibody solution drop (1:250 in PBS + 3% BSA; Cell Signaling, LC3B, #2775; New England Biolabs, Herts, United Kingdom) on parafilm for 24h at 4°C in the dark. Thereafter the coverslips were dipped several times in a large volume (>200ml) of PBS to wash away unbound primary antibody and then incubated as above in fluorescently labelled secondary antibody (1:800 in PBS + 3% BSA; Alexa Fluor® 488 Donkey Anti-Rabbit IgG (H+L), A-21206, Life Technologies Ltd, Paisley, United Kingdom) for 2h at room temperature in the dark. After another wash step, the coverslips were mounted on glass slides using mounting medium that contains (1µg/ml) 4',6-diamidino-2-phenylindole (DAPI) to visualize nuclei. Cells were imaged using a Zeiss Axioplan 2/ISIS confocal microscope (Carl Zeiss Ltd., Cambridge, United Kingdom) with the help of Margaret O'Prey (Beatson Institute for Cancer Research, Glasgow).

2.11 Protein Analysis

Cells used for protein analysis were taken from “maintenance cells” growing in exponential growth phase for at least 48h prior to the experiment and with regular medium change every 48-72h.

2.11.1 Protein Extraction

Cells were washed at least once in ice cold 1X PBS before incubation in cell lysis buffer for 30min on ice. The cell lysis buffer was prepared freshly for each experiment from a stock solution (50mM HEPES, 150mM NaCl, 100mM NaF, 10mM EDTA, 10mM Na₄P₂O₇*10H₂O, 1% Triton X, 0.1% SDS) with freshly added protease inhibitor cocktail tablets (for 10ml lysis buffer one “complete, Mini Protease Inhibitor Cocktail Tablet”,

11836 153 001, Roche). 500ul lysis buffer was used to lyse an approx. 50% confluent 100mm tissue culture dish. Cells were collected with a plastic scraper and the lysate transferred to 1.5ml microcentrifuge tubes. Lysates were then agitated in an Eppendorf Thermomixer at 4000rpm for 15min at 4°C and centrifuged at 12000g for 15min at 4°C. Thereafter the supernatant was transferred to fresh microcentrifuge tubes and stored at -80°C before further use. A small part of the lysate was put aside for protein quantification using the bicinochonic acid (BCA) method.

2.11.2 Protein separation / Polyacrylamide Gel Electrophoresis (SDS-PAGE)

Proteins were separated according to length and mass-to-charge ration using denatured conditions. Briefly, 14µg protein lysate in 10µl lysis buffer (see 2.11.1) were mixed with 10µl 2x sample buffer (100mM TRIS pH 6.8, 2% SDS, 5% β-mercaptoethanol, 15% glycerol, trace amounts of bromophenol blue), boiled at 95°C for 5min and then loaded onto a freshly prepared gel composed of an upper stacking layer (4% acrylamide, 125mM Tris-HCl pH6.8, 0.1% SDS, 0.05% ammonium persulfate (APS), 0.1% N, N, N', N'-tetramethylethylenediamine (TEMED) and a lower separating layer (15% acrylamide, 375mM Tris-HCl pH8.8, 0.1% SDS, 0.05% APS, 0.1% TEMED). A 30% stock solution of 37.5:1 parts acrylamide:bisacrylamide was used to pour gels. Proteins were resolved by applying a constant current of 400mA for approx. 2h.

2.11.3 Protein Immobilisation

Following polyacrylamide gel electrophoresis proteins were immobilized on a polyvinylidene fluoride (PVDF) membrane. A wet-transfer system was used and a constant current of 2A was applied for 1h to transfer the proteins from the polyacrylamide gel onto the PVDF-membrane.

2.11.4 Protein detection

Non-specific binding-sites on the PVDF membrane were immediately blocked by incubation for 1h in blocking buffer (TBS-Tween 0.1%, 3% BSA) at room temperature. Next the membrane was rinsed 3x in wash buffer (TBS-Tween 0.1%), followed by three wash steps for 10min each in wash buffer. Then the membranes were incubated with primary antibodies at the indicated dilutions (see below) in PBS+3% BSA at 4°C overnight. Thereafter the antibody solution was removed and another washing step as before followed. Incubation in horseradish peroxidase (HRP) conjugated secondary antibody (Anti-rabbit IgG, HRP-linked Antibody, #7074, Cell Signaling; Anti-mouse IgG, HRP-linked Antibody, #7076, Cell Signaling) at a dilution of 1:3000 was for 1h at room temperature. After thorough washing the protein-antibody conjugate was visualized by chemiluminescence on autoradiographs using ECL Western Blotting Substrate. Densitometry using ImageJ software (<http://rsb.info.nih.gov/ij/index.html>) was used as a surrogate marker of protein levels.

Antibody	Clone	Cat#	Dilution	Supplier
Atg7		Sc33211	1:1000	Santa Cruz Biotechnology
LC3B		CS2775S	1:1000	Cell Signaling
P38		CS9212	1:1000	Cell Signaling

2.12 Autophagic Flux analysis

To measure autophagic flux, four p53-proficient and four p53-deficient pancreatic cancer cell lines, generated as detailed above (2.9.1), were used. Cells were seeded at equal density in medium containing 1g/L glucose and grown for 24h. For flux analysis lysosomal protease inhibitors Leupeptin (20µm) and NH₄Cl (20mM) were added for 15min as indicated and then the cells were harvested into cell lysis buffer (see 2.11.1) immediately and subjected to Western-Blot analysis. The LC3-II/p38 ratio of individual cell lines was determined using densitometry with ImageJ software, and then averaged for genotype and treatment.

2.13 Metabolic analysis

2.13.1 Oxygen Consumption Rate (OCR) & Extracellular Acidification Rate (ECAR)

OCR and ECAR were measured in a Seahorse FX24 Flux Analyzer (Seahorse Bioscience, Massachusetts, USA) from cells generated as described above. Tumour cells were grown in exponential growth phase for at least 24h in regular cell culture medium (1g/L glucose) and for experiments seeded at a target density of 10000 cells/well 12-24h prior to measurement in 24-well Seahorse plates. 1h before measurement in the Flux Analyzer medium was thoroughly aspirated and replaced with specialized, buffer-free, flux-medium (XF Assay Medium, 102352-000, Seahorse Bioscience) supplemented with 2% FBS, 1g/l glucose, and 1mM L-glutamine. The cells were kept at 37°C at ambient atmosphere for 1h to allow equilibrium and then placed into the Flux Analyzer to determine OCR & ECAR. Antimycin A to block mitochondrial respiration and 2-Deoxy-D-Glucose (2-DG) to block glycolysis were added automatically by the Flux-Analyzer were indicated. Raw-data was normalized to cell number. Normalized values of several individual cell lines from each genotype were averaged to obtain OCR and ECAR values. Values are expressed as average +/- SEM. The data is representative of no less than 3 independent experiments.

2.13.2 Massspectrometry of metabolic intermediates

Exo- and endo-metabolites were measured by LC-MS (Liquid Chromatography Mass Spectrometry) from cells grown in DMEM (10% FCS, 1mM L-glutamine, 0.11g/L pyruvate and P/S) supplemented with 4.5g/L glucose for endometabolites or 1g/L glucose for exometabolites. All assays were done with cells in logarithmic growth phase. Every cell line was seeded in triplicates and no less than 5 different biological replicates were used for each genotype. For measurement of 2-DG uptake cells were grown in DMEM (10% FCS, 1mM L-glutamine, 0.11g/L pyruvate and P/S) supplemented with 1g/L glucose and incubated for 6h with 10mM 2-DG. To measure metabolites 50000 cells/well were seeded in a 6-well plate and 24h later medium was exchanged with fresh medium. Then, after 24h supernatant was harvested to analyse endometabolites. 50µl supernatant were diluted with 150 MilliQ-water and 600µL acetonitrile. Samples were then shaken at

1400rpm for 15min at 4°C and then centrifuged for 15min at 14000g. Supernatants were stored at -80°C for 24h and then analysed by LC-MS. Exometabolites were harvested from cells with extraction solution (50% Methanol, 30% Acetonitrile, 20% MilliQ water) after removal of the supernatant and three washes with PBS. The volume of the required extraction solution was adjusted to 1×10^6 cells/ml. Extraction volumes were calculated from equally treated “counter wells”. All extractions were done using ice-cold reagents, pre-chilled tubes and pre-chilled centrifuges. For statistical analysis no less than 5 biological replicates (taken in triplicates) for each genotype were compared. Metabolites were separated using the Thermo Scientific (Hemel Hempstead, UK) Accela liquid chromatography system. A ZIC-pHILIC column (Merck, Germany) was used for LC separation using gradient elution with a solution of 20mM ammonium carbonate, with 0.1% ammonium hydroxide, and acetonitrile. Metabolites were detected using a Thermo Scientific Exactive high resolution mass spectrometer with electrospray (ESI) ionization, examining metabolites in both positive and negative ion modes, over the mass range of 75-1000 m/z. Data acquisition and processing was done by Gilian McKay (Beatson Institute for Cancer Research, Glasgow).

2.13.3 FDG-PET/CT

All mice were fasted before FDG imaging. At 4-6 h before imaging all mice were given an intravenous injection of Fenestra LC iodine based liver contrast (Advanced Research Technologies, Canada). Mice were anesthetized and given an intravenous bolus of ^{18}F -FDG (~4MBq). After an uptake phase of 30min, positron emission tomography (PET) and computed tomography (CT) images were acquired using an Albira scanner (Bruker, Billerica, MA, USA). Static PET acquisitions were performed for 5minutes and reconstructed using the MLEM algorithm with 12 iterations. CT data was acquired for 12 minutes in high-resolution mode (600 projections) using 45kV and 0.2mA settings. Fused PET-CT images were analysed using PMOD software (PMOD Technologies Ltd, Zurich, Switzerland) to perform qualitative and quantitative assessments of the data. FDG uptake was quantified by calculating the ratio of the maxim SUV (standardized uptake value) within the tumor to the mean SUV within a reference tissue (liver). Data acquisition and processing was done by Agata Mrowinska (Beatson Institute for Cancer Research).

2.14 Statistics

Statistical analysis was done using PASW statistics (IBM, Armonk, New York, USA). Kaplan-Meier survival curves and boxplots were created with PASW statistics software and exported into Adobe Illustrator software (Adobe Systems Incorporated, San Jose, CA, USA). All other graphs were done using both Excel (Microsoft, Reading, Berkshire, United Kingdom) and Adobe Illustrator. Details about the statistical tests used for certain experiments are provided in the legend to each graph.

3 Results

3.1 Effects of genetic deletion of autophagy in the pancreas

3.1.1 Pdx1-Cre efficiently recombines the Atg7flox/flox and Atg5flox/flox alleles

We first questioned the impact of autophagy deletion in the pancreas. To this extend we crossed Pdx1-Cre mice with Atg7flox/flox animals to obtain Pdx1-Cre Atg7^{+/+}, and Pdx1-Cre Atg7^{-/-} mice. Pdx1-Cre Atg7^{-/-} mice were born viable without any visible defects and developed normally before the clinical onset of pancreatic disease at approx. 3 month of age (see below).

Histological examination of pancreata from adult mice showed, as expected, mosaic recombination in the exocrine compartment of the pancreas, i. e. autophagy-deficient and autophagy-proficient tissue exist in parallel in Pdx1-Cre Atg7^{-/-} animals (Figure 3). A characteristic immunohistological staining pattern with three different antibodies was used to discern wild-type from autophagy deficient areas (Figure 3) [159]. Recombined tissue did not show any immunoreactivity with Atg7 antibody, enhanced & aggregated p62 staining, and strong cytoplasmic, homogenous LC3-staining. In contrast, in autophagy-proficient areas the staining pattern was as follow: strong cytoplasmic for Atg7, cytoplasmic & distinct punctate for LC3 and absent to low for p62 (Figure 3) [159]. Homogenous LC3-staining as opposed to a punctate pattern reflects the accumulation of the non-autophagosome-bound, dispersed cytoplasmic LC3-I. LC3-puncta represent the autophagosome-bound form of LC3: LC3-II. Of note, occasionally, large and round LC3 structures were seen in Atg7-null tissue. As has previously been reported, these are LC3-I aggregates and not an indication of autophagosome formation [102], [171]. Similar to the results in Pdx1-Cre Atg7^{-/-} mice, we saw mosaic recombination in Pdx1-Cre Atg5^{-/-} animals with homogenous LC3-I staining, as well as p62-accumulation and aggregation in autophagy-deficient tissue (Figure 4). We did not have antibodies that worked in IHC against Atg5 or Atg12 at our disposal and therefore solely had to rely on a combination of LC3 and p62 staining to assess recombination in these mice. Due to the special features of each immunohistochemistry this is sufficient to discriminate between autophagy-competent and autophagy-incompetent tissue.

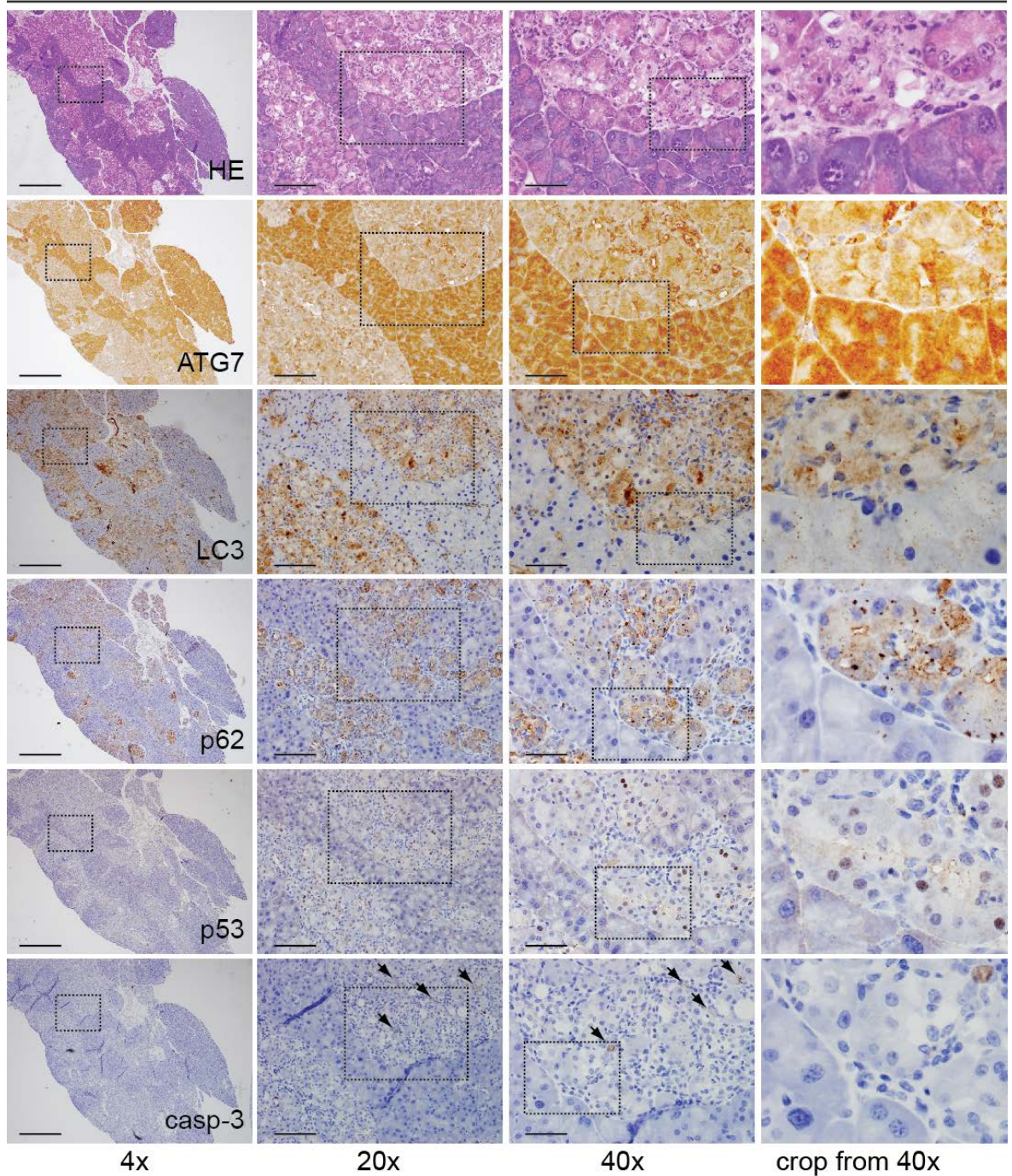
PDX KRas^{wt/wt} ATG7^{-/-} (mosaic)

Figure 3: Histological characterization of Pdx1-Cre Atg7^{-/-} pancreata.

Serial sections of the same region of a pancreas from a 150d old mouse stained with Hematoxylin-Eosin (HE), Atg7, LC3, p62, p53 and caspase-3 are shown. For each staining an overview panel (4x magnification) and 2 higher magnification panels (20x, 40x), as well as a magnified cropped region to show specific staining patterns are provided. The rectangles identify the zoomed areas. Recombined regions (Atg7^{-/-}) are mosaic and can be identified by a lack of Atg7 immunoreactivity, combined with diffuse LC3 staining and p62 accumulation and aggregation in the same part of the pancreas. P53 accumulation and caspase-3 activation are confined to recombined regions and cannot be seen in Atg7^{+/+} areas. Non recombined, i. e., Atg7-proficient (Atg7^{+/+}) have a strong Atg7-staining combined with a distinct punctate LC3-staining pattern and lack p62-accumulation. Scale bars represent 500 μ m (4x panels), 100 μ m (20x) or 50 μ m (40x).

KRas^{wt/wt} ATG5^{-/-} (exocrine, mosaic)

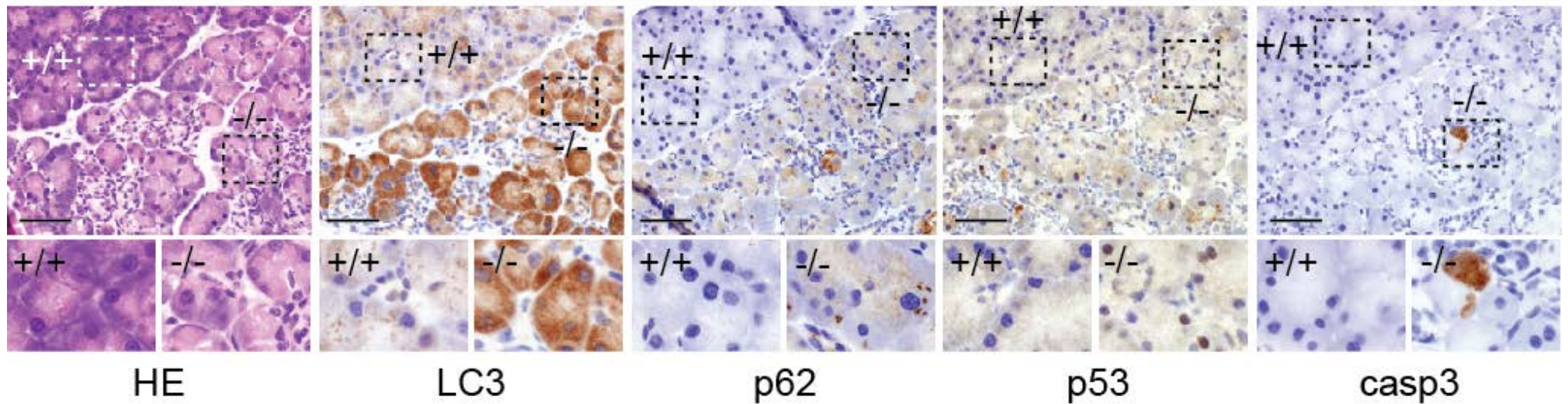
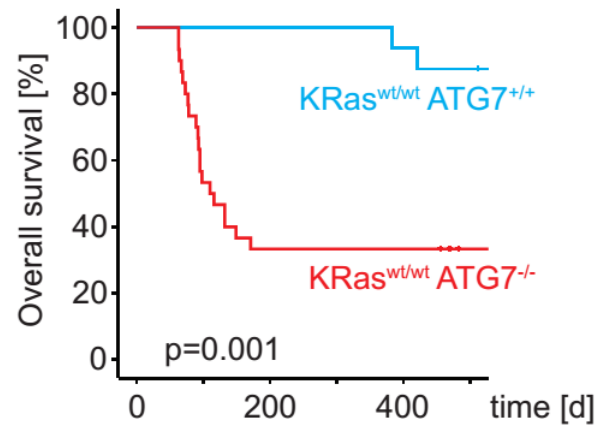


Figure 4: Loss of Atg5 in the pancreas mimics the phenotype of Atg7-loss.

Serial sections of the same pancreatic region stained with HE, LC3, p62, p53 and caspase 3 showing Atg5^{-/-} next to Atg5^{+/+} areas after Pdx1-Cre mediated mosaic recombination in a 101d old mouse. Recombined tissue (-/-) is in the lower right corner and Atg5-wt tissue in the upper right corner of the panels. Representative regions (+/+ and -/-) are cropped (from the area identified by the rectangle) and provided underneath the main panels. Like their Atg7^{-/-} counterparts Atg5^{-/-} areas show strong diffuse staining for LC3, p62 aggregates, have increased levels of p53 and caspase-3 activation. Non-recombined have a distinct, punctate LC3 staining pattern, do not accumulate p62 or p53 and do not activate caspase-3. Scale bars represent 50μm.

3.1.2 Genetic ablation of autophagy in the pancreas reduces survival

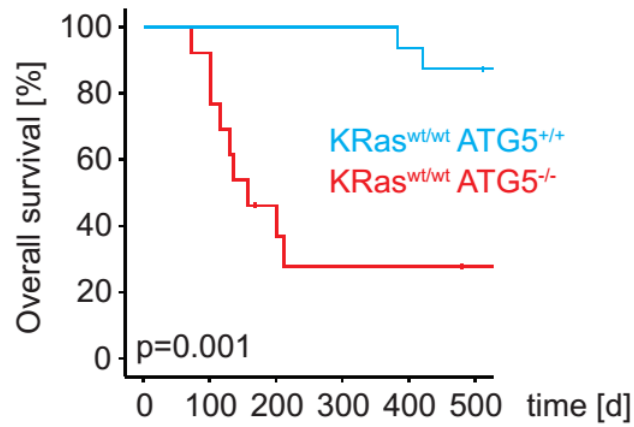
We were interested to learn how autophagy-deletion in the pancreas impacts on survival and therefore conducted a Kaplan-Meier survival analysis of Pdx1-Cre Atg7^{+/+} and Pdx1-Cre Atg7^{-/-} mice (Figure 5). Animals were either sacrificed when they showed signs of disease (compare 2.1) or reached 500d of age. Approx. 60% of Pdx1-Cre Atg7^{-/-} mice became sick at a median age of 110d and had to be culled. Clinically they presented with a hunched posture, inappetence, piloerection and dehydration. These mice also suffered from polyuria (increased urination frequency), because the bedding was frequently found to be wet in cages that housed Pdx1-Cre Atg7^{-/-} mice. Roughly 40% of animals had life spans comparable to wild-type mice and were culled in good health at the end of the experiment. We did not observe a gender specific bias in Pdx1-Cre Atg7^{-/-} mice (Figure 5). As expected, Pdx1-Cre animals virtually did not show any signs of disease during the experiment. Similar results were obtained when comparing cohorts of Pdx1-Cre to Pdx1-Cre Atg5^{-/-} mice (Figure 6).



	n	m/f	median
ATG7^{+/+}	16	5/11	n/a [#]
ATG7^{-/-}	30	18/12	110 +/- 20.3

Figure 5: Loss of Atg7 in the pancreas increases mortality.

Shown is a Kaplan-Meier analysis comparing overall survival of mice either wild-type (blue) or Atg7^{-/-} (red) in the pancreas. Median survival +/- SDEV, number of mice (n) and male/female (m/f) are provided in the table. A log-rank test (Mantel-Cox) was used for statistical analysis. "n/a[#]": 14/16 animals were culled > 500d when completely healthy.



	n	m/f	median
ATG5^{+/+}	16	5/11	n/a*
ATG5^{-/-}	13	8/5	158 +/- 40

Figure 6: Loss of Atg5 in the pancreas increases mortality.

Kaplan-Meier analysis comparing overall survival of mice either Atg5^{+/+} (blue) or Atg5^{-/-} (red) in the pancreas. Note the Atg5^{+/+} cohort is the same cohort as the Atg7^{+/+} cohort in Figure 1d (blue). These are Pdx1-Cre but otherwise wild-type mice. Median survival +/- SDEV, number of mice (n) and male/female (m/f) are provided in the table. A log-rank test (Mantel-Cox) was used for statistical analysis. As in Pdx1-Cre Atg7^{-/-} mice loss of Atg5 reduces survival in a large proportion of mice.

3.1.3 Pancreas specific deletion of autophagy causes destruction of endocrine and exocrine tissue

In order to understand the histopathological features that underlie the strong differences in survival we sacrificed Pdx1-Cre and Pdx1-Cre Atg7^{-/-} mice at fixed time points between 35d and 150d of age and harvested pancreatic tissue for histological analysis (Figure 7, Figure 8). Whereas both the endocrine (Figure 8) and exocrine (Figure 7) compartment never showed any morphological irregularities in Atg7-wild-type mice at all times, there were striking anomalies in Pdx1-Cre Atg7^{-/-} pancreata, especially at later time points. H&E stained sections revealed that normal pancreatic architecture was disrupted and an inflammatory cell infiltrate was present. Exocrine tissue was homogenous and glassy in appearance and cells seemed vacuolated on occasion, all of which are histological features of necrosis (Figure 7). Furthermore, especially at later time points the islets of Langerhans showed a grossly distorted morphology, i. e. ballooning of cells and vanishing of cell borders, again consistent with necrosis (Figure 8). Notably, histological changes appeared to be more extensive in endocrine tissue compared to the exocrine compartment, which retained its regular morphology to a certain degree. In addition, normal, i. e. non recombined acini were present in Pdx1-Cre Atg7^{-/-} pancreata (compare Figure 3). This is in line with the mosaic expression pattern of Pdx1 especially in exocrine pancreatic tissue. In adult animals Pdx1 expression is virtually restricted to islet cells, where mosaicism is less pronounced [45], [67], [80]. Similar results were obtained from Pdx1-Cre Atg5^{-/-} mice (Figure 4).

We intended to shed light on the molecular factors that contribute to the pancreatic destruction in Pdx1-Cre Atg7^{-/-} mice. P53 is an important inducer of cell death [120] and has been reported to interact with Atg7 [105]. Mice culled at fixed time points between 35-150d of age were analysed (Figure 7, Figure 8). We found a striking induction of nuclear p53 in autophagy deficient, exocrine tissue but not in non-recombined areas (Figure 7). P53 accumulation was most pronounced at 35d of age and then declined and reached a plateau at later times (Figure 7, Figure 9). A similar spatio-temporal activation pattern was seen for cleaved caspase-3, which is a central executioner of apoptotic cell death [103] and is also involved in necrotic cell death [120] (Figure 7, Figure 9). The percentage of p53-positive cells was always higher than the corresponding value for cleaved caspase-3 (Figure 9). Interestingly, neither significant p53 accumulation nor cleaved caspase-3 was detected at all times in endocrine tissue (Figure 8). In other words, despite showing extensive destruction, islets cells did not stain positive for p53 and cleaved caspase-3.

Similar results were obtained in Pdx1-Cre Atg5^{-/-} mice (Figure 10), albeit a time line was not possible due to the relatively small number of available animals compared to the leading Pdx1-Cre Atg7 cohort.

To determine if p53 and caspase-3 activation are a consequence or at least partly causative for the early death of Pdx1-Cre Atg7^{-/-} mice, we interbred p53^{flox/flox} animals (see 2.2.5) to generate and compare Pdx1-Cre p53^{+/+} Atg7^{-/-} and Pdx1-Cre p53^{-/-} Atg7^{-/-} mice. Figure 11 shows that p53-deletion significantly delays the early death observed in the Pdx1-Cre Atg7^{-/-} cohort but does not rescue it. Cleaved caspase-3 levels are reduced in acini of Pdx1-Cre p53^{-/-} Atg7^{-/-} animals when compared to the age-matched Pdx1-Cre p53^{+/+} Atg7^{-/-} group. Most strikingly the early peaked activation of caspase-3 at 35d is absent in p53^{-/-} animals (Figure 12).

We did not observe caspase-3 activation in endocrine tissue in both groups. Animals in both cohorts showed the same clinical signs of illness such as inappetence and polyuria. This implies a) that the acinar cell death is partly the result of p53 accumulation and caspase-3 activation and b) that the death mechanism in endocrine cells does not involve the induction of p53 and caspase-3. Taken together all aforementioned results suggested that necrosis might be the leading cause of pancreatic destruction and that an additional death program involving p53 and caspase-3 exists in exocrine tissue that accelerates death of both the organ and the mouse.

The combination of clinical signs and the histopathological findings with acinar and extensive islet-destruction raised the possibility that animals died from pancreatic insufficiency. From the results presented so far this was likely but we wanted to prove pancreatic dysfunction biochemically and discern between global (exocrine & endocrine), isolated exocrine or isolated endocrine insufficiency. We therefore secured blood plasma and stool samples from moribund and age matched healthy animals of the indicated genotypes (Figure 13). For obvious reasons it was not possible to faste sick mice before acquisition of blood samples and therefore mice were considered to be in a randomly fed state which could theoretically affect blood glucose levels. To compensate for this potential pitfall we included fructosamine in the analysis of endocrine pancreatic function. Fructosamine is a term for ketoamine products that stem from the attachment of carbohydrates to proteins. Fructosamine reflects an average of blood glucose levels over a period of 2 to 3 weeks and is independent of short-lived glucose spikes (that could potentially result from ingestion of food or intermittent starvation periods) [146], [179]. To

assess exocrine pancreatic function we relied on blood parameters (amylase, lipase, cholesterol, triglycerides) and faecal elastase. Amylase breaks down dietary starch into sugars. Lipase turns over lipids and as a direct result, blood lipid content (cholesterol, triglycerides) can be influenced by the exocrine pancreas. When purely relying on those two parameters to assess exocrine pancreatic function, results are sometimes complicated by the fact that the exocrine pancreas is not the only source of these enzymes. Additionally, it is also possible that enzyme levels appear to be normal, despite impaired exocrine function. For example it is plausible, that in a combination of exocrine insufficiency (which lowers blood enzyme levels) and pancreatitis (which increases blood enzyme levels) amylase and lipase levels are within the normal range [90], [118]. We therefore included fecal elastase as a reliable indicator of pancreatic exocrine function [183]. The combination of blood borne and faecal parameters allows an accurate evaluation of the exocrine compartment (Figure 13).

Moribund Pdx1-Cre Atg7^{-/-} animals had significantly elevated glucose and fructosamine levels compared to age matched wild-type controls. This proved impaired glucose metabolism in sick Pdx1-Cre Atg7^{-/-} mice and the diagnosis diabetes is complemented by the previously mentioned clinical signs inappetence and polyuria. Exocrine function was not affected (Figure 13). Similar results were obtained for Pdx1-Cre Atg5^{-/-} mice (Figure 14).

Pdx1-Cre p53^{-/-} Atg7^{+/+} mice did not develop disease within 200d of life and had normal pancreatic morphology and function (Figure 15). In Pdx1-Cre Atg7^{-/-} animals p53-deletion did not influence the impaired glucose homeostasis, i. e. when mice were moribund they were diabetic, regardless of p53 status (Figure 15). Exocrine function was again not affected in all genotypes.

In summary moribund Pdx1-Cre Atg7^{-/-} with or without p53 suffer from isolated endocrine pancreatic insufficiency. Seemingly, the exocrine compartment is functionally not compromised despite prominent histopathological abnormalities. Possible explanations for this result are a) mosaic recombination in acinar tissue and therefore healthy exocrine tissue in Pdx1-Cre Atg7^{-/-} mice sufficient to maintain function, b) comparatively high regenerative potential of acinar cells compared to islet cells and c) strong recombination in the endocrine compartment that has very little potential to sustain injury [140], [28].

3.1.4 Genetic ablation of autophagy in the pancreas does not lead to cancer

It is important to mention that we did not observe pre-malignant lesions or invasive pancreatic cancer in Pdx1-Cre Atg7^{-/-} mice aged up to 500d, regardless of p53 status. Also, in all Atg7-proficient animals pancreatic cancer did not occur during their lifespan, again regardless if p53 was present or not.

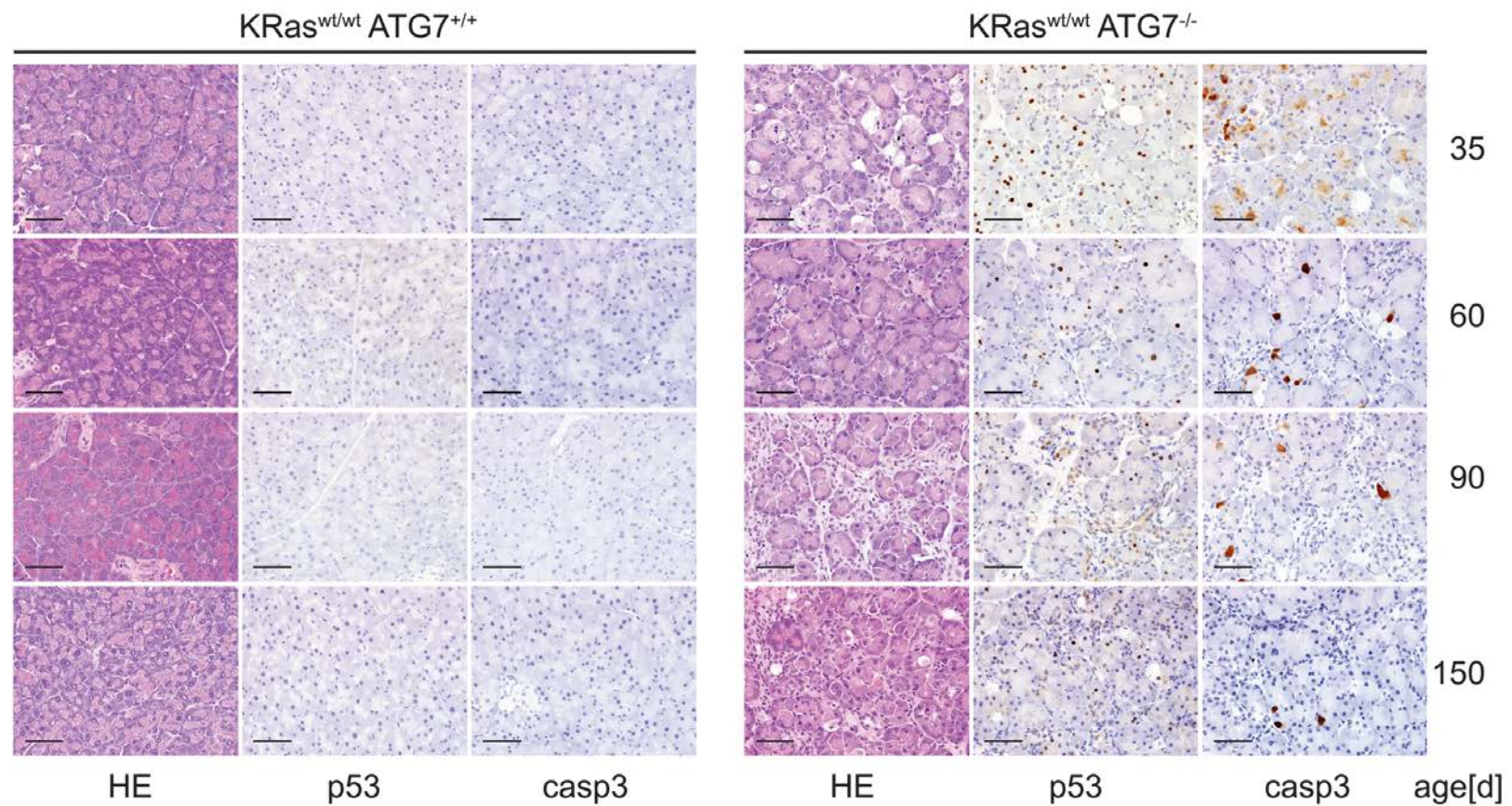


Figure 7: Effects of loss of autophagy on pancreatic acinar tissue over time.

Representative examples of pancreatic acinar tissue stained with HE, p53 and caspase-3 from mice of the indicated genotypes. Animals have been sacrificed at specified time points. In wt-acini ($KRas^{wt/wt} Atg7^{+/+}$) p53 and caspase-3 staining is virtually completely negative during all times. In $Atg7^{-/-}$ acinar tissue p53-levels and caspase-3 activation are strikingly enhanced and peaked at 35d of age. At later time points p53-levels and caspase-3 activation are maintained albeit at a lower level (quantified in Figure 9). Scale bars represent 50 μ m.

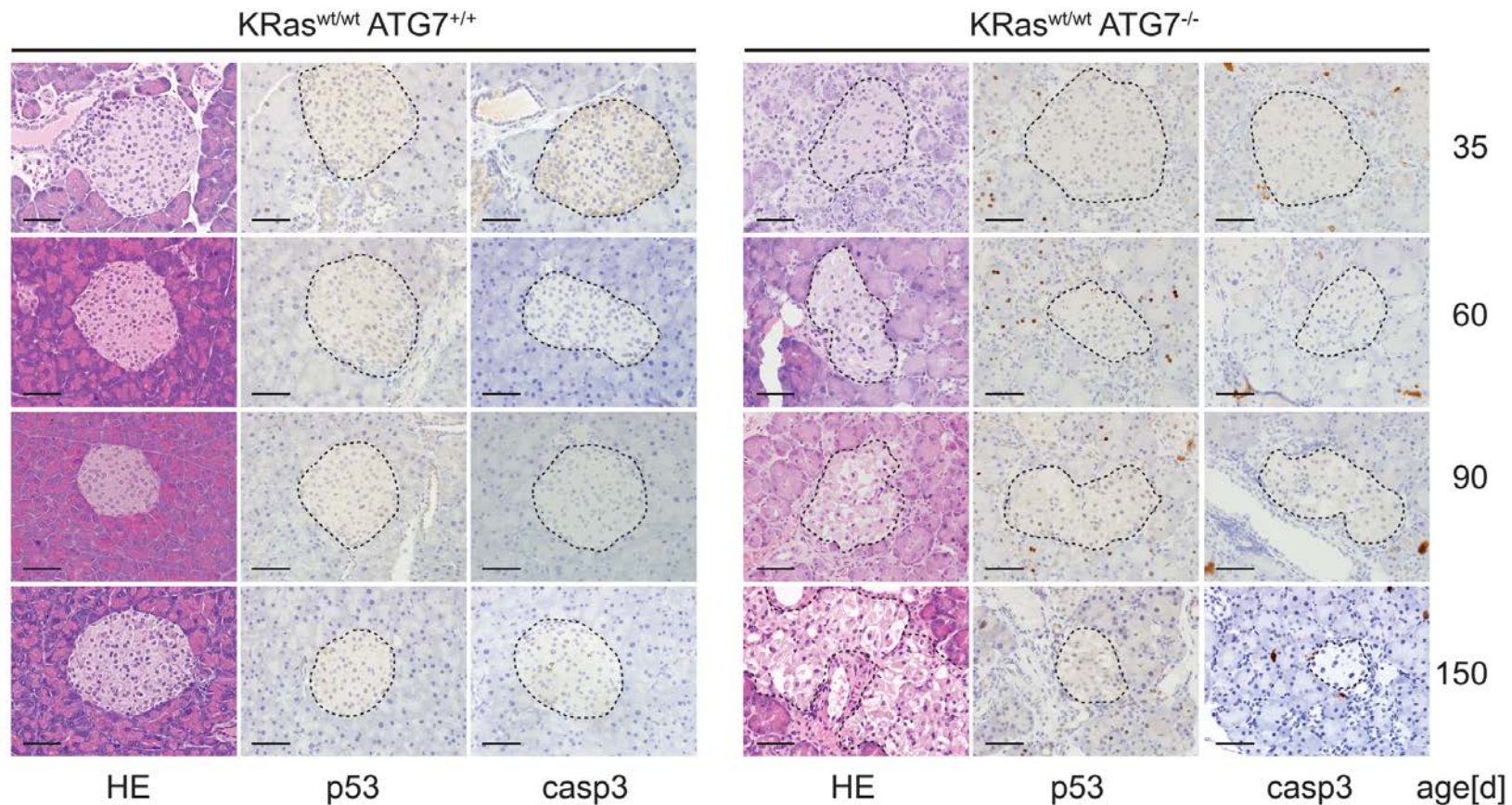


Figure 8: Effects of loss of autophagy on pancreatic endocrine tissue (islets) over time.

Representative examples of pancreatic endocrine tissue stained with HE, p53 and caspase-3 from mice of the indicated genotypes that have been sacrificed at defined time points. For better identification islets are encircled in most panels. Wt-islets (left three columns) are histologically normal at all time points; p53 and caspase-3 staining is virtually completely absent. HE staining of islets in *Atg7*^{-/-} islets (*Pdx1 Atg7*^{-/-}, right three columns) shows progressive morphological disintegration over time. At 35d of age islets look histologically largely normal but cells balloon and progressively disintegrate over time. This destruction is not accompanied by significant p53-accumulation or caspase-3 activation in islets at all times. Notably all increases in p53 levels and caspase-3 activation are confined to acinar tissue. Scale bars represent 50µm.

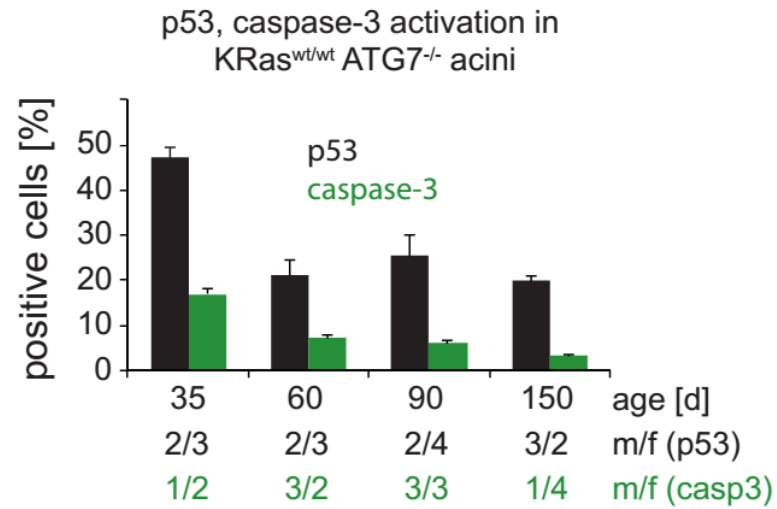


Figure 9: Quantification of p53 accumulation and caspase-3 activation in Atg7^{-/-} acinar tissue over time.

Quantification (median, SEM) of p53 (black) and caspase-3 (green) activation in Atg7-deficient acinar tissue (Pdx1-Cre Atg7^{-/-}) of mice sacrificed at the indicated time points. P53- or caspase-3 activation in wt-pancreas is virtually absent at all times.

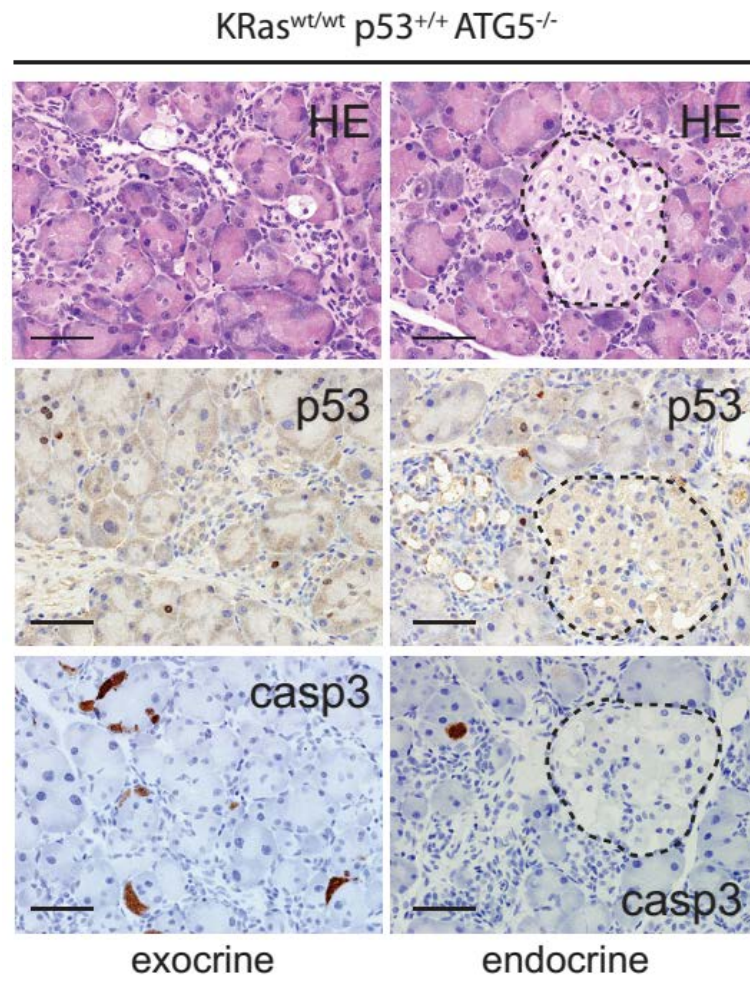
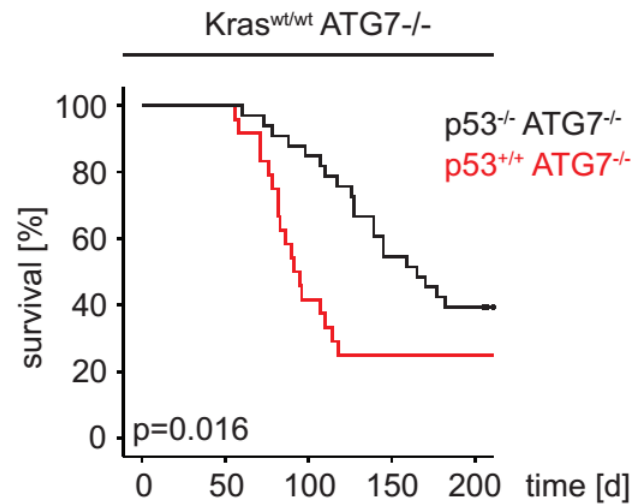


Figure 10: Effects of Atg5 deletion on exocrine and endocrine pancreatic tissue.

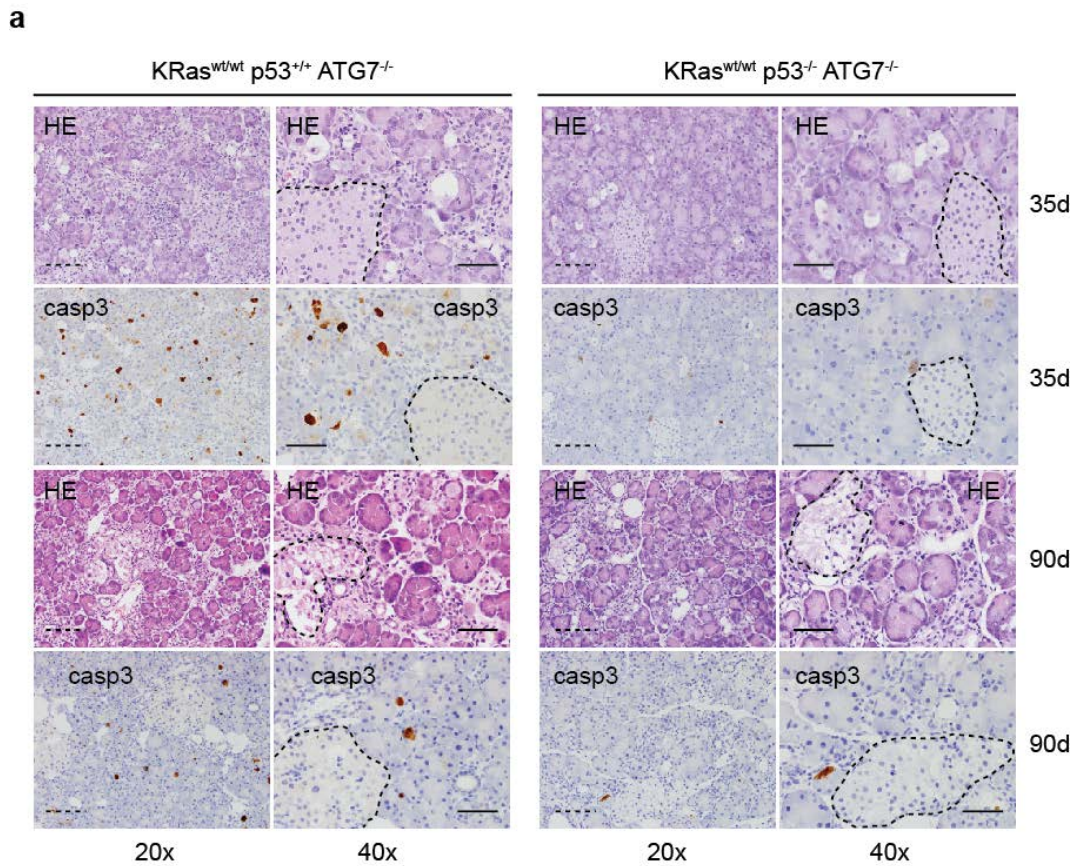
Shown are representative HE, p53 and caspase-3 images of Atg5-deficient exocrine and endocrine (islets) pancreatic tissue from mice with an average age of 113d show increased p53 and caspase-3 activity only in acinar tissue but not in islets. Notably islets (encircled) display the same destructive morphological changes as Atg7^{-/-} islets. Scale bars represent 50 μ m.



	n	m/f	median
p53^{+/+}	24	11/13	91 +/- 6
p53^{-/-}	33	17/16	165 +/- 18

Figure 11: Additional deletion of p53^{-/-} in PDX-Cre Atg7^{-/-} animals delays early death.

Kaplan-Meier analysis comparing overall survival of Pdx1-Cre Atg7^{-/-} that are either p53^{+/+} (red) or p53^{-/-} (black). Median survival +/- SDEV, number of mice (n) and male/female (m/f) are provided in the table. Additional deletion of p53 in Atg7^{-/-} pancreata only delays the early death but does not rescue it completely. A log-rank test (Mantel-Cox) was used for statistical analysis.



b

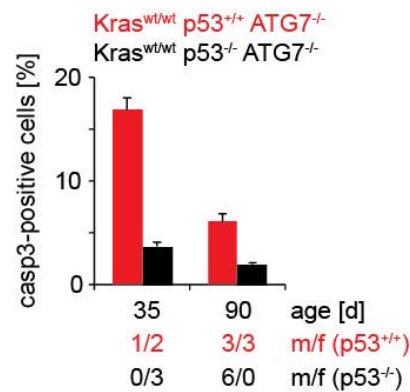


Figure 12: The absence of p53 in Pdx1-Cre Atg7^{-/-} mice abrogates exocrine caspase-3 activation but does not prevent exocrine and endocrine tissue destruction.

A) Representative HE, caspase-3 images from Atg7-deficient exocrine and endocrine tissue that is either p53^{+/+} (left two columns) or p53^{-/-} (right two columns). For each genotype and staining a lower magnification (20x) and a higher (40x) magnification panel is shown containing both exocrine (acini) and endocrine (islets, encircled in 40x panels) tissue. Acinar caspase-3 levels are significantly reduced in p53^{-/-} Atg7^{-/-} pancreata compared to p53^{+/+} Atg7^{-/-} pancreata. Islets are caspase-3 negative and show similar destructive morphological changes in both groups. **B)** Caspase-3 activation is quantified (Median, SEM) and statistical analysis was done using a Mann-Whitney U test. The male/female ratio is provided. Scale bars represent 100 μ m (lower magnification panels) and 50 μ m (higher magnification).

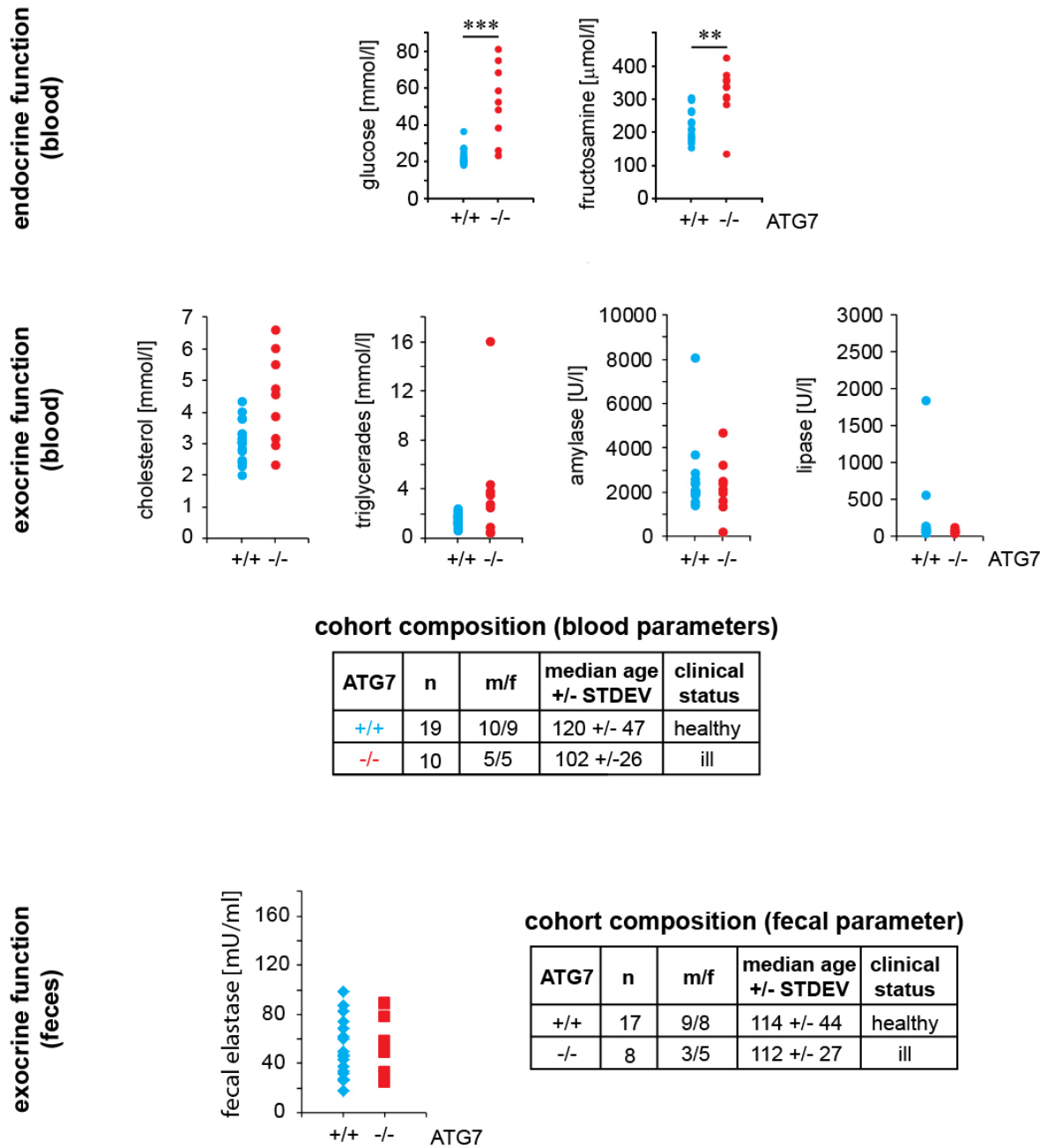


Figure 13: Biochemical profiling of Pdx1-Cre Atg7^{+/+} and Pdx1-Cre Atg7^{-/-} mice.

Biochemical analysis of islet (endocrine) function in moribund Atg7^{-/-} mice (red) or age matched healthy ctrl mice (blue). Exocrine function as assessed by a combination of parameters: a) blood cholesterol, blood triglycerades, blood amylase, blood lipase and b) fecal elastase. These were not altered in moribund Pdx1-Cre Atg7^{-/-} mice compared to age matched wt-mice. Detailed information about the mice used for biochemical analysis is provided in the tables. For statistical analysis a Mann-Whitney U test was used. “****”=p<0.001, “**” = p<0.01.

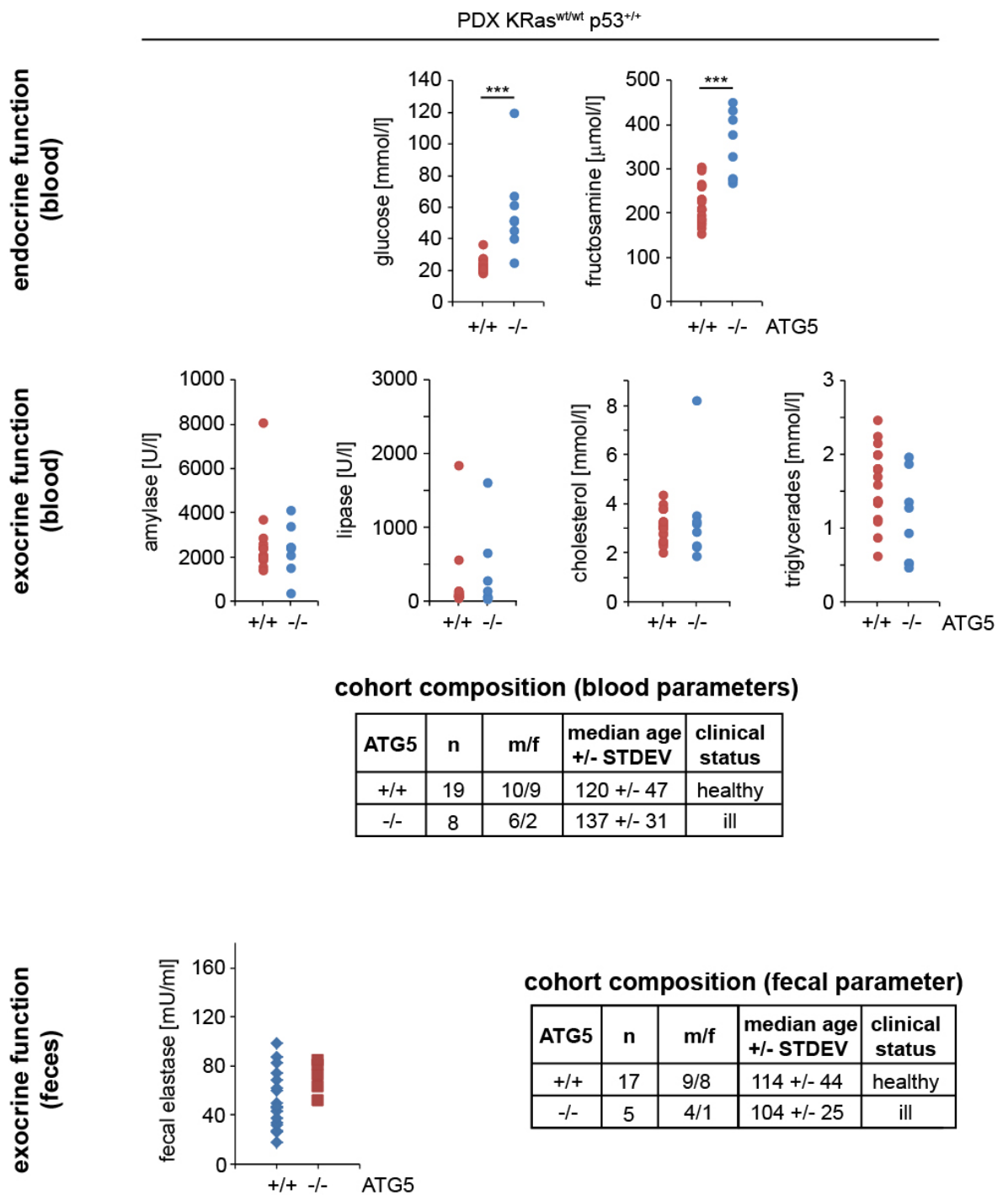


Figure 14: Biochemical profile of Pdx1-Cre Atg5^{+/+} compared to Pdx1-Cre Atg5^{-/-} mice.

Assessment of endocrine (glucose, fructosamine) and exocrine blood serum parameters shows a diabetic phenotype (increased glucose and fructosamine) in moribund Pdx1-Cre Atg5^{-/-} animals but not their age matched Atg5^{+/+} counterparts. Exocrine pancreatic blood parameters are not altered in moribund Atg5^{-/-} mice. Detailed information about both groups is provided in the table. For statistical analysis a Mann-Whitney U test was used. “***”=p<0.001. **E)** Fecal elastase levels as a read-out for pancreatic exocrine function are not different between both groups.

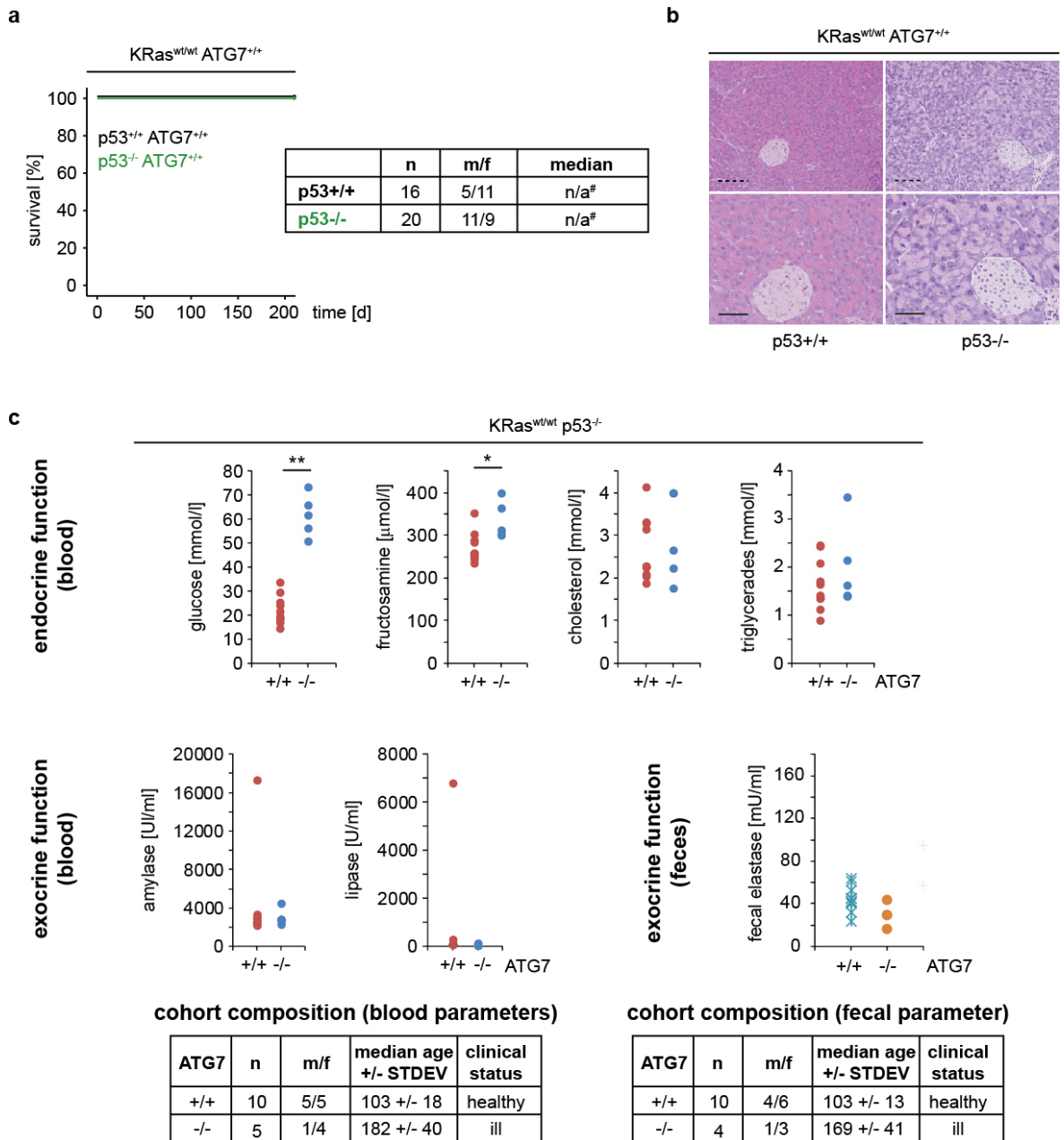


Figure 15: Loss of p53 in the pancreas does not affect survival or pancreatic function.

A) Kaplan-Meier analysis comparing overall survival of mice that are either p53-proficient (blue) or p53-deficient (green) in the pancreas. Atg7 is wt in both cohorts. Detailed information about the cohorts is provided in the table. No death was observed for 200d and mice were sacrificed in complete health. B) HE staining from pancreatic tissue of p53^{+/+} and p53^{-/-} animals (93d of age) is provided in a lower overview magnification (20x, top row) and a higher magnification (40x, bottom row). Morphology is not altered in p53^{-/-} pancreata. Scale bars represent 100 μ m (lower magnification panels) and 50 μ m (higher magnification). C) Assessment of endocrine (glucose, fructosamine) and exocrine blood parameters shows a diabetic phenotype (increased glucose and fructosamine) in moribund Pdx1-Cre p53^{-/-} Atg7^{-/-} animals but not their age matched Pdx1-Cre p53^{-/-} Atg7^{+/+} counterparts. Exocrine pancreatic blood parameters are not altered in ill mice. For statistical analysis a Mann-Whitney U test was used. “***”=p<0.01, “*”=p<0.05. Fecal elastase levels as a read-out for pancreatic exocrine function are not different between both groups. Detailed information about the mice is provided.

3.1.5 Conclusions: autophagy-deletion in the pancreas

We used a pancreas specific Pdx1-Cre recombinase to delete either one of the essential autophagy regulating genes Atg7 or Atg5 in the pancreas of mice. This causes, primarily in the exocrine compartment, a mosaic loss of autophagy. In contrast, the endocrine cells are more universally affected. The absence of autophagy causes widespread damage of both pancreatic compartments and reduces overall survival of approx. 60% of mice. Tissue destruction showed morphological features of necrosis in both the exocrine and endocrine pancreas. The exocrine compartment possessed an additional p53-dependent cell death component that could be rescued by p53-deletion. Autophagy-compromised, moribund mice were diabetic, regardless of the p53 status but the exocrine function appeared normal in mice of all genotypes and health statuses. Signs of pancreatic premalignancy or overt pancreatic cancer were not detected in mice of all aged up 500d.

3.2 Effects of autophagy deletion in the pancreas in the presence of oncogenic KRasG12D

Having established that autophagy-deletion does not cause cancer in pancreata that express two copies of wild-type KRas we next questioned what is the situation if an oncogenic version of KRas is present. The protooncogene KRas is mutated in the vast majority of human pancreatic cancer. Its oncogenic activation is believed to be one of the earliest events in the genesis of pancreatic ductal adenocarcinoma that triggers the event from PanIN formation to development of invasive cancer [72], [125], [34]. We therefore crossed Pdx1-Cre KRasG12D/wt mice (compare 2.2.2) that accurately recapitulate the PanIN to PDAC sequence of human pancreatic cancer [67] with Atg7flox/flox animals to create Pdx1-Cre KRasG12D/wt Atg7^{+/+} and Pdx1-Cre KRasG12D/wt Atg7^{-/-} cohorts.

3.2.1 Genetic ablation of autophagy in the pancreas in mice expressing oncogenic KRas reduces survival

Kaplan-Meier survival analysis showed that virtually all mice in the Atg7-null cohort succumb to death before they reached 250d of age. In contrast the median overall-survival time in the Pdx1-Cre KRasG12D/wt cohort was 348 days (Figure 16). Importantly Figure 16 includes all deaths, i. e. death from pancreatic cancer and death from alternative causes such as pancreatic insufficiency (see below) or benign papilloma growth exceeding the limits defined in the project license (1.5cm in any diameter) and others (compare 2.1). A Kaplan-Meier survival analysis adjusted to only include death from pancreatic cancer is discussed in 3.2.4.

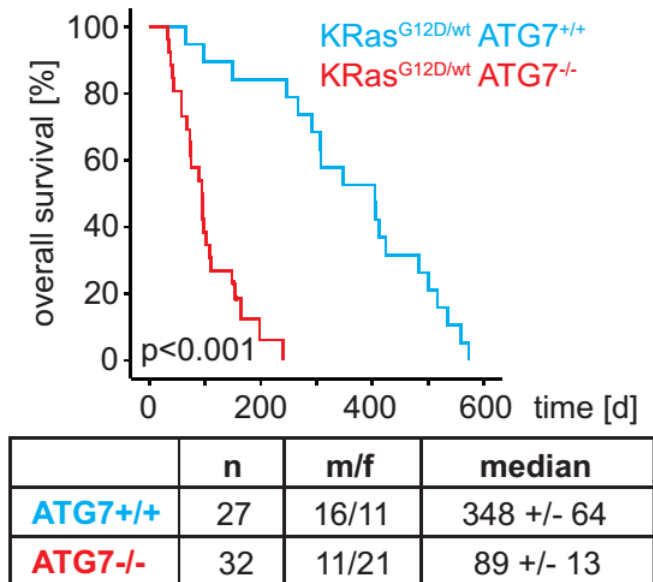


Figure 16: Overall survival of Pdx1-Cre KRasG12D/wt mice with (red) and without (blue) additional deletion of Atg7.

Kaplan-Meier analysis comparing overall survival of KRasG12D/wt mice that are either Atg7+/+ (blue) or Atg7-/- (red). Detailed information about the analysed mice is provided in the table. A log-rank test (Mantel-Cox) was used for statistical analysis.

3.2.2 Pancreas specific deletion of autophagy leads to enhanced PanIN formation in mice expressing oncogenic KRas

Histological examination showed a drastic increase in ductal lesions in pancreata from 150d old Pdx1-Cre KRasG12D/wt Atg7^{-/-} mice when compared to organs from Pdx1-Cre KRasG12D/wt Atg7^{+/+} animals of the same age (Figure 17). On H&E stained sections these lesions showed morphological features reminiscent of premalignant PanIN: flat or papillary columnar or cuboidal cells with different degrees of nuclear abnormalities [168]. The Alcian blue/PAS stain specifically stains mucins and therefore can be employed to differentiate normal ductal cells (that do not produce mucins) from PanIN cells that generate mucins [67]. As shown in Figure 17 on serial sections of the same area virtually all lesions in Pdx1-Cre KRasG12D/wt Atg7^{-/-} mice stain bright purple and are therefore confirmed to be PanINs both morphologically (H&E) and with a specific dye (Alcian blue/PAS). By comparison age-matched autophagy competent mice (Pdx1-Cre KRasG12D/wt Atg7^{+/+}) have far fewer precursor lesions (Figure 17). Figure 17 shows for both genotypes serial sections of the same pancreatic region processed with different histological stains. All PanINs from Pdx1-Cre KRasG12D/wt Atg7^{-/-} pancreata show the staining pattern for absent autophagy: no immunoreactivity with Atg7 antibody, homogenous cytoplasmic LC3 reactivity and p62-aggregation. In contrast Atg7-proficient PanINs stain strongly with Atg7 immunoglobulins, have distinct LC3-puncta and absent p62 immunoreactivity (Figure 17). Similar results were obtained from Pdx1-Cre KRasG12D/wt Atg5^{-/-} mice compared to Pdx1-Cre KRasG12D/wt Atg5^{+/+} animals (Figure 18).

It is noteworthy that PanIN are initiated by oncogenic KRasG12D and are therefore the result of Pdx1-Cre induced recombination. Theoretically if recombination of one locus (lox-Stop-lox KRasG12D) occurs in a cell, then all other loxP sites should also be excised (i. e. the Atg7^{flox/flox} and Atg5^{flox/flox} regions). Therefore all PanINs are expected to be of the same genotype and mosaicism in precursor lesions should not occur as it does in acini from Pdx1-Cre Atg7^{-/-} mice. In this regard, we never observed autophagy-proficient PanINs as determined by immunohistochemistry in Pdx1-Cre KRasG12D/wt Atg7^{-/-} mice.

A quantification of PanIN numbers showed that in Pdx1-Cre KRasG12D/wt Atg7^{-/-} the PanIN count is higher in the first 150d of age, with a peak in 60d old mice. At 200d the PanIN number drops to levels of the control group. PanIN numbers in Pdx1-Cre

KRasG12D/wt Atg7^{+/+} animals steadily rise with time and by 200d match the count in the Pdx1-Cre KRasG12D/wt Atg7^{-/-} cohort (Figure 19).

Figure 17:

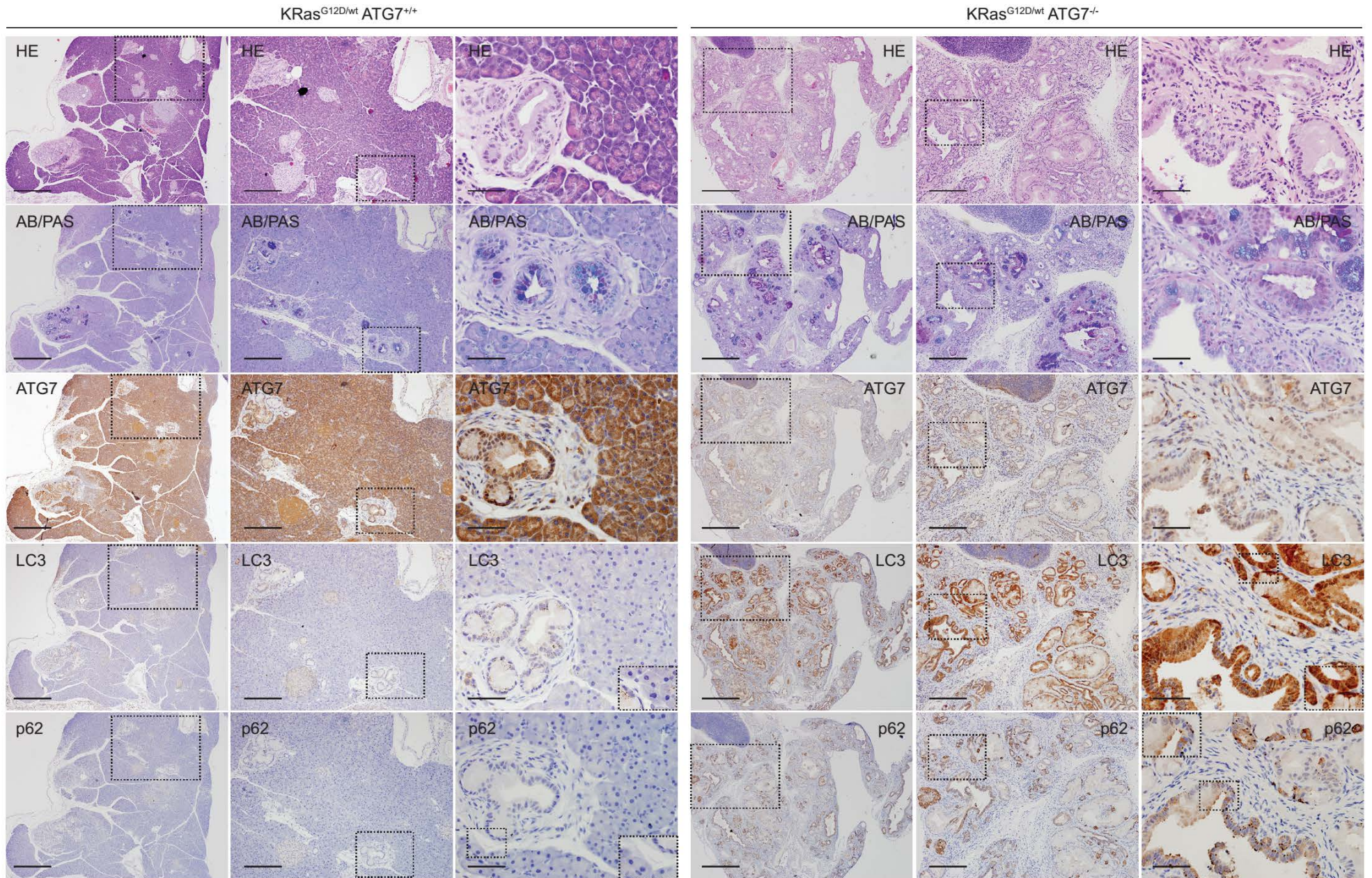


Figure 17: Effect of PDX-Cre mediated Atg7-loss in the pancreas of mice expressing mutant KRasG12D.

Serial sections of the same region of pancreata from a 150d old mice that expresses mutant KRasG12D in the pancreas and are either Atg7^{+/+} (left 3 columns) or Atg7^{-/-} (right 3 columns) stained with Hematoxylin-Eosin (HE), Atg7, LC3, p62. For each staining an overview panel (4x magnification) and 2 higher magnification panels (10x, 40x) are provided. For LC3 and p62 cropped region to show specific staining patterns are added. The rectangles identify the zoomed areas. Scale bars represent 500 μ m (low magnification panels), 200 μ m (medium magnification panels) and 50 μ m (high magnification panels).

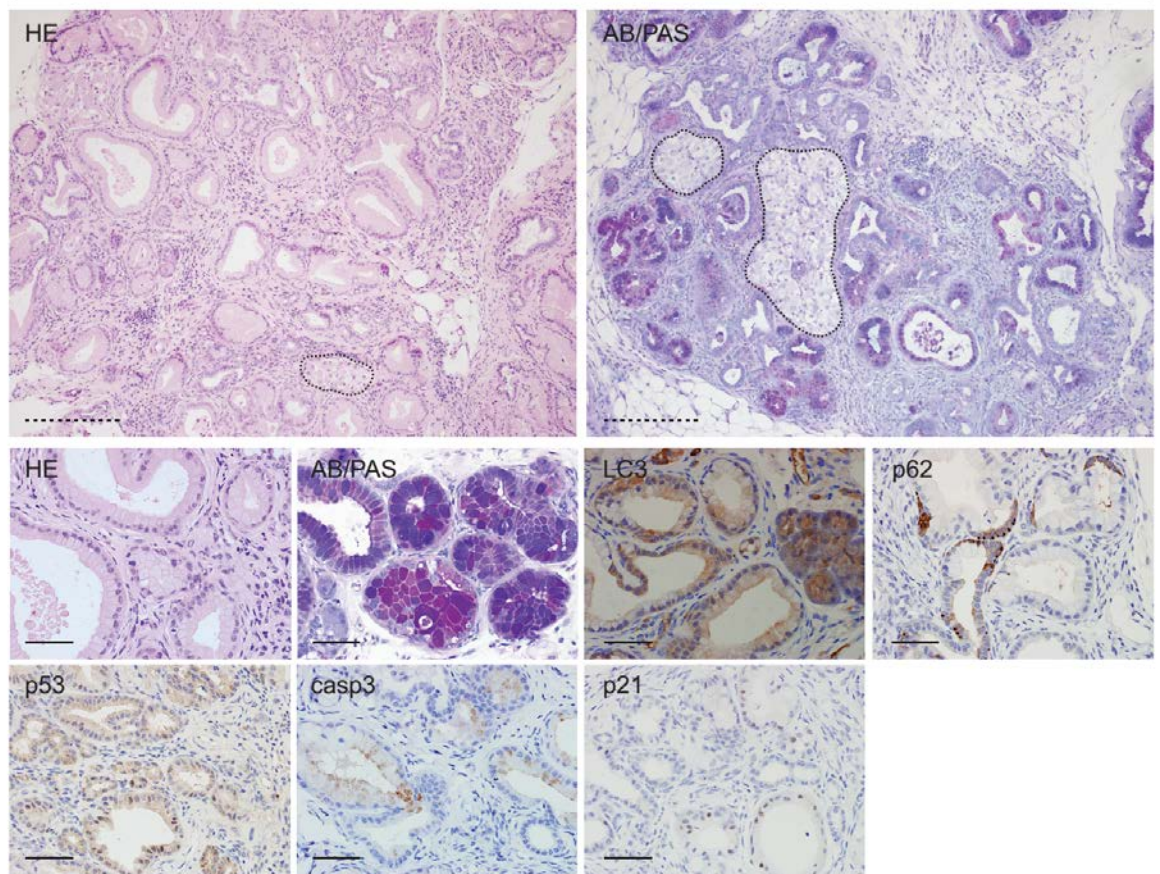


Figure 18: Loss of Atg5 in the pancreas of PDX-Cre KRasG12D/wt mice mimics the phenotype of Atg7-loss in pancreata expressing mutant KRasG12D.

Representative sections stained with HE, AB/PAS, LC3, p62, p53 and caspase 3 of pancreatic tissue from on average 93d old mice. PanIN number is increased compared to autophagy-proficient pancreata expressing mutant KRasG12D (overview HE and AB/PAS panels). PanIN stain positive for Alcian blue/PAS, p53 and p21. Loss of autophagy is shown by p62 accumulation and a diffuse LC3-staining pattern. Islets in the overview panels are encircled. Scale bars represent 200µm (dotted) and 50µm (solid).

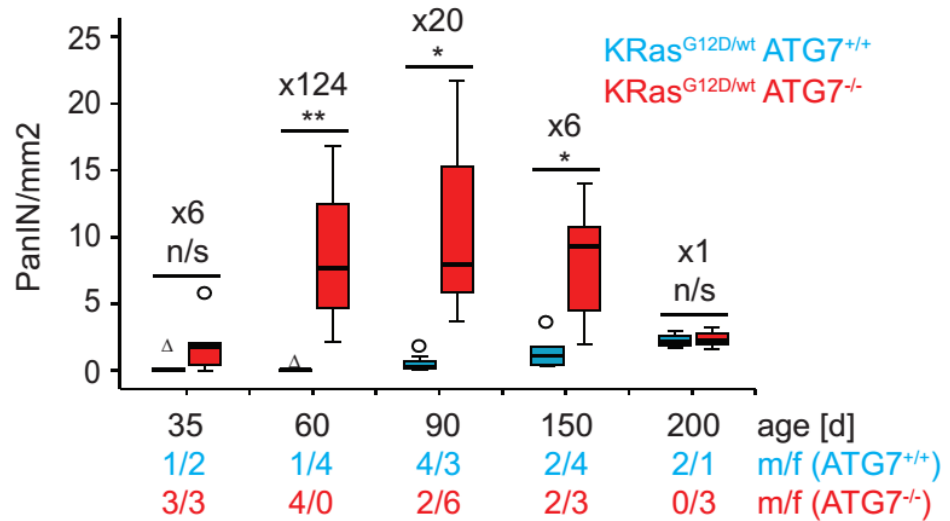


Figure 19: Comparison of total PanIN numbers in Pdx1-Cre KRas^{G12D/wt} mice that are either Atg7^{-/-} (red) or Atg7^{+/+} (blue) over time.

Quantification of PanIN from mice of the indicated genotype aged 35-200 days. Fold increase and the male/female ratio are shown for each time point. For statistical analysis a Mann-Whitney U test was used. “***”=p<0.01, “*”=p<0.05. Error bars are STDEV.

3.2.3 Autophagy-deficient PanINs activate a cell death program

As detailed before in chapter 3.1, Atg7-deletion in the pancreas resulted in a strong induction of p53 and caspase-3 in acinar cells of mice expression two copies of wild-type KRas. Oncogenic KRasG12D has been shown to induce a p53-dependent senescence program as a barrier to tumour formation [145] and autophagy has been implicated in the regulation of senescence [192]. We wanted to know if deletion of autophagy modulates p53-levels and caspase-3 activation in PanIN cells. We also questioned if PanINs in Pdx1-Cre KRasG12D/wt Atg7^{-/-} mice show evidence of senescence like their Atg7-proficient counterparts do. To this extend we stained pancreatic sections from Pdx1-Cre KRasG12D/wt Atg7^{+/+} and Pdx1-Cre KRasG12D/wt Atg7^{-/-} mice 35-150d for p53, caspase-3 and the senescence markers Sa- β -Gal (senescence associated β -galactosidase) and the cyclin-dependent kinase inhibitor 1 (p21/WAF1). Exemplary pictures from 150d old mice are shown in Figure 17 and Figure 20. A quantification of both parameters was undertaken for mice aged 90-150d (Figure 21). Earlier time points could not be assessed due to the lower number of PanIN lesions in younger Pdx1-Cre KRasG12D/wt Atg7^{+/+} pancreata. P53 was readily activated in PanINs of both genotypes. However, the Atg7-status did not significantly impact on p53 levels. In contrast caspase-3 levels were significantly enhanced in autophagy-deficient PanINs (Pdx1-Cre KRasG12D/wt Atg7^{-/-}) at all times (Figure 21).

Notably senescent parameters p21 and Sa- β -Gal were visible in PanINs of both genotypes, implying that Atg7 is not required for induction of the senescence program in PanINs (Figure 20). Similar results were obtained when comparing Pdx1-Cre KRasG12D/wt Atg5^{-/-} mice to their autophagy-proficient counterparts (Figure 18). Again, due to the comparatively small cohort compared to the leading Atg7 mice a time course analysis was not possible.

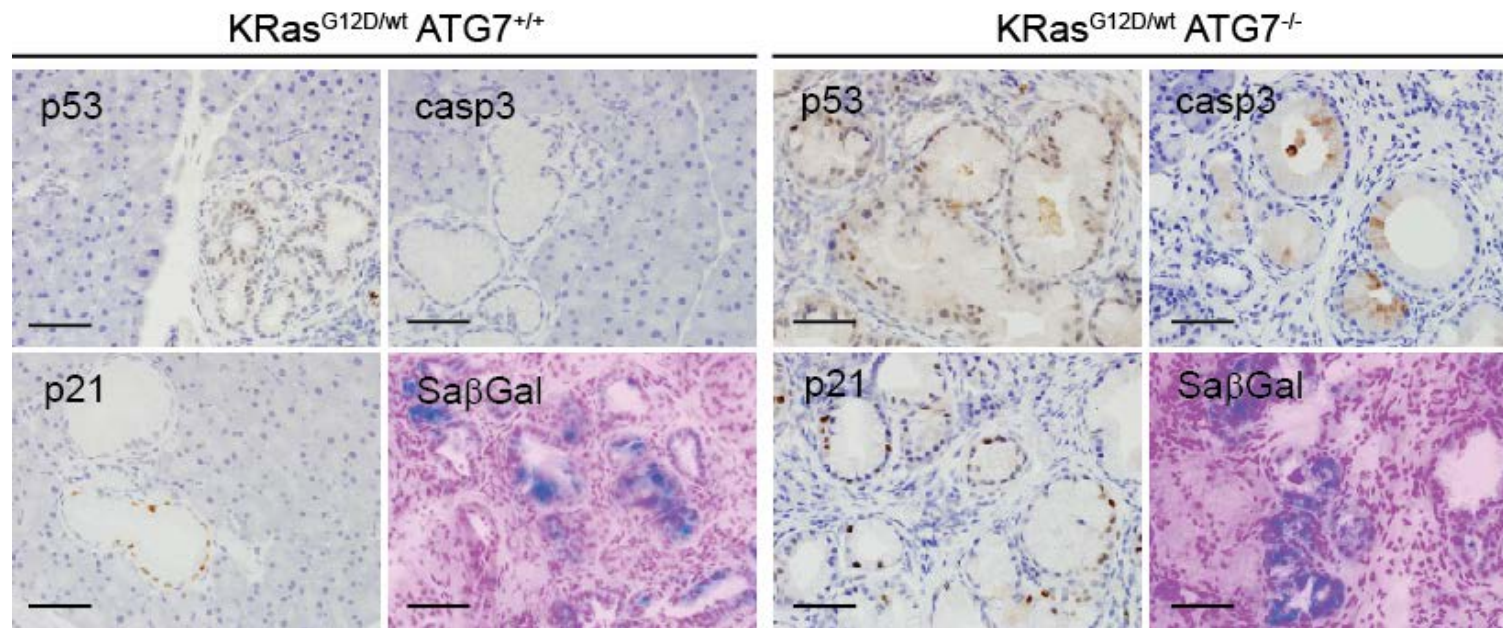


Figure 20: Atg7-deficient PanINs show markers of senescence and activate a cell death program.

Shown are representative p53, casp3, p21 and SaβGal stainings from 150d old mice of both genotypes. Scale bars represent 50μm (solid).

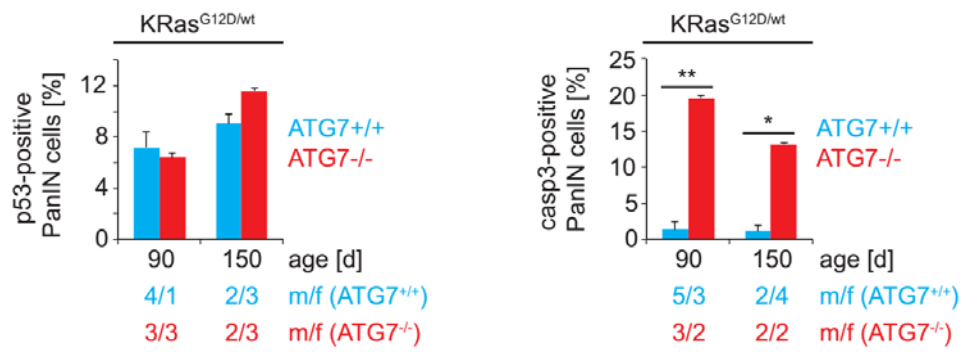


Figure 21: Quantification of p53 and caspase-3 activation in PanINs.

P53 and caspase-3 activation of the indicated genotypes were quantified (median, SEM) in mice of 90 and 150d of age. The male/female ratio is provided. For statistical analysis a Mann-Whitney U test was used. “***”=p<0.01, “*” = p<0.05.

3.2.4 Genetic ablation of autophagy blocks development of pancreatic cancer

After having histologically analysed all Pdx1-Cre KRasG12D/wt Atg7^{-/-} samples we never found evidence of invasive cancer in these mice. A Kaplan-Meier survival analysis adjusted to only include death from pancreatic cancer is presented below in Figure 22. While in line with published data [67] roughly 1/3 of autophagy competent animals (Pdx1-Cre KRasG12D/wt Atg7^{+/+}) succumbed to death from PDAC at a median age of 484 days, not a single mouse in the Pdx1-Cre KRasG12D/wt Atg7^{-/-} cohort had developed even microscopic evidence of pancreatic cancer. This was against the background of an up to 100-fold increased pre-malignancy burden (Figure 19) very surprising.

Considering that all Pdx1-Cre KRasG12D/wt Atg7^{-/-} animals were dead just before the control colony started succumbing to PDAC we were left with two possibilities: a) Pdx1-Cre KRasG12D/wt Atg7^{-/-} do not form tumours or b) they could form tumours but die from pancreatic insufficiency similar to Pdx1-Cre Atg7^{-/-} animals before a potential onset of cancer. To address this we took advantage of the PanIN progression model, i. e. PanIN start out as low grade PanIN1A/B and over time progress to more dysplastic PanIN2 and 3 [70]. We quantified (with the help of Jennifer Morton, Beatson Institute of Cancer Research) the percentage of PanIN1A/B, 2, 3 relative to the total number of PanINs per histological section from mice of both cohorts with a median age of 150d (Figure 23). Whereas Pdx1-Cre KRasG12D/wt Atg7^{+/+} pancreata contain significant numbers of PanIN 2 and even high grade PanIN3, the overwhelming majority of PanIN in Pdx1-Cre KRasG12D/wt Atg7^{-/-} mice are low grade PanIN1A/B, with occasional PanIN2 and virtually no PanIN3 (Figure 23). This argues that in an autophagy-deficient situation PanIN progression is blocked and as a consequence tumour development is impaired.

Kaplan-Meier analysis comparing tumour free survival of Pdx1-Cre KRasG12D/wt Atg5^{+/+} vs Pdx1-Cre KRasG12D/wt Atg5^{-/-} animals showed that a subset of mice lacking Atg5 in the pancreas live up to 500d without ever developing tumours (Figure 24). This strongly reinforces the notion that the absence of autophagy blocks the PanIN to PDAC progression in mice. In other words autophagy is required for tumour formation in this context.

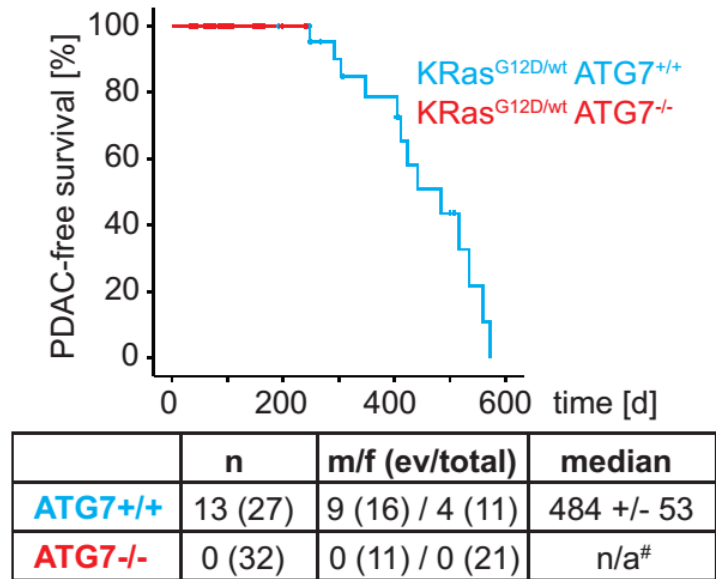


Figure 22: Tumour free survival of Pdx1-Cre KRasG12D/wt Atg7+/+ compared to Pdx1-Cre KRasG12D/wt Atg7+/+ mice.

Kaplan-Meier analysis comparing PDAC-free survival of KRasG12D/wt mice that are either Atg7+/+ (blue) or Atg7-/- (red). Detailed information about the analysed mice is provided in the table.

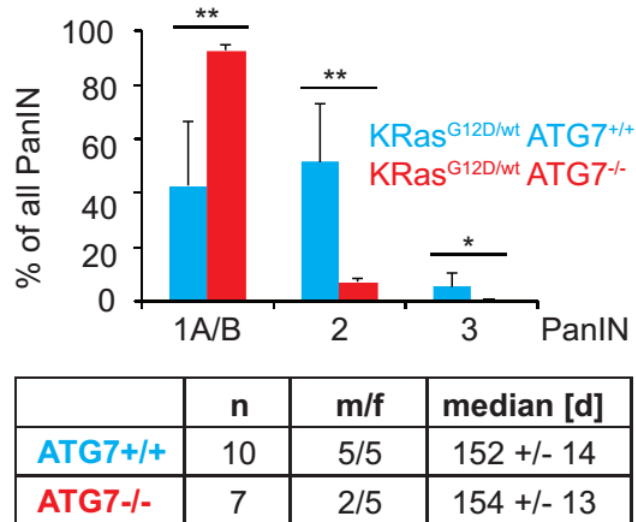


Figure 23: PanIN grading in Pdx1-Cre KRasG12D/wt Atg7^{+/+} and Pdx1-Cre KRasG12D/wt Atg7^{-/-} mice.

PanIN grading of pancreata from 150d old PDX-Cre KRasG12D/wt mice that are either Atg7^{+/+} (blue) or Atg7^{-/-} (red). Detailed information about the analysed mice is provided in the table. For statistical analysis a Mann-Whitney U test was used. “***”=p<0.01, “*”=p<0.05. Error bars are STDEV. PanIN grading was done with help from Jennifer Morton (Beatson Institute for Cancer Research, Glasgow).

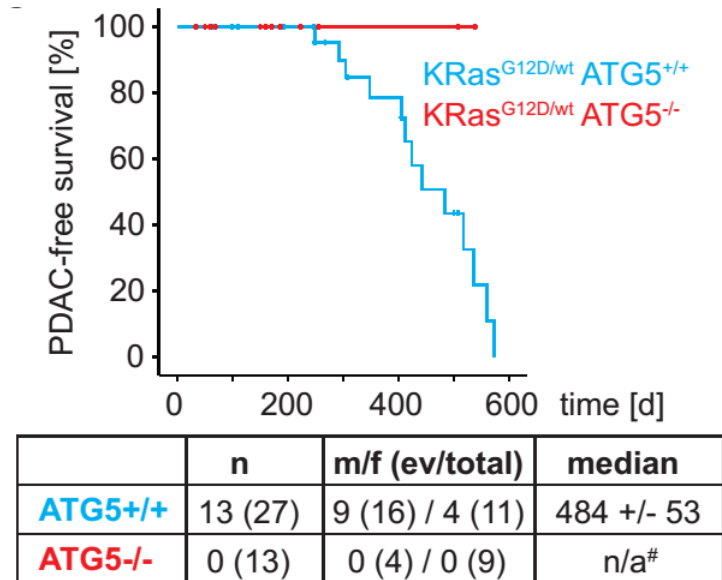


Figure 24: Tumour free survival of Pdx1-Cre KRasG12D/wt Atg5+/+ compared to Pdx1-Cre KRasG12D/wt Atg5-/- mice.

PDAC-free survival of KRasG12D/wt mice that lack Atg5 (red) compared to autophagy-proficient KrasG12D/wt mice (blue). Median survival +/- SDEV, number of mice and male/female (m/f) ratio are also provided. The number of mice succumbing to PDAC is shown (ev), followed by the total number (all) of mice of the same genotype. “n/a[#]”: none of the animals succumbed to PDAC. A log-rank test (Mantel-Cox) was used for statistical analysis.

3.2.5 Genetic ablation of autophagy in the pancreas in mice expressing oncogenic KRas causes endocrine but not exocrine dysfunction

Having established that deletion of autophagy blocks pancreatic cancer development we were left to clarify the cause of the early death in Pdx1-Cre KRasG12D/wt mice that lack either both copies of Atg7 or both copies of Atg5. In analogy to the results obtained for Pdx1-Cre Atg7^{-/-} (with two copies of wild-type KRas), we found that moribund Pdx1-Cre KRasG12D/wt Atg7^{-/-} mice suffered from endocrine but not exocrine insufficiency (Figure 25). We did not have a sufficient number of samples to do a similar analysis in Pdx1-Cre KRasG12D/wt Atg5^{-/-} animals. Considering previous data that implies a strong resemblance between deletion of Atg7 or Atg5, I would consider it likely that a similar situation exists upon deletion of Atg5.

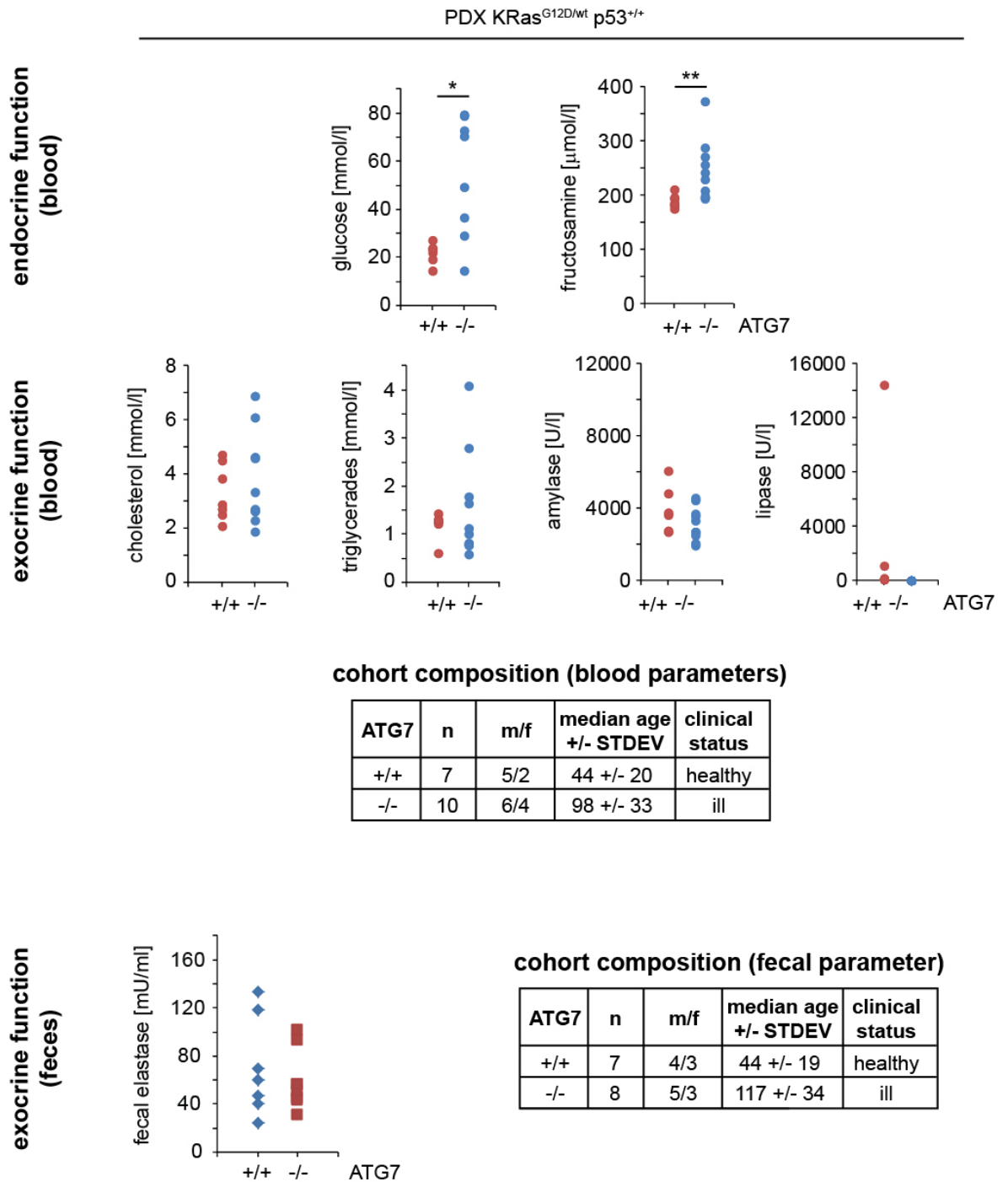


Figure 25: Biochemical profiling of Pdx1-Cre KRas^{G12D/wt} mice with and without genetic deletion of Atg7.

Assessment of endocrine (glucose, fructosamine) and exocrine blood serum parameters shows a diabetic phenotype (increased glucose and fructosamine) in moribund PDX-Cre KRas^{G12D/wt} Atg7^{-/-} animals but not in their PDX-Cre KRas^{G12D/wt} Atg7^{+/+} counterparts. Exocrine pancreatic blood parameters are not altered in ill mice. Fecal elastase levels as a read-out for pancreatic exocrine function are not different between both groups. Detailed information about the cohorts is provided in the tables. For statistical analysis a Mann-Whitney U test was used. “***”=p<0.01, “*”=p<0.05.

3.3 P53-modulates the effects of autophagy on pancreatic cancer development

In the previous chapters I have outlined how autophagy deletion blocks tumour formation in mice that expressed two copies of wild-type p53. We decided to interbreed p53^{flox/flox} mice to Pdx1-Cre KRas^{G12D/wt} Atg7^{+/+} and Pdx1-Cre KRas^{G12D/wt} Atg7^{-/-} animals to generate and compare Pdx1-Cre KRas^{G12D/wt} p53^{-/-} Atg7^{+/+} and Pdx1-Cre KRas^{G12D/wt} p53^{-/-} Atg7^{-/-} colonies. We also generated the respective Atg5 cohorts. In short we were interested to see how autophagy deletion impacts on pancreatic cancer that arises from p53-deficient cells for several reasons. A) PDAC develops rapidly in p53^{-/-} mice [65], [68] and usually at a time before pancreatic insufficiency becomes clinically apparent in our model system. B) We have shown that Atg7-deletion leads to p53-accumulation in acinar cells that are believed to be a potential source of cancer (via transdifferentiation into ductal and PanIN cells) [6], [169]. C) P53 has been shown to coordinate metabolic processes, including autophagy [187], [123], [48].

3.3.1 Simultaneous, genetic deletion of p53 and autophagy in pancreata expressing oncogenic KRas permits and accelerates tumour development

Kaplan-Meier tumour-free survival analysis showed that as expected nearly all mice in the Pdx1-Cre KRas^{G12D/wt} p53^{-/-} Atg7^{+/+} cohort succumb to PDAC with a median onset of 69d (Figure 26). Surprisingly the Atg7-deficient control colony (Pdx1-Cre KRas^{G12D/wt} p53^{-/-} Atg7^{-/-}) not only developed cancer in virtually 100% of cases but also had to be culled significantly earlier with a median survival time of 50d (Figure 26). Of note, censored animals in both colonies were found dead and showed too much decay upon dissection to properly assess if a tumour was present or not.

Tumours developing in Pdx1-Cre KRas^{G12D/wt} p53^{-/-} Atg7^{-/-} were histologically confirmed to be autophagy-deficient (Figure 27).

Our results implied that in a p53-deficient situation genetic loss of autophagy might accelerate tumour formation in stark contrast to the p53-proficient situation where autophagy inhibition completely blocked tumourigenesis. Since Kaplan-Meier survival data presented in Figure 26 essentially only refers to time of death (with evidence of

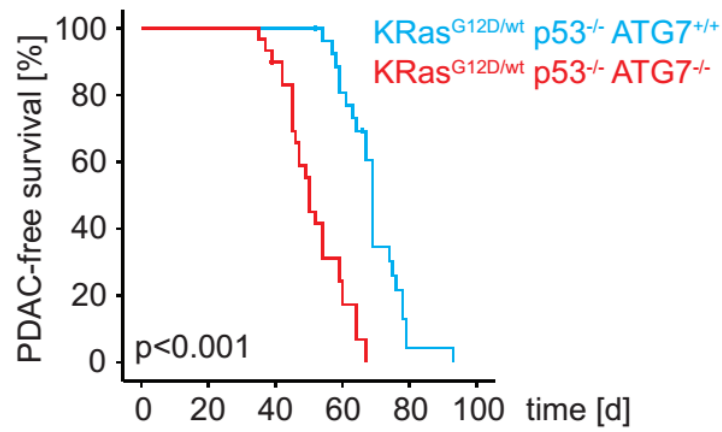
pancreatic cancer). It does not give information about the time of tumour onset or rule out that the early death in the *Atg7*^{-/-} cohort is due to a combination of ill pancreatic health (pancreatic insufficiency) with just the additional presence of a tumour. To address these issues we sacrificed mice of both genotypes at fixed time points between 21 and 35d of age and recorded if a tumour was present or not, the animal weight and the tumour weight (Figure 28).

At 21d of age, tumours were absent in both cohorts. However, 28d old animals in the *Pdx1-Cre KRasG12D/wt p53*^{-/-} *Atg7*^{-/-} cohort had pancreatic cancer in about 70% of cases compared to <20% in the *Atg7*^{+/+} control group (Figure 28). Furthermore tumours had significantly greater mass in the *Atg7*^{-/-} group, both in absolute values and relative to bodyweight. The bodyweight did not differ between groups. A similar picture is seen in mice sacrificed at 35d of age, with 100% of cases now having a tumour in the *Atg7*^{-/-} cohort and only 67% in the control group. Again autophagy-deficient tumours are heavier (Figure 28). Figure 29 shows representative H&E sections from mice of both cohorts sacrificed at the indicated time points. At 21d of age PDAC is absent but PanINs are visible in both groups. Notably at that stage PanIN number is equal in both groups (Figure 30). At 29d of age nearly all pancreatic tissue is comprised of tumour in the *Atg7*^{-/-} cohort, with no evidence of invasive cancer in the *Atg7*^{+/+} control group. At 35d of age, tumour cells infiltrate still broadly present normal pancreatic tissue in *Pdx1-Cre KRasG12D/wt Atg7*^{+/+} mice whereas the “pancreas” is virtually 100% tumour in the *Atg7*^{-/-} cohort (Figure 29). Taken together this data clearly shows that pancreatic cancer developed earlier in *Pdx1-Cre KRasG12D/wt p53*^{-/-} *Atg7*^{-/-} animals compared to *Pdx1-Cre KRasG12D/wt p53*^{-/-} *Atg7*^{+/+} mice.

Biochemical analysis of endocrine and exocrine pancreatic function from mice that were moribund did not show a difference between both cohorts (Figure 31). In other words *Pdx1-Cre KRasG12D/wt p53*^{-/-} *Atg7*^{-/-} mice did not suffer from endocrine dysfunction. This proved that animals represented in Figure 26 die from pancreatic cancer and especially that *Pdx1-Cre KRasG12D/wt p53*^{-/-} *Atg7*^{-/-} mice did not die prematurely due to a failure of endocrine or exocrine function.

Similar survival results were obtained in the respective *Atg5* cohorts (Figure 32). *Pdx1-Cre KRasG12D/wt p53*^{-/-} *Atg5*^{-/-} mice developed cancer in 100% of cases with a very rapid median time to death of 26d compared to the 69d of the control group (Figure 32).

Histological examination proved that tumours in Pdx1-Cre KRasG12D/wt p53^{-/-} Atg5^{-/-} mice were indeed autophagy incompetent (homogenous LC3 pattern, p62 aggregation) (Figure 33). We did not perform biochemical analysis of the Atg5^{-/-} mice due to the fact that they were too small (approx. 5g) to obtain enough blood. However, a median time to death of 25d with 100% of mice bearing a tumour almost certainly excludes pancreatic insufficiency. Regardless of genotype we never observed clinical pancreatic insufficiency in any mouse that was not at least 1-2 month older.



	n (ev/total)	m/f (ev/total)	median
ATG7^{+/+}	24 (27)	12 (14) / 12 (13)	69 +/- 1
ATG7^{-/-}	29 (30)	17 (17) / 12 (13)	50 +/- 1

Figure 26: Tumour free survival of Pdx1-Cre $KRas^{G12D/wt} p53^{-/-} Atg7^{+/+}$ vs mice Pdx1-Cre $KRas^{G12D/wt} p53^{-/-} Atg7^{-/-}$.

Kaplan-Meier analysis comparing PDAC-free survival in $KRas^{G12D/wt} p53^{-/-}$ mice that are either $Atg7^{+/+}$ (blue) or $Atg7^{-/-}$ (red). Median survival +/- SDEV, number of mice and male/female (m/f) ratio are provided in the tables. The number of mice succumbing to PDAC is specified (ev), followed by the total number (all) of mice of the same genotype. A log-rank test (Mantel-Cox) was used for statistical analysis.

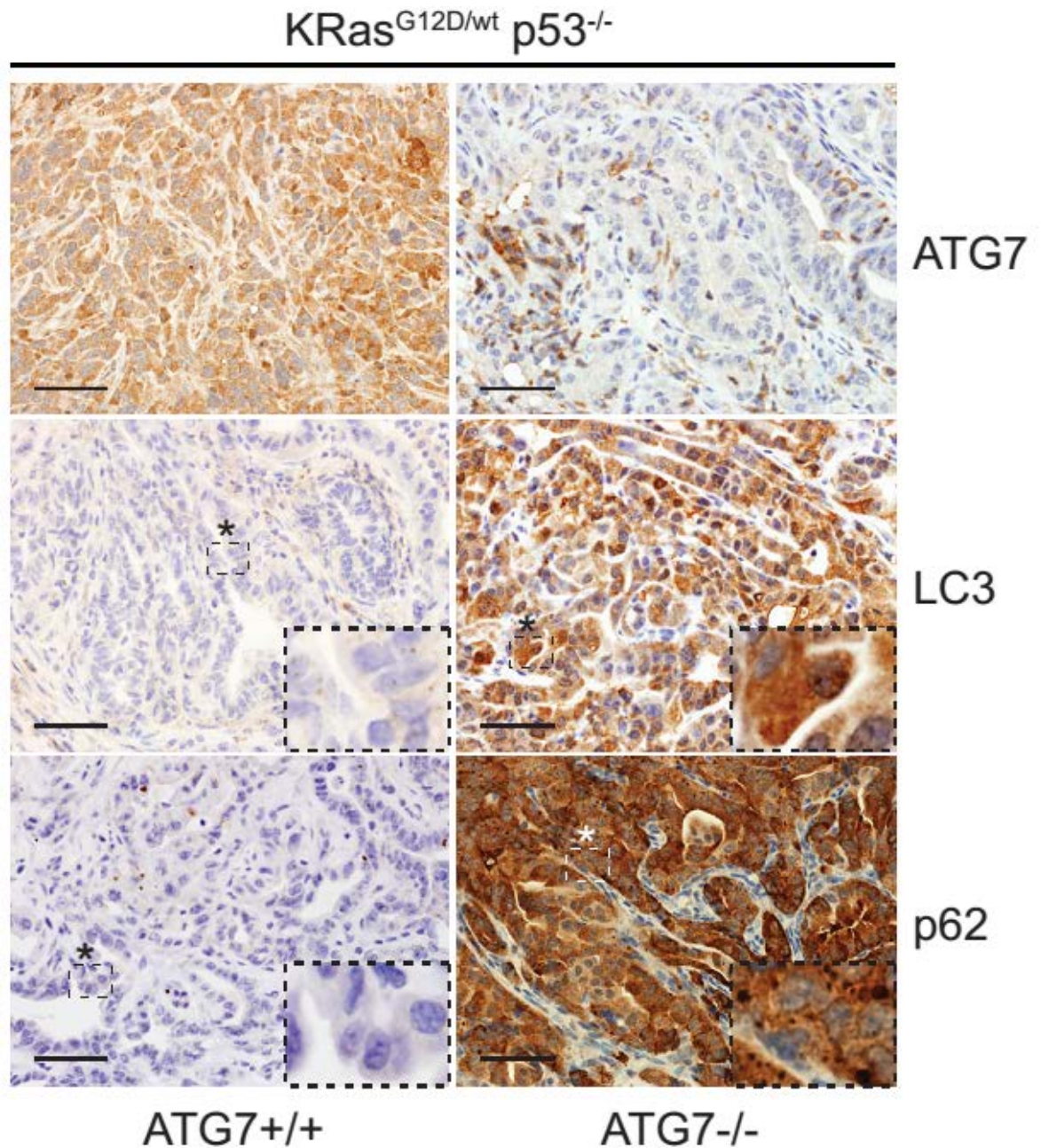


Figure 27: PDACs from Pdx1-Cre KRas^{G12D/wt} p53^{-/-} Atg7^{-/-} mice are autophagy deficient. Pancreatic tumours of the indicated genotypes stained for Atg7, LC3 and p62. Strong diffuse LC3-stain, p62 accumulation and aggregation and the absence of Atg7 immunoreactivity confirm that tumours arise from Atg7^{-/-} tissue in the absence of p53. Inserts are magnified crops from the same images to show specifics of LC3 and p62 staining. Scale bars represent 50 μ m.

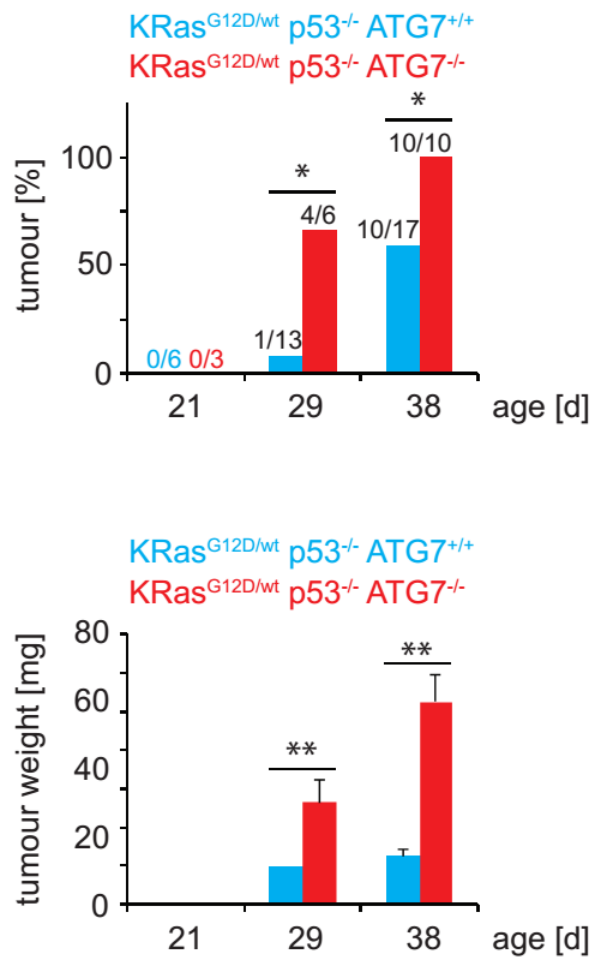


Figure 28: Early tumour onset in Pdx1-Cre $KRas^{G12D/wt} p53^{-/-}$ mice, when *Atg7* is deleted. Tumour incidence in mice from the indicated genotypes, sacrificed at 21, 29 and 38d of age. Numbers in the diagram represent tumour bearing mice vs all mice. Significance was assessed with a Fisher's Exact test. "*" = $p < 0.05$. Weight of tumours (median, SEM) from mice of the specified genotypes culled at the indicated time points. For statistical analysis a Mann-Whitney U test was used. "***" = $p < 0.01$.

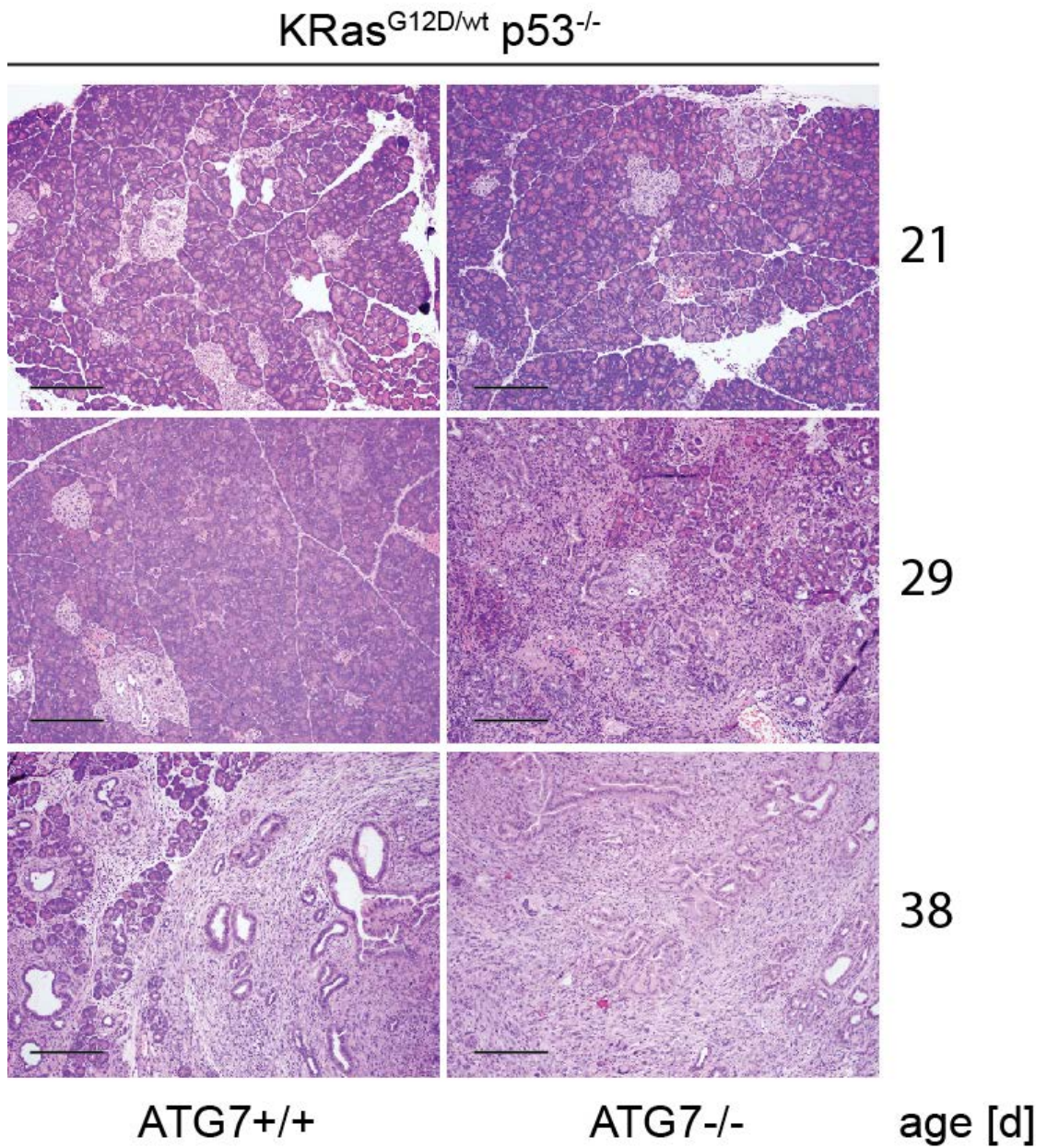
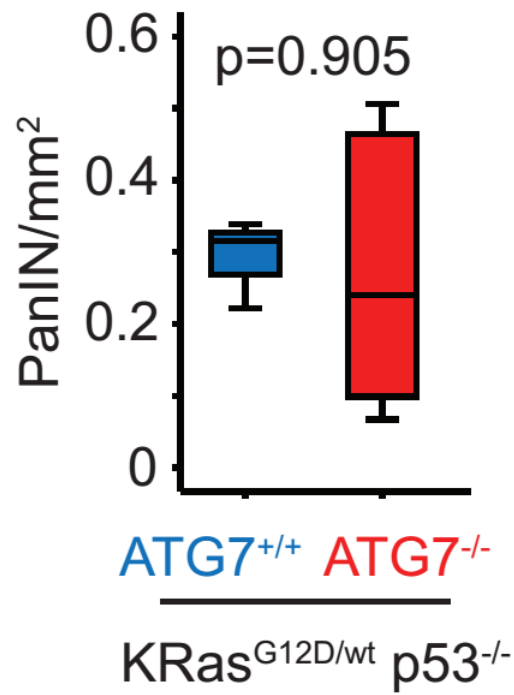


Figure 29: Representative H&E images reflecting the different tumour onset in Pdx1-Cre KRas^{G12D/wt} p53^{-/-} Atg7^{+/+} and Pdx1-Cre KRas^{G12D/wt} p53^{-/-} Atg7^{-/-} mice. Shown are representative HE stainings of pancreata from the indicated time points and genotypes. Scale bars represent 200 μ m.



ATG7	n	m/f	median age +/- STDEV	clinical status
+/+	6	3/3	21	healthy
-/-	3	2/1	21	healthy

Figure 30: Comparison of PanIN numbers in 21d old Pdx1-Cre KRas^{G12D/wt} p53^{-/-} mice Atg7^{+/+} and Pdx1-Cre KRas^{G12D/wt} p53^{-/-} Atg7^{-/-}.

ATG7 deletion (red, n=5) does not increase the number of PanIN/mm² tissue in mice sacrificed 21d after birth compared to ATG7 proficient mice of the same age (blue, n=3). Detailed information about mice used for the analysis is provided.

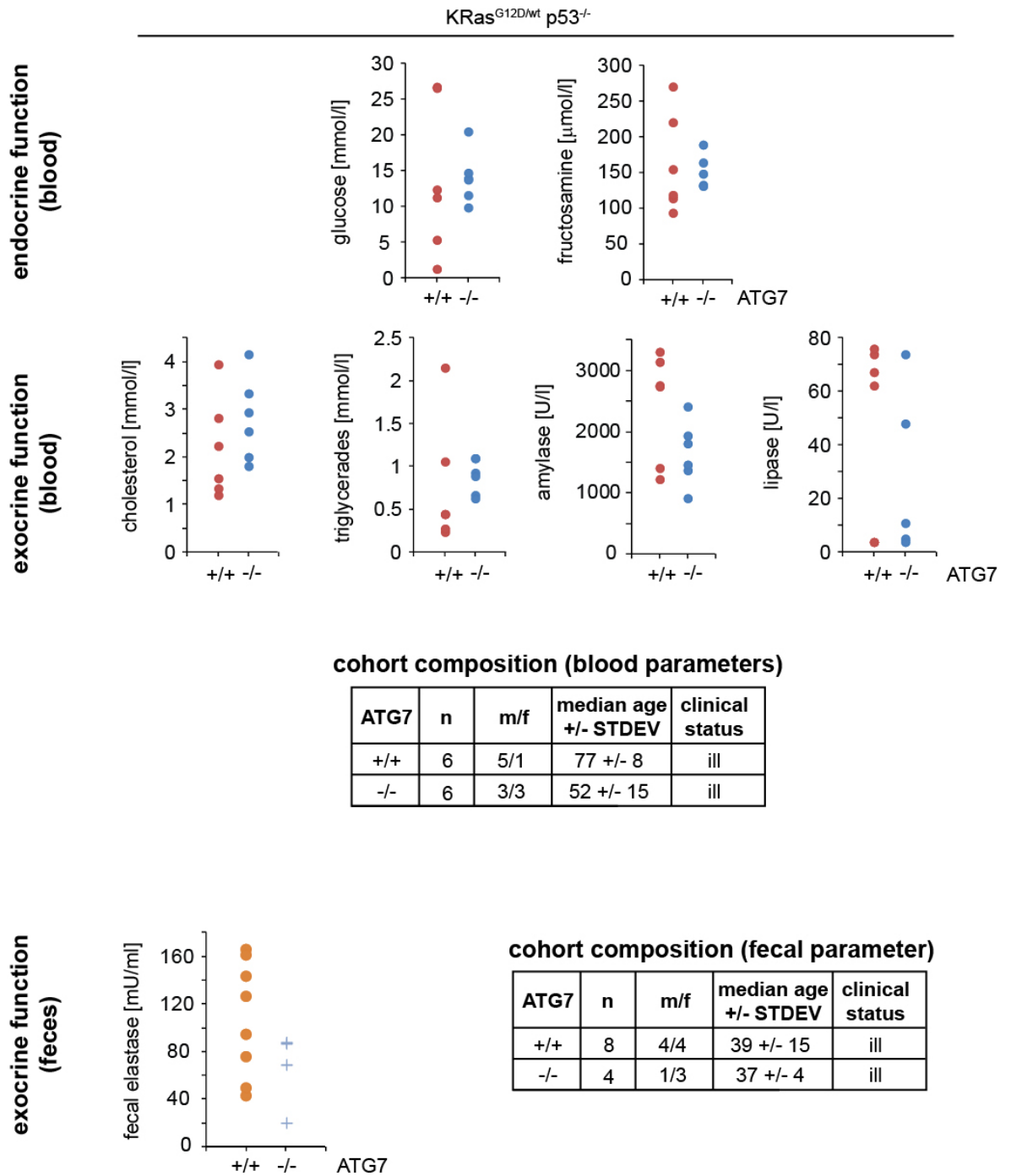
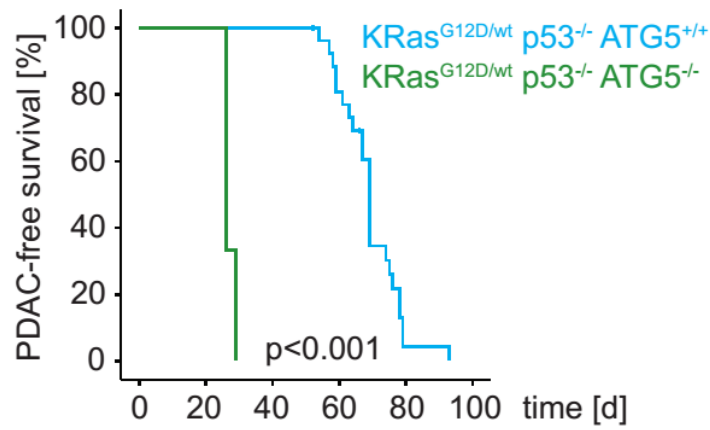


Figure 31: Biochemical profiling of tumour-bearing, moribund Pdx1-Cre KRas^{G12D/wt} p53^{-/-} mice +/- Atg7.

All mice represented in this figure were moribund and had to be sacrificed because of malignancy. Assessment of endocrine (glucose, fructosamine) and exocrine blood serum parameters does not show a difference between both genotypes. Likewise fecal elastase activity is not different between both groups. Information about the cohorts is provided in the tables.



	n (ev/total)	m/f (ev/total)	median
ATG5^{+/+}	24 (27)	12 (14) / 12 (13)	69 +/- 1
ATG5^{-/-}	3 (3)	1 (1) / 2 (2)	26 +/- 1

Figure 32: Tumour free survival of Pdx1-Cre $KRas^{G12D/wt} p53^{-/-} Atg5^{+/+}$ vs Pdx1-Cre $KRas^{G12D/wt} p53^{-/-} Atg5^{-/-}$ mice.

Kaplan-Meier analysis comparing PDAC-free survival of $KRas^{G12D/wt} p53^{-/-}$ mice that are either $Atg5^{+/+}$ (blue) or $Atg5^{-/-}$ (green). Median survival +/- SDEV, number of mice and male/female (m/f) ratio are provided in the tables. The number of mice succumbing to PDAC is specified (ev), followed by the total number (all) of mice of the same genotype. A log-rank test (Mantel-Cox) was used for statistical analysis.

KRas^{G12D/wt} p53^{-/-} ATG5^{-/-}

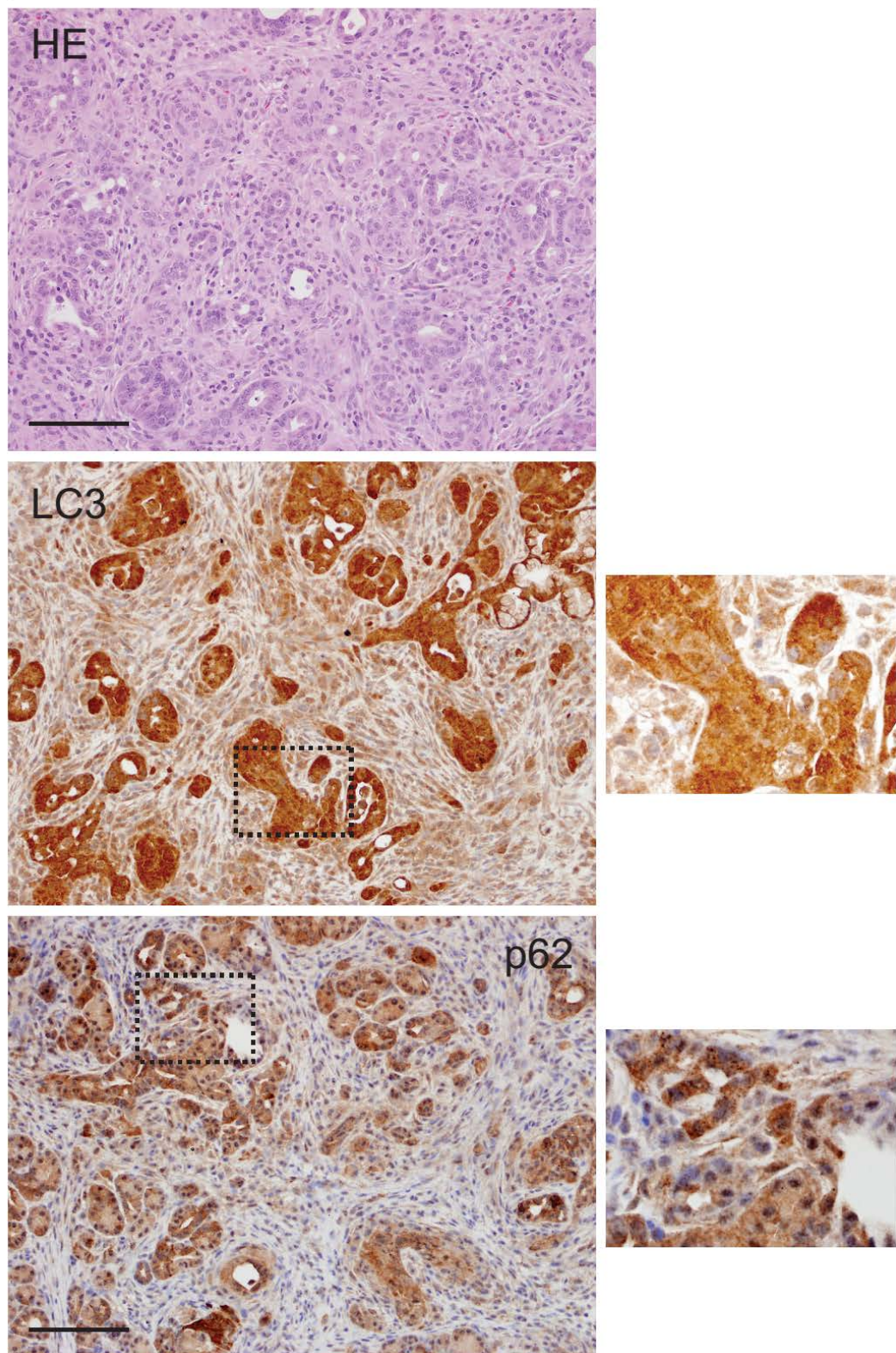


Figure 33: PDACs from Pdx1-Cre KRasG12D/wt p53^{-/-} Atg5^{-/-} mice are autophagy deficient. HE, LC3 and p62 staining of a tumour from a PDX-Cre KRasG12D/wt p53^{-/-} Atg5^{-/-} mouse confirms that the tumour is arising from autophagy deficient tissue as evidenced by strong, diffuse LC3-staining and p62-accumulation. For each staining a representative overview and a magnified cropped region to show LC3 and p62 staining specifics are identified by a dotted rectangle. Scale bars represent 100µm.

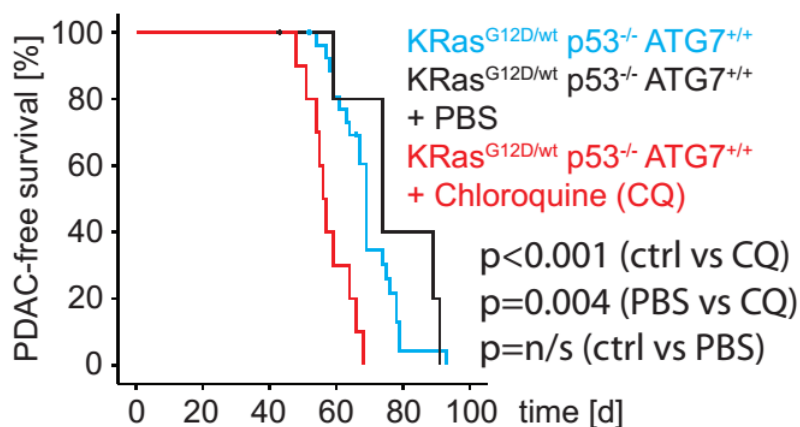
3.3.2 Pharmacological inhibition of autophagy in Pdx1-Cre KRasG12D/wt p53^{-/-} mice accelerates tumour development

Considering that bi-allelic deletion of either Atg5 or Atg7 in Pdx1-Cre KRasG12D/wt p53^{-/-} mice drastically accelerates tumour onset proves that it is indeed the lack of autophagy rather than an autophagy-independent effect of Atg7 or Atg5 that is responsible for the observed phenotypes. If genetic inhibition of autophagy accelerates tumour onset in certain scenarios this challenges the assumption that it is a beneficial option to impair autophagy in tumour therapy at least under certain conditions. We wanted to verify the genetic data and see if we could reproduce the findings in Pdx1-Cre KRasG12D/wt p53^{-/-} animals with pharmacological inhibition of autophagy by means of chloroquine (CQ) injection (Figure 34). CQ is a drug that is historically used to prevent malaria but has sparked the interest of cancer researchers in recent years because it has shown tumour suppressive properties in certain settings, that have been at least partially attributed to its inhibitory effect on autophagy [93], [2]. CQ inhibits lysosomal function by increasing the pH within lysosomes and as a result autolysosomal content is not degraded, i. e. autophagy is blocked. It is important to mention that it is increasingly challenged if the cell death promoting effects of CQ are the results of autophagy inhibition or are the consequence of alternative functions of the drug [138]. Nonetheless, it still remains the only clinically, readily available drug to inhibit autophagy *in vivo*.

Pdx1-Cre KRasG12D/wt p53^{-/-} mice were treated from 28d of age with CQ or vehicle control (PBS) until mice had to be culled because of tumour burden. CQ was administered daily by intraperitoneal injection at a dose of 30mg/kg body weight until mice developed signs of pancreatic cancer (abdominal distension, inappetence, hunched appearance). In line with the genetic data, pharmacological inhibition of autophagy reduced the survival time (Figure 34). Importantly, all mice in the treatment and control group succumbed to PDAC. Representative histological, H&E stained sections are provided in Figure 35.

To assess if pharmacological inhibition, like genetic deletion, of autophagy increases PanIN burden we treated Pdx1-Cre KRasG12D/wt mice from 60d – 90d of age with chloroquine. At the end of the experiment we did not detect any histological differences between the two groups (Figure 36) and PanIN numbers were equal in both cohorts (Figure 36). CQ treatment did not impact on pancreatic function as assessed by biochemical analysis (Figure 36). When combining the genetic and pharmacological data it is unlikely

that an increased PanIN burden is the cause of the accelerated tumour onset in the autophagy deficient situation.



	n (ev/total)	m/f (ev/total)	median
ctrl	24 (27)	12 (14) / 12 (13)	69 +/- 1
PBS	5 (6)	3 (3) / 2 (3)	74 +/- 8
CQ	10 (10)	3 (3) / 7 (7)	56 +/- 2

Figure 34: Chloroquine (CQ) treatment accelerates tumour onset in Pdx1-Cre KRasG12D/wt p53^{-/-} mice.

Shown is a Kaplan-Meier analysis comparing PDAC-free survival KRasG12D/wt p53^{-/-} mice that are treated with chloroquine (CQ, red) or vehicle (PBS, black). Untreated mice of the same genotype are in blue. Median survival +/- SDEV, number of mice and male/female (m/f) ratio are provided in the tables. The number of mice succumbing to PDAC is specified (ev), followed by the total number (all) of mice of the same genotype. A log-rank test (Mantel-Cox) was used for statistical analysis.

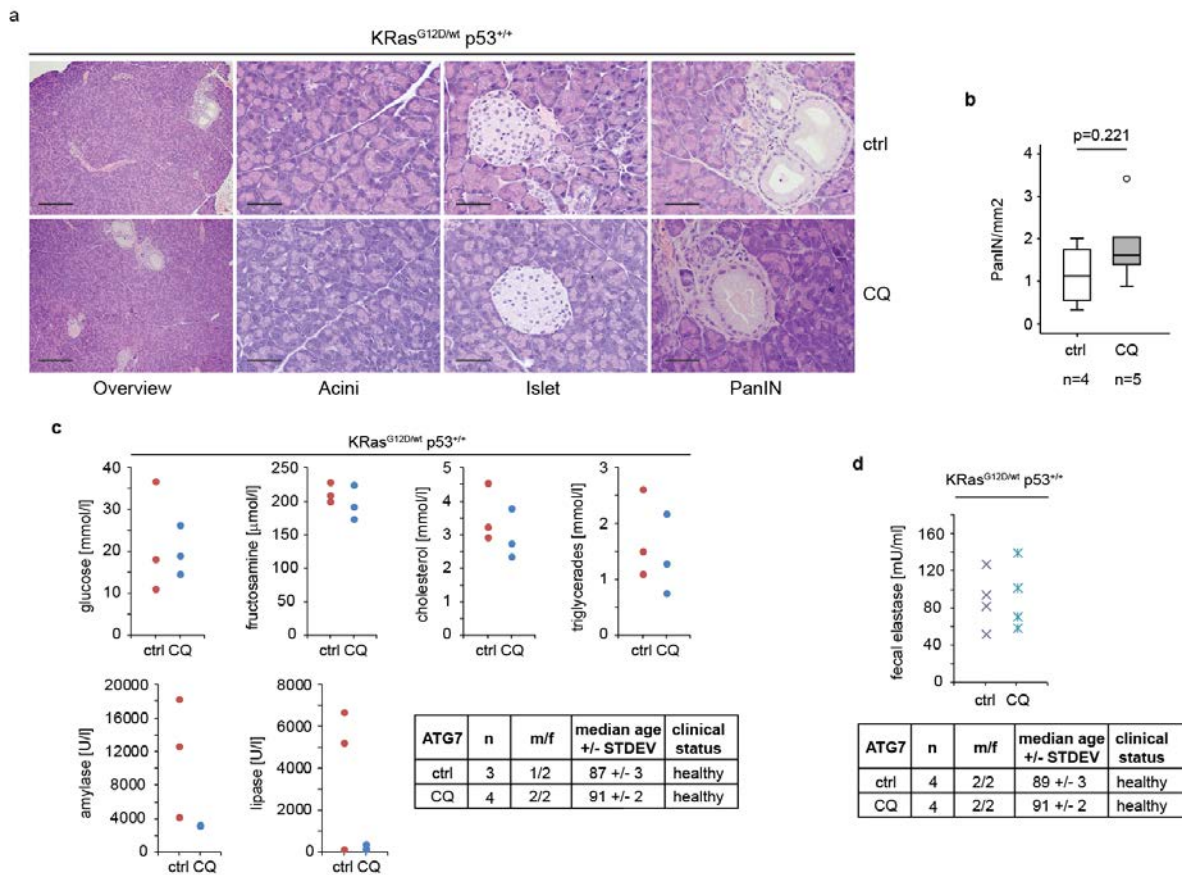


Figure 36: Chloroquine treatment does not affect pancreatic morphology and function in Pdx1-Cre KRasG12D/wt p53+/+ mice.

A) Representative HE images of pancreata from Pdx1-Cre KRasG12D/wt treated with vehicle control (PBS) or chloroquine from 51-59d of age for 36d. For each group an overview panel and a representative higher magnification panel of exocrine pancreatic tissue (acini), endocrine tissue (islets) and a PanIN is provided. Scale bars represent 200µm (dotted) and 50µm (solid). There are no histological differences between both groups evident. **B)** PanIN quantification. CQ-treatment does not alter the number of PanINs. **C)** Assessment of endocrine (glucose, fructosamine) and exocrine blood serum parameters does not show a difference between both genotypes. **D)** Likewise fecal elastase activity is not different between both groups. Information about the cohorts is provided in the tables.

3.3.3 Conclusion: Autophagy deletion in the pancreas expressing oncogenic KRas

In the previous chapters I have presented data to indicate that the role of autophagy in pancreatic cancer development is intrinsically linked to the p53 status.

In pancreata expressing mutant KRasG12D and two copies of wild-type p53 genetic impairment of either one of the essential autophagy genes Atg7 or Atg5 blocks the PanIN to PDAC progression; albeit autophagy inhibition leads to a temporary, drastic overload with premalignant lesions. Autophagy deficient PanINs readily execute the senescence response with p53 accumulation, p21 induction and enhanced activity of Sa- β -Gal. Unlike their autophagy competent counterparts they activate a cell death program as shown by activation of caspase-3. Like autophagy-incompetent mice expressing two copies wild-type KRas (Pdx1-Cre Atg7^{-/-} or Pdx1-Ctr Atg5^{-/-}), animals that harbour a single allele of oncogenic KRas and lack autophagy in the pancreas (Pdx1-Cre KRasG12D/wt Atg7^{-/-}) succumb to death early from endocrine pancreatic dysfunction.

This situation changes drastically when autophagy was genetically inactivated or pharmacologically impaired in mice expressing oncogenic KRas and lacking both alleles of p53 in pancreatic cells (Pdx1-Cre KRasG12D/wt p53^{-/-} Atg7^{-/-} or Pdx1-Cre KRasG12D/wt p53^{-/-} Atg5^{-/-}). The absence of p53 permits tumour formation in virtually all pancreata that were rendered genetically or pharmacologically autophagy-deficient and also significantly accelerated tumour onset. Importantly we have shown that all tumours from Pdx1-Cre KRasG12D/wt p53^{-/-} Atg7^{-/-} (or Atg5^{-/-}) animals arise from autophagy-deleted tissue. Pancreatic function was not different between autophagy-competent vs autophagy-deficient cohorts, effectively ruling out pancreatic insufficiency as the cause of the early lethality.

In summary loss of p53 switches autophagy from being a tumour promoter (p53^{+/+}) to being a tumour suppressor (p53^{-/-}).

3.4 Characterization of ATG7 proficient and deficient pancreatic tumours

We were keen to understand how and why the p53 status dictates the role of autophagy in pancreatic cancer development. As detailed before p53 can regulate autophagy and important metabolic processes [123] and we therefore focused our analysis thereon.

3.4.1 Loss of p53 reduces autophagy in pancreatic tumours

To see how the p53 status impacts on autophagy in pancreatic cancer *in vivo* we stained sections from tumours that arose in Pdx1-Cre KRasG12D/wt p53^{+/+} and Pdx1-Cre KRasG12D/wt p53^{-/-} animals and stained with an antibody against LC3 (Figure 37).

Tumours from p53-proficient animals harboured more LC3-puncta compared to tumour tissue from p53-deficient mice, raising the possibility that tumours from p53-proficient animals have increased autophagy compared to p53^{-/-} tumours (Figure 37). Of course enhanced LC3 punctation is only a reflection of increased autophagosome accumulation and does not prove increased autophagic flux, i. e. the complete degradation of autophagosomal content and not just the entrapment of cytoplasmic material within autophagosomes [144]. We therefore needed to devise a way that allowed functional analysis of tumour cells. To this extent several different tumour cell lines were generated from individual tumours of the genotypes indicated in Figure 38. Mirroring the *in vivo* results, tumour cell lines that were generated from p53-proficient PDACs had more LC3-puncta (Figure 38a) and increased levels of the autophagosome bound LC3-II compared to p53-deficient cell lines (Figure 38b). We were also able to generate cell lines from Atg7-deficient tumours (Pdx1-Cre KRasG12D/wt p53^{-/-} Atg7^{-/-}) and propagate them under the same conditions as autophagy competent cell lines (Figure 38b). To finally prove that p53-null cells have indeed reduced autophagic flux we employed the lysosomal protease inhibitors leupeptin and NH₄Cl (Figure 38c). If autophagy proceeds to lysosomal degradation (and therefore “fluxes”) then LC3-II levels are increased after treatment with the aforementioned inhibitors. If autophagy is blocked before the formation of autolysosomes then inhibitor treatment does not affect LC3-II levels [144]. Treatment of cell lines from both groups (p53-proficient, p53⁺ vs p53-deficient, p53⁻) showed that LC3-II levels increase after treatment, regardless of genotype (Figure 38c). This indicates that cell lines of both genotypes execute full autophagy (they “flux”). However, the average

increase of LC3-II (quantified relative to p38) is approx. 2-fold higher in the p53-proficient than in the p53-deficient group. This means that in the same time approx. twice as much autophagosomes are turned over in p53^{+/+} cells than in p53^{-/-} cells (Figure 38c). Therefore autophagic flux is increased in tumour cell lines generated from a p53-proficient background. In combination with the notion that in Pdx1-Cre KRasG12D/wt p53^{-/-} mice, autophagy-deficient tumours develop these results suggest that p53-deletion reduces the requirement for autophagy below a certain threshold at which it is dispensable for cellular survival.

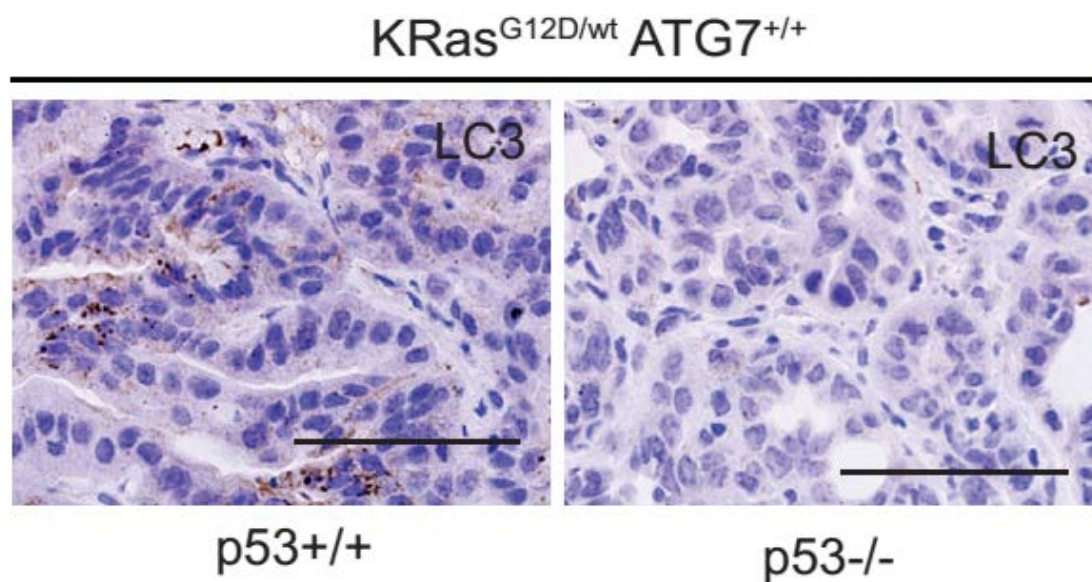


Figure 37: Increased LC3-puncta accumulation in PDACs from Pdx1-Cre KRasG12D/wt p53^{+/+} compared to Pdx1-Cre KRasG12D/wt p53^{-/-} mice.

Tumours from Pdx1-Cre KRasG12D/wt p53^{-/-} Atg7wt/wt exhibit fewer autophagosomes than tumours from Pdx1-Cre KRasG12D/wt p53^{+/+} Atg7wt/wt mice. Representative IHC images showing punctate staining of LC3 are shown.

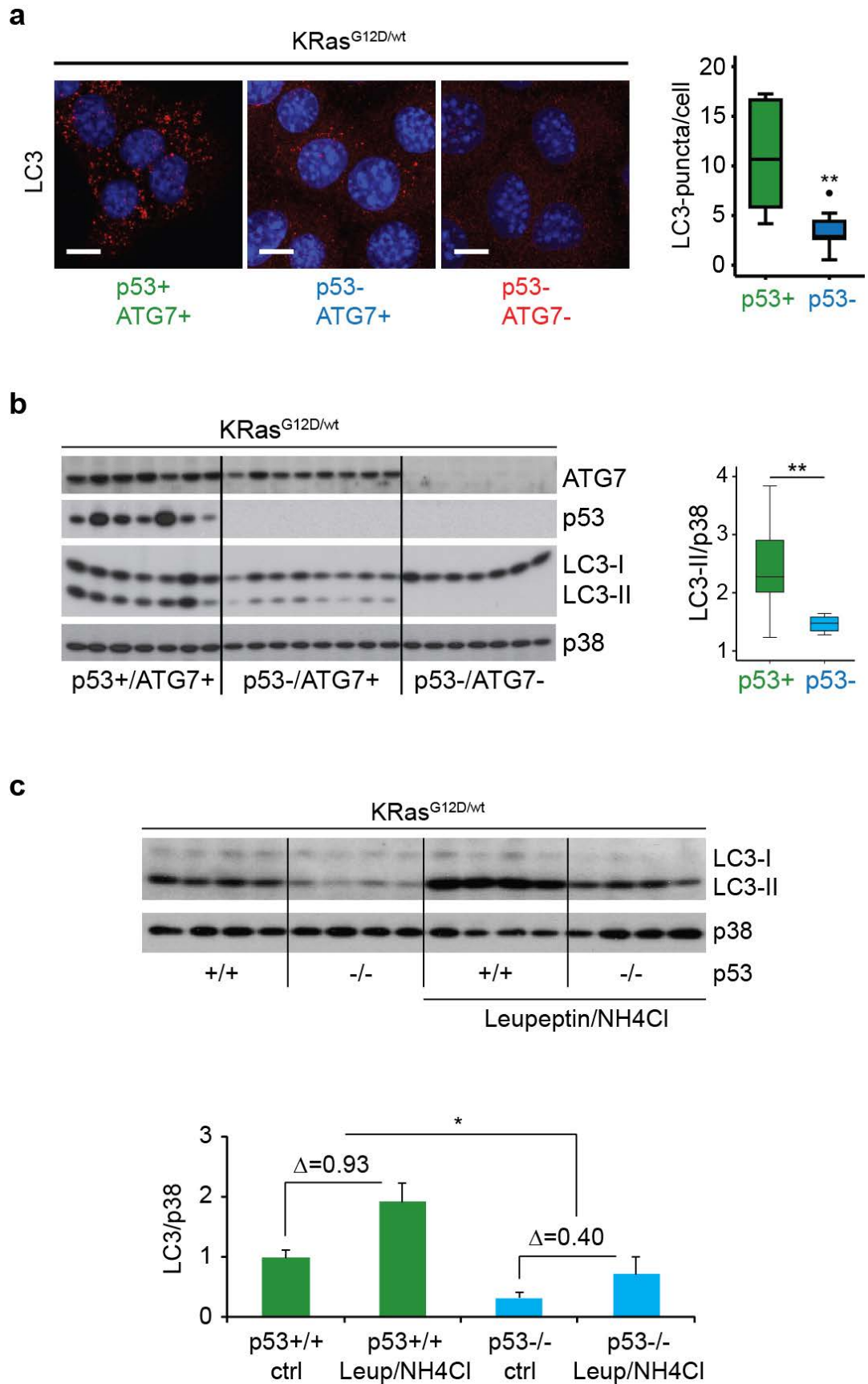


Figure 38: Autophagic flux is increased in cell lines generated from PDACs that developed in Pdx1-Cre KRas^{G12D/wt} p53^{+/+} vs Pdx1-Cre KRas^{G12D/wt} p53^{-/-} mice.

Maximum projection of 15 confocal slices from representative images of cell lines derived from PDX KRas^{G12D/wt} ATG7^{+/+} tumours that either developed from a p53-positive (p53⁺ & ATG7⁺) or p53-negative background (p53⁻ & ATG7⁺). ATG7-negative tumour

cells (p53- & ATG7-) do not show any punctate staining and serve as a negative control. LC3-puncta are shown as red puncta and DAPI was used as nuclear counterstain. Statistics were done with a non-parametric Mann-Whitney test counting the puncta of no less than 50 randomly chosen cells of each cell line (n=8 for p53-/- cell lines, n=7 for p53+/+ cell lines). For statistical analysis a Mann-Whitney U test was used. “**”=p<0.01. Scale bars represent 10µm. Cell lines from tumours which developed in the absence of p53 show lower levels of LC3-II compared to those that developed in p53-proficient tissue. Each lane represents a cell line derived from an individual tumour of the indicated genotypes. Quantification of LC3-II levels is provided as bar graph. c, Western blot and densitometry analysis shows greater LC3-II accumulation in p53-proficient than in p53-deficient cell lines after treatment with lysosomal protease inhibitors Leupeptin/NH4Cl indicating greater autophagic flux in the former. A quantification of the increase in LC3-II (densitometry LC3-II/p38, average + SEM) is provided. Statistical analysis was done with a t-test. “*” = p<0.05.

3.4.2 Atg7 deficiency increases glycolysis and anabolism in p53/- tumours *in vitro*

Autophagy fulfils critical functions in cellular homeostasis, energy production and provision of biosynthetic precursors of which there is a high demand in rapidly growing cancer cells [61], [48]. We hypothesized that if autophagy is lost then the tumour cells must have acquired alternative means to sustain their rapid growth. One such compensatory mechanism could be the promotion and modification of glucose utilization, both of which have been shown to be regulated by the p53 status (see 1.4.1).

The Seahorse Bioscience XF24 Extracellular Flux Analyzer allows real-time and simultaneous measurement of two key determinant of energy metabolism in a microplate: a) ExtraCellular Acidification Rate (ECAR) as a likely readout of glycolysis and b) Oxygen Consumption Rate (OCR) as readout of mitochondrial respiration and oxidative phosphorylation (OXPHOS).

We assessed a number of early passage Pdx1-Cre KRasG12D/wt p53/- cell lines that were either autophagy-proficient (Atg7+/+, n=8) or autophagy-deficient (Atg7-/-, n=7) for OCR and ECAR (Figure 39a). We did not observe a statistically significant difference in OCR between cell lines of both genotypes (Figure 39a). In contrast ECAR was significantly elevated in autophagy deficient cell lines (Pdx1-Cre KRasG12D/wt p53/- Atg7-/-) compared to autophagy proficient controls (Pdx1-Cre KRasG12D/wt p53/- Atg7+/+) (Figure 39b). ECAR only measures the extracellular acidification rate but it does not clarify what is the source of the pH drop. This can arise through: a) increased lactate production and secretion or b) other causes such as extracellular accumulation of ketone bodies. To complicate matters further lactate is primarily derived from fermentation of glucose but in certain scenarios can also be generated from glutamine [22]. 2-Deoxy-D-Glucose (2-DG) competitively inhibits glycolysis by competing with glucose for membrane-bound glucose transporters and by inhibition of the first rate-limiting enzyme of glycolysis, hexokinase II [25], [188]. We monitored ECAR in real-time after addition of 2-DG and observed a nearly complete obliteration of the ECAR difference between autophagy proficient (Pdx1-Cre KRasG12D/wt p53/- Atg7+/+) and autophagy deficient cell lines (Pdx1-Cre KRasG12D/wt p53/- Atg7-/-) (Figure 39c). This dealt with the two aforementioned caveats of ECAR measurement. Our results implied that the increased ECAR in autophagy deficient cells was at least mostly due to enhanced lactate production and glucose seemingly was the main source of lactate.

Using a liquid chromatography mass spectrometry (LC-MS) to measure exometabolites (extracellular metabolites) and endometabolites (intracellular metabolic intermediates) we substantiated our characterization of glucose utilization in autophagy competent and incompetent cells. Gillian McKay (Beatson Institute for Cancer Research) analysed the samples and processed the data to a format compatible with Microsoft Excel. Analysis of exometabolites revealed that autophagy defective cells (Pdx1-Cre KRasG12D/wt p53^{-/-} Atg7^{-/-}) were marked by a higher glucose consumption as well as an increased lactate secretion compared to their autophagy proficient controls (Pdx1-Cre KRasG12D/wt p53^{-/-} Atg7^{+/+}) (Figure 40). Furthermore we found significantly elevated levels of glucose, intracellular intermediates of glycolysis (glucose-6-phosphate, pyruvate) and intracellular intermediates of the anabolic pentose phosphate pathway (ribose-phosphate, seduheptulose-7-phosphate) in autophagy deficient cells (Figure 40).

The TCA cycle (compare 1.2.2) is an indispensable metabolic node that generates redox carriers and intermediates that fuel a variety of anabolic processes. Our aforementioned analysis of endometabolites included intermediates of the TCA cycle. These were not significantly different between Pdx1-Cre KRasG12D/wt p53^{-/-} Atg7^{+/+} and Pdx1-Cre KRasG12D/wt p53^{-/-} Atg7^{-/-} cells and therefore in our system the TCA cycle is seemingly not compromised in autophagy deficient cells (Figure 41).

Taken together we have shown that autophagy deletion in p53-null tumour cells leads to increased glucose uptake that is in part used to fuel the anabolic pentose phosphate pathway. Importantly autophagy-deficient PDAC cells are able to maintain the TCA cycle and therefore to feed anabolic pathways.

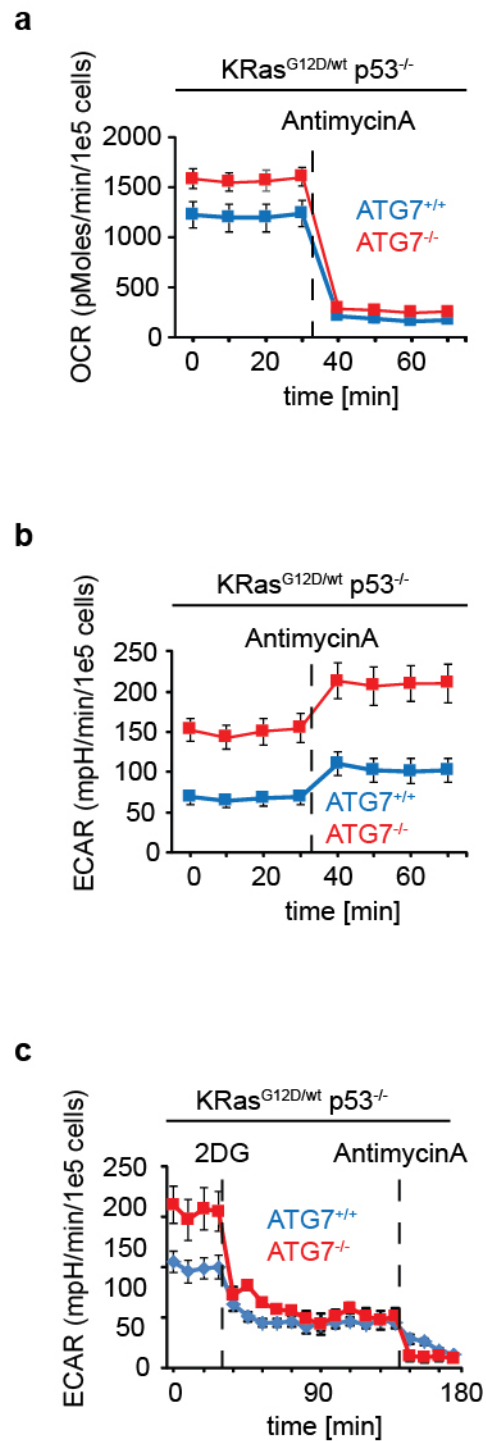


Figure 39: Metabolic profiling of Pdx1-Cre *KRas*^{G12D/wt} *p53*^{-/-} *Atg7*^{+/+} and Pdx1-Cre *KRas*^{G12D/wt} *p53*^{-/-} *Atg7*^{-/-} tumour cells.

Average Oxygen Consumption Rate (OCR, a) and ExtraCellular Acidification Rate (ECAR, b) of 8 *Atg7*^{+/+} (blue) vs 7 *Atg7*^{-/-} (red) cell lines shows increased ECAR in autophagy-deficient cells. C) Treatment with 2-DG (10mM) reduces ECAR and abrogates the difference between cell lines derived from *Atg7*^{+/+} and *Atg7*^{-/-} tumours. Antimycin A was added where indicated to block mitochondrial respiration.

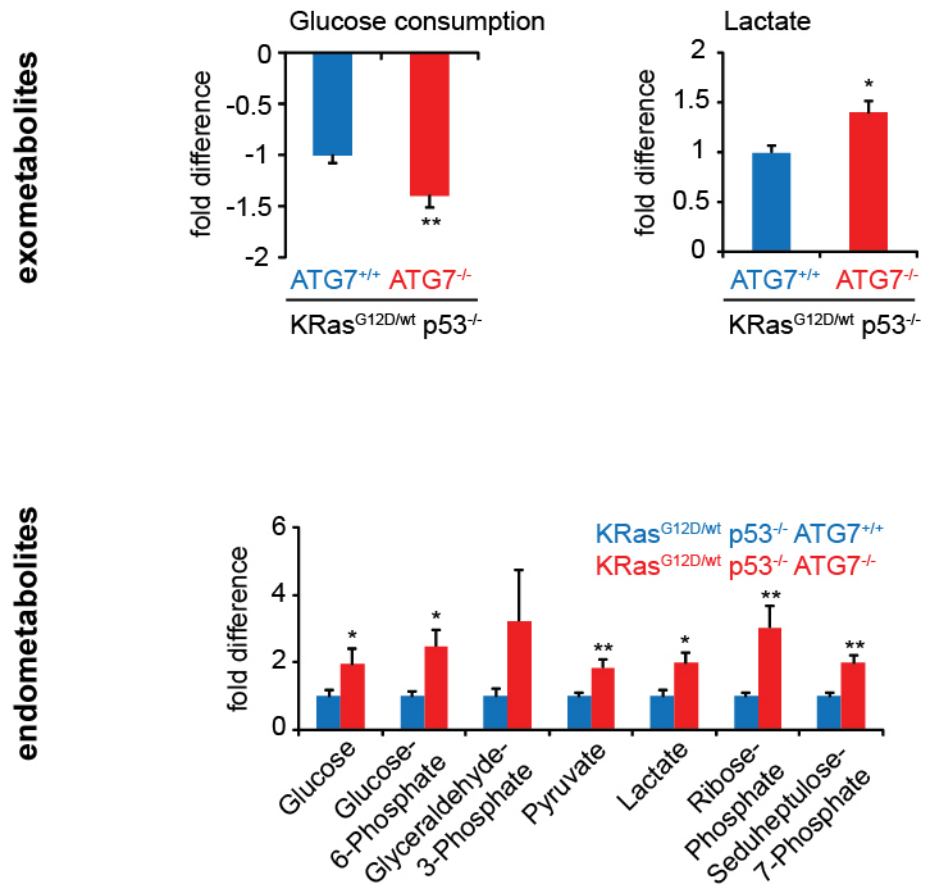


Figure 40: LCMS analysis of exometabolites and endometabolites in autophagy proficient and deficient tumour cells.

LC-MS analysis revealed increased glucose consumption from medium and extracellular lactate accumulation in Atg7^{-/-} cell lines (red) and compared to Atg7^{+/+} cell lines (blue). LC-MS of intracellular glycolytic and pentose phosphate pathway intermediates shows enhanced accumulation in Atg7^{-/-} tumour cell lines. A Mann-Whitney U test was used to ascertain significance. “**” = p<0.01, “*” = p < 0.05.

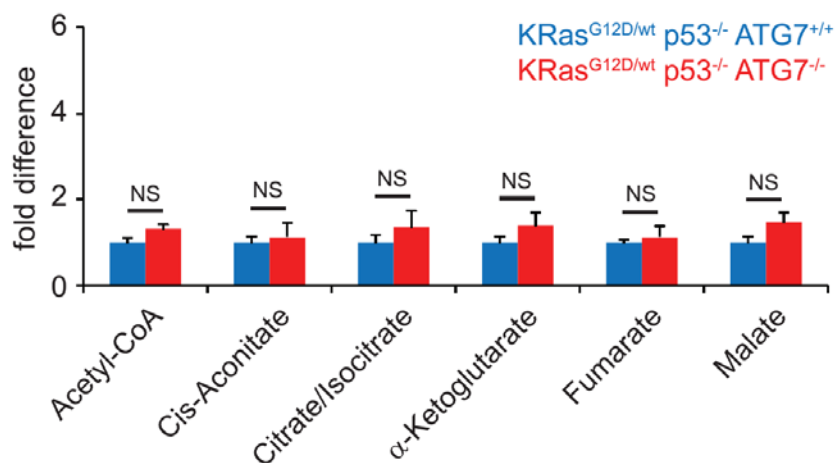


Figure 41: ATG7-deficiency does not reduce intracellular TCA-cycle intermediates or Acetyl-CoA levels.

Intracellular TCA-cycle metabolites were assessed by LC-MS and expressed as fold difference compared to $ATG7^{+/+}$ tumour cell lines ($Pdx1-Cre$ $KRas^{G12D/wt}$ $p53^{-/-}$). Values represent the average of no less than 5 biological replicates measured in triplicates for each genotype. Error bars are SEM. Differences are not significant ("NS", Mann Whitney U test).

3.4.3 Atg7 deficient tumours have increased glucose uptake compared to Atg7 proficient tumours *in vivo*

Cells cultured *in vitro* switch their metabolism towards glycolysis and therefore it is often difficult to transfer results obtained from cell lines to the *in vivo* situation [79]. Positron emission tomography (PET) with the glucose analogue 2-[fluorine-18] fluoro-2-deoxy-D-glucose (18F-FDG) as positron emitting tracer in combination with computed tomography (CT) allows the detection of tumours and quantification of regional glucose uptake. Inside the cell 18F-FDG is phosphorylated to 18F-FDG-6-phosphate and then cannot be metabolized further or exit the cell. Hence the activity of 18F-FDG is a good indicator of localized glucose uptake. Merging the information from 18F-FDG PET scans with CT images enables the accurate localization of regional glucose uptake within its anatomical context [89], [35].

On occasion CT imaging is improved by using contrast agents to heighten the contrast mainly of soft tissue. Fenestra LC (ART Advanced Research Technologies Inc., Canada) is commonly used for demarcation of the liver in CT scans [199]. Fenestra agents contain contrast-enhancing iodinated lipids in combination with special substances that cause these lipids to accumulate in the hepatobiliary system and thereby to enhance liver discrimination (<http://www.art.ca/en/imaging-agents/technology.php/>). Fenestra does not interfere with glucose uptake.

We subjected tumour bearing Pdx1-Cre KRasG12D/wt p53^{-/-}-Atg7^{+/+} and Pdx1-Cre KRasG12D/wt p53^{-/-} Atg7^{-/-} mice to 18F-FDG PET/CT imaging to study the glucose uptake *in vivo* (Figure 42). Images were taken, quantified and exported to a format compatible with AMIDE imaging software (<http://amide.sourceforge.net/>) by Agata Mrowinska (Beatson Institute for Cancer Research, Glasgow). In line with physiological high glucose uptake in the brain, enhanced tracer accumulation in the heart and bladder signal intensity was high in these organs. Liver demarcation was well defined and the 18F-FDG PET signal was homogeneously low in mice of both genotypes. Importantly we were able to detect and quantify locally enriched 18F-FDG uptake in pancreatic tumours (marked by the cross in Figure 42). All three Atg7^{-/-} animals had a higher SUV_{max} (maximum standardized uptake value) compared to Atg7^{+/+} animals (Figure 42) confirming that autophagy deficient tumours have increased glucose uptake *in vivo*. Importantly by using SUV_{max} (i. e. the highest signal intensity in the region of interest),

our quantification of ^{18}F -FDG uptake is independent of tumour size and animal weight. In other words it is excluded that a higher value is merely the reflection of a larger tumour.

We were also able to reproduce the *in vivo* findings with ^{18}F -FDG PET *in vitro* with 2-DG. After 6h treatment with 2-DG we harvested Pdx1-Cre KRasG12D/wt p53^{-/-} Atg7^{+/+} and Pdx1-Cre KRasG12D/wt p53^{-/-} Atg7^{-/-} cell lines and measured intracellular accumulation of 2-DG and its metabolite 2-DG 6-phosphate (2-DG-6P) by liquid chromatography mass spectrometry (Gillian McKay). As expected, 2-DG and 2-DG-6P accumulated more in autophagy deficient than in autophagy competent cells (Figure 43).

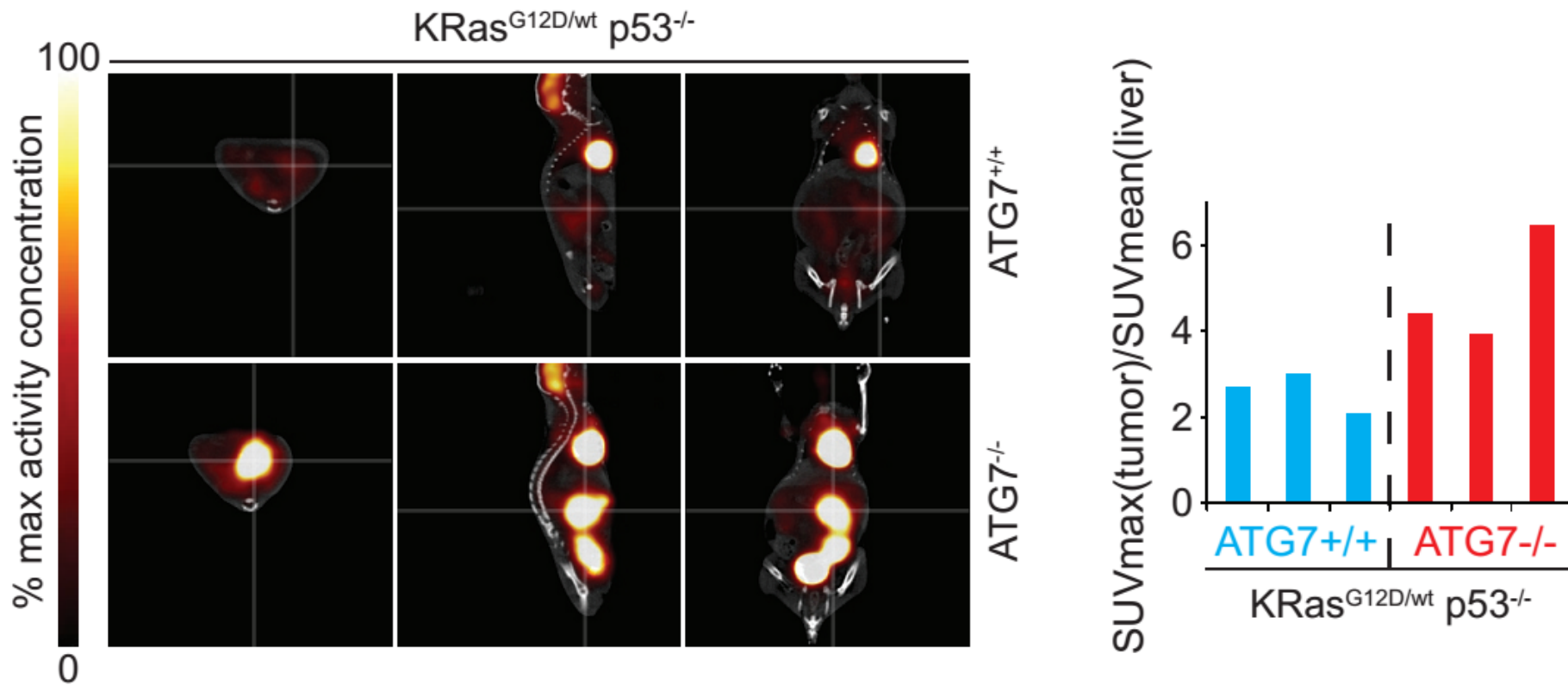


Figure 42: 18F-FDG PET/CT imaging of autophagy proficient and autophagy deficient tumour in vivo.

Irrespective of genotype, local and physiological enrichment 18F-FDG uptake can be seen in the brain, heart and bladder (due to the section only in the Atg7^{-/-} mouse) in the sagittal and coronal views (middle and right panels, respectively). This is due to enrichment of 18F-FDG in the blood, the high glucose uptake in the brain, and the 18F-FDG excretion into the urin. 18F-FDG uptake is seen in pancreatic tumours (marked by the intersection of the translucent lines in each panel). The signal is much higher in Atg7^{-/-} animals compared to Atg7^{+/+} mice. Quantification of 18F-FDG uptake in 3 ATG7 wild-type and 3 Atg7-deficient mice, expressed as a ratio the ratio of the maxim SUV within the tumour to the mean SUV within a reference tissue (liver) is shown on the right.

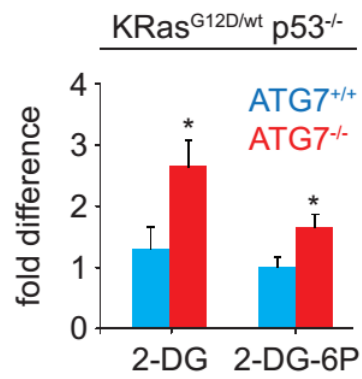


Figure 43: 2-DG uptake and phosphorylation in Atg7^{-/-} and Atg7^{+/+} tumour cell lines. LC-MS analysis show increased accumulation of 2-DG and its metabolite 2-DG-6-Phosphate in Atg7-proficient (blue) and Atg7-deficient (red) cell lines.

3.4.4 Conclusion: Role of autophagy in p53-deficient tumours

We have shown *in vitro* and *in vivo* that tumours arising from p53-deficient tissue have decreased autophagy when compared to PDACs that developed in mice that had two copies of wild-type p53. This lead as to believe that in the absence of p53, the requirement for autophagy to sustain cellular survival is lowered beneath a certain threshold at which it was completely dispensible. At the beginning of this chapter (3.4) we postulated that autophagy deficient tumour cells have adopted mechanisms that compensate for the loss of autophagy and that a modified glucose metabolism might be part of it. Indeed we found *in vitro* and *in vivo* that in autophagy defective tumours glucose uptake is increased relative to autophagy competent tumours. Using a mass spectrometry approach we furthermore saw an enhanced accumulation of metabolic intermediates of the anabolic pentose phosphate pathway in cell lines generated from Pdx1-Cre KRasG12D/wt p53^{-/-} Atg7^{-/-} PDACs compared to their Atg7^{+/+} counterparts. Importantly neither OXPHOS nor the TCA cycle were impaired in cell lines derived from Pdx1-Cre KRasG12D/wt p53^{-/-} Atg7^{-/-} cell lines compared to Pdx1-Cre KRasG12D/wt p53^{-/-} Atg7^{+/+} cells. In summary autophagy-deficient tumour cells have increased glucose uptake and use it to fuel both glycolytic and anabolic pathways, which considering their function can theoretically replace some core traits of autophagy.

4 Discussion

In my thesis I addressed the question how deletion of autophagy impacts on pancreatic cancer development *in vivo*. This is important because autophagy is increasingly being targeted in cancer treatment but that rationale is based on relatively little scientific *in vivo* data.

By breeding mice that express a Cre recombinase under the control of the pancreatic transcription factor Pdx1 to different mouse strains that contain an inducible allele of oncogenic KRas (LSL-KRasG12D), floxed alleles of p53 (p53flox/flox), or floxed alleles of either Atg7 or Atg5 (Atg7flox/flox, Atg5flox/flox), we were able to generate different mouse cohorts to genetically dissect the role of autophagy in pancreatic cancer.

We first confined our analysis to mice that express two copies of wild-type KRas. Here, genetic deletion of autophagy in the pancreas caused cell death with morphological features of necrosis in the endocrine and exocrine compartment. Autophagy-deficient regions are marked by an inflammatory infiltrate completing the histological diagnosis of chronic pancreatitis. Mareninova and colleagues reported that in pancreatitis autophagy is impaired. As a consequence of deregulated lysosomal hydrolases (cathepsins B and L) the fusion of autophagosomes with lysosomes is retarded. This results in an imbalance between trypsin and its inactive form trypsinogen in acinar cells and causes acinar vacuolation and necrotic cell death [129], [52]. Autophagosome accumulation after chemical induction of pancreatitis with the cholecystokinin analogue cerulein was also reported by Hashimoto and colleagues [63]. In the same study, mice that expressed a Cre recombinase under the control of the rat elastase I promoter/enhancer (EL-Cre2) were crossed to Atg5flox/flox mice [62] (compare 2.2.4) to obtain animals that are autophagy-deficient (mosaic) in acinar tissue. Notably EL-Cre2 is not expressed in islet cells. Chemically induced pancreatitis was markedly reduced in EL-Cre2 Atg5^{-/-} pancreata compared to wild-type controls. Interestingly, when monitored for up to two month EL-Cre2 Atg5^{-/-} animals did not show signs of acinar destruction ([63]). In summary the studies by Mareninova and Hashimoto imply that impaired autophagic flux is at least partially responsible for the pathological events in pancreatitis and that inhibition of the early steps of autophagy alleviates the severity of chemically induced pancreatitis [129], [63]. At first sight this is difficult to reconcile with the findings of my study in which genetic deletion of autophagy invariably leads to pancreatitis with acinar vacuolation and inflammatory infiltration. It is possible that Hashimoto and colleagues did not see

pancreatic destruction in EL-Cre2 Atg5^{-/-} mice because animals have been monitored for a comparatively short time (2 month) and complete deletion of autophagy has not 100% been ascertained. It can also not be ruled out that the differences are caused by diverse effects of the Pdx1-promoter and the rat elastase I promoter/enhancer. It is also conceivable that chemically induced pancreatitis has a different, underlying pathophysiology compared to pancreatitis after prolonged, genetic inhibition of autophagy. In this regard it is worth mentioning that genetic ablation of autophagy in the lung causes inflammation (pneumonia) that is certainly caused by a different mechanism than the proposed trypsin/trypsinogen imbalance in pancreatitis because trypsin is not expressed in the lung [55].

Apparently restricted to acinar cells, an additional p53 dependent cell death program contributed to pancreatic damage in Pdx1-Cre Atg7^{-/-} mice. Added genetic deletion of p53 delayed, but did not rescue the demise of the animal. Loss of p53 seemingly had no impact on the destruction of Atg7-negative islet cells. This was not surprising when taking into account that in our model system a) dying endocrine cells never accumulated p53 and b) the morphological extent of islet destruction appeared similar during all time points in Pdx1-Cre Atg7^{-/-} mice regardless of p53 status. It has been suggested that the severity of pancreatitis is reflected in the cell death mechanism that is activated in acinar cells. Mild forms of acute pancreatitis are associated predominantly with apoptotic cell death that is marked by caspase activation, whereas necrosis primarily marks severe forms of the disease [10], [53]. Caspases are not merely executors of apoptosis in the context of pancreatitis but have also been shown to protect from a possibly more detrimental necrotic cell death [130]. This is consistent with my finding that Pdx1-Cre Atg7^{-/-} animals have an early activation peak of p53 and caspase-3 that later plateaus at a lower level. It is feasible that genetic loss of Atg7 causes damage to which cells initially respond with apoptosis induction. Since autophagy never recovers, acinar cell injury persists, is unresolved and cells switch to necrotic cell death. In line with my data, additional deletion of p53 in Pdx1-Cre Atg7^{-/-} mice (Pdx1-Cre p53^{-/-} Atg7^{-/-}) then would abrogate the initial apoptotic death component which could explain the delayed death in Pdx1-Cre p53^{-/-} Atg7^{-/-} animals compared to Pdx1-Cre p53^{+/+} Atg7^{-/-} mice.

Biochemical analysis of pancreatic function substantiated the claim that it is primarily the endocrine compartment that cannot withstand deletion of autophagy. We only found evidence of endocrine but never of exocrine insufficiency in moribund mice where autophagy had been deleted in the pancreas. Numerous studies have shown the importance of autophagy for β -cell function and survival [82], [40], [33], [133]. By interbreeding mice that express a Cre-recombinase under control of the rat insulin gene (Rip) [46] to Atg7^{flox/flox} mice [96] (compare 2.2.3) two groups independently generated mice with genetic deletion of autophagy in pancreatic β -cells [82], [33]. It was found that Rip-Cre Atg7^{-/-} mice develop diabetes and that autophagy-deficient islets have gross morphological alterations that resemble the changes described in my study. Interestingly neither of the two studies reported decreased survival of diabetic mice aged for at least 20 weeks [82], [33]. Possible explanations for the increased mortality of diabetic mice in my study could be that a) Rip-Cre does not recombine in all β -cells [46], or b) that the additional inflammatory component of the exocrine pancreas (pancreatitis) which is not present in Rip-Cre Atg7^{-/-} mice tips the balance in diabetic mice towards death, or c) mice have been culled when the animals could still cope with the consequences of impaired glucose metabolism.

In summary, genetic deletion of autophagy in the pancreas causes destruction of both, the endo- and exocrine compartment. Histological, survival and biochemical data identified the progressive destruction of the islets of Langerhans as the primary cause of increased mortality in mice with genetic deletion of autophagy in the pancreas. Early premalignant lesions (PanINs) or invasive cancer did not occur in mice aged > 500d.

We then questioned the role of autophagy in mice expressing one allele of oncogenic KRas^{G12D}. Pdx1-Cre KRas^{G12D}/wt mice develop multiple PanINs of which only a few in approx. 1/3 of mice finally progress to invasive carcinoma between 300-500d of age [67]. Our own mouse colony of the aforementioned genotype (Pdx1-Cre KRas^{G12D}/wt Atg7^{+/+}) essentially resembled previously published data. Strikingly, if in addition autophagy was deleted by removal of either Atg7 or Atg5 (Pdx1-Cre KRas^{G12D}/wt Atg7^{-/-} or Pdx1-Cre KRas^{G12D}/wt Atg5^{-/-}) PanINs accumulated drastically but never progressed to cancer during the lifespan of the mice. There are several possible explanations why PanINs accumulate in pancreata that express oncogenic KRas and have additional, genetic deletion of autophagy. A) Genetic deletion of autophagy leads to widespread pancreatic inflammation. Chronic pancreatitis has been shown to be required for PanIN formation and PanIN to PDAC progression in adult Pdx1-Cre KRas^{G12D}/wt

mice. Furthermore pharmacological induction of chronic pancreatitis exacerbates PanIN formation in pancreata expressing oncogenic Ras [51], [49]. B) Loss of autophagy delays the onset of senescence [192]. It is conceivable that a delayed proliferation arrest allows more time to form PanINs. My study has not clarified the reasons for the PanIN accumulation. A possible way to address this would be to treat Pdx1-Cre KRasG12D/wt Atg7^{-/-} or Pdx1-Cre KRasG12D/wt Atg5^{-/-} mice with anti-inflammatory drugs to alleviate pancreatitis. Thereby it would be possible to discern if the increased PanIN numbers are inherently a consequence of genetic deletion of autophagy or secondary due to inflammation. Whatever is the cause for the drastic PanIN accumulation, in autophagy-deficient pancreatic tissue, they all have in common an inability to progress to invasive cancer. It is currently unclear why autophagy-deficient PanINs that arise from a p53-proficient background cannot progress to PDAC. A contributing component may be that PanINs from Pdx1-Cre KRasG12D/wt Atg7^{-/-} and Pdx1-Cre KRasG12D/wt Atg5^{-/-} mice initiate a cell death program that involves the activation of caspase-3 and leads to their progressive decline whereas autophagy-proficient PanINs are less prone to death. Oncogenic KRas increases glucose uptake in pancreatic tumours and diverts glycolytic intermediates into the anabolic pentose phosphate pathway (PPP) [190]. Autophagy has been reported to be required to sustain the vital TCA-cycle [54], [189]. It is therefore tempting to speculate that autophagy-deficient PanINs do not progress, stay senescent and ultimately demise because of a compromised TCA cycle that cannot fuel anabolic pathways and therefore the increased need for biosynthetic precursors in cancer cells cannot be met.

We were interested to learn how autophagy impacts on tumour development in Pdx1-Cre KRasG12D/wt p53^{-/-} mice because loss of p53 has broad implications for cellular metabolism [123], [187] and permits the rapid progression from PDAC to invasive cancer possibly by abrogating the senescence barrier [145]. From a practical point of view we also wanted to generate mouse cohorts with and without autophagy that developed carcinoma before they died from pancreatic insufficiency.

We found that deletion of both copies of p53 created a permissive environment for KRasG12D driven pancreatic tumours to form in the absence of autophagy. Importantly this was the case if autophagy was either genetically deleted (Pdx1-Cre KRasG12D/wt p53^{-/-} Atg7^{-/-}, Pdx1-Cre KRasG12D/wt p53^{-/-} Atg5^{-/-}) or pharmacologically inhibited with chloroquine (CQ) in Pdx1-Cre KRasG12D/wt p53^{-/-} mice. In a p53-null background virtually all mice developed tumours when autophagy was inhibited. Tumour onset was

significantly earlier compared to autophagy proficient PDACs (Pdx1-Cre KRasG12D/wt p53^{-/-}). PDACs arising from p53^{+/+} pancreatic cells had increased levels of autophagy when compared to tumours developing from p53^{-/-} cells. When additionally considering, that only in the absence of p53 genetic deletion of autophagy invasive cancer can develop then it is conceivable that loss of p53 lowers the requirement of autophagy below a certain threshold at which it is completely dispensable. Consequently we hypothesized that if p53-null cells can progress to form tumours in the absence of autophagy, then they likely have acquired alternative means to fulfil important functions of autophagy. In line with this assumption, we found that autophagy deficient PDACs (Pdx1-Cre KRasG12D/wt p53^{-/-} Atg7^{-/-}) have increased glucose uptake *in vivo* and *in vitro*. Furthermore p53-null, autophagy-deficient pancreatic cancer cells (Pdx1-Cre KRasG12D/wt p53^{-/-} Atg7^{-/-}) compared to their autophagy-proficient counterparts (Pdx1-Cre KRasG12D/wt p53^{-/-} Atg7^{+/+}) have increased glycolysis and elevated levels of intermediates of the PPP *in vitro*. Importantly OXPHOS and the TCA-cycle are not significantly different between both groups.

As mentioned before, in pancreatic cancer oncogenic KRas increases glucose flux through the glycolytic pathway and the PPP [190]. Loss of p53 increases glycolysis through a variety of different mechanisms [123], [48]. It is plausible therefore that the absence of p53 facilitates increased uptake and diversion of glucose into the PPP and cells require autophagy less for the provision of biosynthetic precursors. This is in line with our finding that cell lines from p53-deficient tissue have reduced autophagy compared to cell lines from autophagy-proficient tissue. When in addition autophagy is absent (Pdx1-Cre KRasG12D/wt p53^{-/-} Atg7^{-/-}) glycolysis is increased and the PPP is fuelled compared to autophagy-competent cells (Pdx1-Cre KRasG12D/wt p53^{-/-} Atg7^{+/+}). Our data clearly shows that in the absence of p53 autophagy is not required for tumour formation or maintenance of cellular metabolism. The accelerated tumour onset is probably due to several factors. It has been shown that autophagy protects from DNA damage and maintains genomic stability [86], [134]. The converse argument that loss of autophagy increases DNA damage and facilitates genomic instability to promote tumour progression has consequently been established in the same studies [86], [134]. Therein lies a possible explanation for the early onset of tumours from p53-null tissue that lack autophagy compared to p53-null, autophagy-proficient tumours. Autophagy might no longer be required to maintain metabolism, but it still protects from genotoxic stress. In reverse it could mean that loss of autophagy can be metabolically compensated but increased genomic instability then promotes tumour development. Besides, increased glucose uptake

and provision for anabolic pathways as seen in the autophagy-deficient situation is also supportive for tumour growth [19], [123], [48]. Lactate itself is an energy-rich metabolite and it is an emerging concept that tumour cells themselves feed on lactate [12], [151]. It might be possible that autophagy-deficient cancer cells not only produce more lactate but also have increased usage of lactate to fuel growth. This clearly merits further investigation.

It is important to mention, that while we showed that pharmacological treatment with the autophagy inhibitor CQ, like genetic inhibition, accelerates tumour onset, this result has to be interpreted carefully. CQ undoubtedly inhibits autophagy but its cytotoxic effects can be independent of autophagy [138]. Furthermore in our study CQ was systemically administered by repeated intraperitoneal injections. As a consequence not only PanINs and cancer cells are exposed to the drug but also the tumour microenvironment and circulating blood cells. It cannot be ruled out with absolute certainty that the tumour promoting effects are therefore not the result of autophagy inhibition within precursor lesions or cancer cells but are rather the consequence of “side effects” of the drug. In this regard it is also worth mentioning that CQ-treatment of mice with pancreatic cancer has been reported to prolong survival [189]. In contrast to our study tumours developed from a p53-proficient background and treatment started when tumours were most likely already established. We initiated chloroquine treatment in p53-null mice at 28d of age. At this time the mice were virtually tumour free. It is also possible, that in the study by Yang and colleagues [189], the cell death promoting effects of chloroquine superseded the potential consequences of genomic destabilization after inhibition of autophagy.

It is unclear to what extent our results are transferable to other cancer entities, i. e. tumours from different tissues and tumours driven by other oncogenes. A recent study by Guo and colleagues found that autophagy suppresses the progression of lung cancer driven by oncogenic KRas, even in the absence of p53 [55]. Aside from the obviously different tumour origin there is another critical difference to our study. Lung cancer initiation by KRasG12D with all additional genetic manipulation was triggered by administration of adenoviral Cre-recombinase in adult mice i. e. the animals were essentially wild-type mice into adulthood [55]. In contrast, recombination in our cohorts occurred embryonically (E8.5) and it is conceivable that this caused a “reprogramming” of cells. In line with this assumption are reports that have shown that cancer development from oncogenic KRas is highly context dependent [50], [106], [49]. Especially it was shown that while young

pancreatic cells are susceptible to oncogenic transformation after activation of oncogenic KRas, older cells are remarkably resistant to oncogene stress [49].

A caveat of the currently available data, including the work I presented in my thesis, is the fact that autophagy was inhibited at a time when tumours were absent. It is clearly desirable to do similar studies and inhibit autophagy (genetically and pharmacologically) after the onset of PDAC and other cancer entities.

In summary our study has shown that the tumour suppressor p53 is a critical determinant for the role of autophagy in pancreatic cancer development. Loss of p53 converts autophagy from a tumour promoter to a tumour suppressor. This is the first study to report a molecular switch *in vivo* that explains the dichotomy of autophagy in cancer.

Appendices

Rightslink® by Copyright Clearance Center

https://s100.copyright.com/AppDispatchServlet



RightsLink®

[Home](#)
[Account Info](#)
[Help](#)


Title: The multiple roles of autophagy in cancer:

Logged in as:
Mathias Rosenfeldt

Author: Mathias T. Rosenfeldt, Kevin M. Ryan

[LOGOUT](#)

Publication: Carcinogenesis

Publisher: Oxford University Press

Date: 07/01/2011

Copyright © 2011, Oxford University Press

Order Completed

Thank you very much for your order.

This is a License Agreement between Mathias T Rosenfeldt ("You") and Oxford University Press ("Oxford University Press"). The license consists of your order details, the terms and conditions provided by Oxford University Press, and the [payment terms and conditions](#).

[Get the printable license.](#)

License Number	3214261417567
License date	Aug 22, 2013
Licensed content publisher	Oxford University Press
Licensed content publication	Carcinogenesis
Licensed content title	The multiple roles of autophagy in cancer:
Licensed content author	Mathias T. Rosenfeldt, Kevin M. Ryan
Licensed content date	07/01/2011
Volume number	32
Issue number	7
Type of Use	Thesis/Dissertation
Requestor type	Academic/Educational institute
Format	Print and electronic
Portion	Abstract
Will you be translating?	No
Author of this OUP article	Yes
Order reference number	
Title of your thesis / dissertation	Autophagy and Cancer (working title)
Expected completion date	Dec 2013
Estimated size(pages)	180
Publisher VAT ID	GB 125 5067 30
Total	0.00 USD

[ORDER MORE...](#)
[CLOSE WINDOW](#)

Copyright © 2013 [Copyright Clearance Center, Inc.](#) All Rights Reserved. [Privacy statement](#).
Comments? We would like to hear from you. E-mail us at customercare@copyright.com



RightsLink®

[Home](#)
[Account Info](#)
[Help](#)


Title: The multiple roles of autophagy in cancer:

Logged in as:
Mathias Rosenfeldt

Author: Mathias T. Rosenfeldt, Kevin M. Ryan

[LOGOUT](#)

Publication: Carcinogenesis

Publisher: Oxford University Press

Date: 07/01/2011

Copyright © 2011, Oxford University Press

Order Completed

Thank you very much for your order.

This is a License Agreement between Mathias T Rosenfeldt ("You") and Oxford University Press ("Oxford University Press"). The license consists of your order details, the terms and conditions provided by Oxford University Press, and the [payment terms and conditions](#).

[Get the printable license.](#)

License Number	3214261331974
License date	Aug 22, 2013
Licensed content publisher	Oxford University Press
Licensed content publication	Carcinogenesis
Licensed content title	The multiple roles of autophagy in cancer:
Licensed content author	Mathias T. Rosenfeldt, Kevin M. Ryan
Licensed content date	07/01/2011
Volume number	32
Issue number	7
Type of Use	Thesis/Dissertation
Requestor type	Academic/Educational institute
Format	Print and electronic
Portion	Text Extract
Number of pages requested	9
Will you be translating?	No
Author of this OUP article	Yes
Order reference number	
Title of your thesis / dissertation	Autophagy and Cancer (working title)
Expected completion date	Dec 2013
Estimated size(pages)	180
Publisher VAT ID	GB 125 5067 30
Total	0.00 USD

[ORDER MORE...](#)
[CLOSE WINDOW](#)

Copyright © 2013 Copyright Clearance Center, Inc. All Rights Reserved. [Privacy statement](#).
Comments? We would like to hear from you. E-mail us at customercare@copyright.com



RightsLink®

[Home](#)
[Account Info](#)
[Help](#)


Title: The multiple roles of autophagy in cancer:

Logged in as:
Mathias Rosenfeldt

Author: Mathias T. Rosenfeldt, Kevin M. Ryan

[LOGOUT](#)

Publication: Carcinogenesis

Publisher: Oxford University Press

Date: 07/01/2011

Copyright © 2011, Oxford University Press

Order Completed

Thank you very much for your order.

This is a License Agreement between Mathias T Rosenfeldt ("You") and Oxford University Press ("Oxford University Press"). The license consists of your order details, the terms and conditions provided by Oxford University Press, and the [payment terms and conditions](#).

[Get the printable license.](#)

License Number	3214261029980
License date	Aug 22, 2013
Licensed content publisher	Oxford University Press
Licensed content publication	Carcinogenesis
Licensed content title	The multiple roles of autophagy in cancer:
Licensed content author	Mathias T. Rosenfeldt, Kevin M. Ryan
Licensed content date	07/01/2011
Volume number	32
Issue number	7
Type of Use	Thesis/Dissertation
Requestor type	Academic/Educational institute
Format	Print and electronic
Portion	Figure/table
Number of figures/tables	4
Will you be translating?	No
Author of this OUP article	Yes
Order reference number	
Title of your thesis / dissertation	Autophagy and Cancer (working title)
Expected completion date	Dec 2013
Estimated size(pages)	180
Publisher VAT ID	GB 125 5067 30
Total	0.00 GBP

[ORDER MORE...](#)
[CLOSE WINDOW](#)

Copyright © 2013 [Copyright Clearance Center, Inc.](#) All Rights Reserved. [Privacy statement](#).
Comments? We would like to hear from you. E-mail us at customercare@copyright.com

Bibliography

- [1] Kehinde Adekola, Steven T. Rosen, and Mala Shanmugam. Glucose transporters in cancer metabolism. *Curr Opin Oncol*, Aug 2012.
- [2] Ravi K. Amaravadi, Jennifer Lippincott-Schwartz, Xiao-Ming Yin, William A. Weiss, Naoko Takebe, William Timmer, Robert S. DiPaola, Michael T. Lotze, and Eileen White. Principles and current strategies for targeting autophagy for cancer treatment. *Clin Cancer Res*, 17(4):654–666, Feb 2011.
- [3] Ravi K Amaravadi, Duonan Yu, Julian J Lum, Thi Bui, Maria A Christophorou, Gerard I Evan, Andrei Thomas-Tikhonenko, and Craig B Thompson. Autophagy inhibition enhances therapy-induced apoptosis in a myc-induced model of lymphoma. *J Clin Invest*, 117(2):326–336, Feb 2007.
- [4] Anja Apel, Hanswalter Zentgraf, Markus W Büchler, and Ingrid Herr. Autophagy—a double-edged sword in oncology. *Int J Cancer*, Apr 2009.
- [5] Elizabeth L Axe, Simon A Walker, Maria Manifava, Priya Chandra, H. Llewelyn Roderick, Anja Habermann, Gareth Griffiths, and Nicholas T Ktistakis. Autophagosome formation from membrane compartments enriched in phosphatidylinositol 3-phosphate and dynamically connected to the endoplasmic reticulum. *J Cell Biol*, 182(4):685–701, Aug 2008.
- [6] Nabeel Bardeesy and Ronald A. DePinho. Pancreatic cancer biology and genetics. *Nat Rev Cancer*, 2(12):897–909, Dec 2002.
- [7] Grégory Bellot, Raquel Garcia-Medina, Pierre Gounon, Johanna Chiche, Danièle Roux, Jacques Pouyssegur, and Nathalie M Mazure. Hypoxia-induced autophagy is mediated through hypoxia-inducible factor induction of bnip3 and bnip3l via their bh3 domains. *Mol Cell Biol*, 29(10):2570–2581, May 2009.
- [8] Karim Bensaad, Eric C. Cheung, and Karen H. Vousden. Modulation of intracellular ros levels by tigar controls autophagy. *EMBO J*, 28(19):3015–3026, Oct 2009.

- [9] Karim Bensaad, Atsushi Tsuruta, Mary A Selak, M. Nieves Calvo Vidal, Katsunori Nakano, Ramon Bartrons, Eyal Gottlieb, and Karen H Vousden. Tigar, a p53-inducible regulator of glycolysis and apoptosis. *Cell*, 126(1):107–120, Jul 2006.
- [10] M. Bhatia. Apoptosis of pancreatic acinar cells in acute pancreatitis: is it good or bad? *J Cell Mol Med*, 8(3):402–409, 2004.
- [11] Amanda Blackford, Giovanni Parmigiani, Thomas W. Kensler, Christopher Wolfgang, Siân Jones, Xiaosong Zhang, D Willams Parsons, Jimmy Cheng-Ho Lin, Rebecca J. Leary, James R. Eshleman, Michael Goggins, Elizabeth M. Jaffee, Christine A. Iacobuzio-Donahue, Anirban Maitra, Alison Klein, John L. Cameron, Kelly Olino, Richard Schulick, Jordan Winter, Bert Vogelstein, Victor E. Velculescu, Kenneth W. Kinzler, and Ralph H. Hruban. Genetic mutations associated with cigarette smoking in pancreatic cancer. *Cancer Res*, 69(8):3681–3688, Apr 2009.
- [12] Gloria Bonuccelli, Diana Whitaker-Menezes, Remedios Castello-Cros, Stephanos Pavlides, Richard G. Pestell, Alessandro Fatatis, Agnieszka K. Witkiewicz, Matthew G. Vander Heiden, Gemma Migneco, Barbara Chiavarina, Philippe G. Frank, Franco Capozza, Neal Flomenberg, Ubaldo E. Martinez-Outschoorn, Federica Sotgia, and Michael P. Lisanti. The reverse warburg effect: glycolysis inhibitors prevent the tumor promoting effects of caveolin-1 deficient cancer associated fibroblasts. *Cell Cycle*, 9(10):1960–1971, May 2010.
- [13] K. A. Brand and U. Hermfisse. Aerobic glycolysis by proliferating cells: a protective strategy against reactive oxygen species. *FASEB J*, 11(5):388–395, Apr 1997.
- [14] Andrei V Budanov and Michael Karin. p53 target genes sestrin1 and sestrin2 connect genotoxic stress and mtor signaling. *Cell*, 134(3):451–460, Aug 2008.
- [15] Ken Cadwell, John Y Liu, Sarah L Brown, Hiroyuki Miyoshi, Joy Loh, Jochen K Lennerz, Chieko Kishi, Wumesh Kc, Javier A Carrero, Steven Hunt, Christian D Stone, Elizabeth M Brunt, Ramnik J Xavier, Barry P Sleckman, Ellen Li, Noboru Mizushima, Thaddeus S Stappenbeck, and Herbert W Virgin. A key role for autophagy and the autophagy gene atg16l1 in mouse and human intestinal paneth cells. *Nature*, 456(7219):259–263, Nov 2008.

- [16] Ken Cadwell, Khushbu K Patel, Masaaki Komatsu, Herbert W Virgin, and Thaddeus S Stappenbeck. A common role for atg1611, atg5 and atg7 in small intestinal paneth cells and crohn disease. *Autophagy*, 5(2):250–252, Feb 2009.
- [17] Huynh Cao, Duong LE, and Li-Xi Yang. Current status in chemotherapy for advanced pancreatic adenocarcinoma. *Anticancer Res*, 33(5):1785–1791, May 2013.
- [18] Bindu P. Chandrasekharan, Vasantha L. Kolachala, Guillaume Dalmaso, Didier Merlin, Katya Ravid, Shanthi V. Sitaraman, and Shanthi Srinivasan. Adenosine 2b receptors (a2bar) on enteric neurons regulate murine distal colonic motility. *FASEB J*, 23(8):2727–2734, Aug 2009.
- [19] Jin-Qiang Chen and Jose Russo. Dysregulation of glucose transport, glycolysis, tca cycle and glutaminolysis by oncogenes and tumor suppressors in cancer cells. *Biochim Biophys Acta*, 1826(2):370–384, Dec 2012.
- [20] Mingyi Chen, Michael Van Ness, Yangtong Guo, and Jeffrey Gregg. Molecular pathology of pancreatic neuroendocrine tumors. *J Gastrointest Oncol*, 3(3):182–188, Sep 2012.
- [21] F. Chiaradonna, R. M. Moresco, C. Airoidi, D. Gaglio, R. Palorini, F. Nicotra, C. Messa, and L. Alberghina. From cancer metabolism to new biomarkers and drug targets. *Biotechnol Adv*, 30(1):30–51, Jan 2012.
- [22] Stephen Yiu Chuen Choi, Colin C. Collins, Peter W. Gout, and Yuzhuo Wang. Cancer-generated lactic acid: a regulatory, immunosuppressive metabolite? *J Pathol*, 230(4):350–355, Aug 2013.
- [23] Anna Colell, Jean-Ehrland Ricci, Stephen Tait, Sandra Milasta, Ulrich Maurer, Lisa Bouchier-Hayes, Patrick Fitzgerald, Ana Guio-Carrion, Nigel J Waterhouse, Cindy Wei Li, Bernard Mari, Pascal Barbry, Donald D Newmeyer, Helen M Beere, and Douglas R Green. Gapdh and autophagy preserve survival after apoptotic cytochrome c release in the absence of caspase activation. *Cell*, 129(5):983–997, Jun 2007.
- [24] Francesco Colotta, Paola Allavena, Antonio Sica, Cecilia Garlanda, and Alberto Mantovani. Cancer-related inflammation, the seventh hallmark of cancer: links to genetic instability. *Carcinogenesis*, May 2009.

- [25] D. J. Combs, D. S. Reuland, D. B. Martin, G. B. Zelenock, and L. G. D'Alecy. Glycolytic inhibition by 2-deoxyglucose reduces hyperglycemia-associated mortality and morbidity in the ischemic rat. *Stroke*, 17(5):989–994, 1986.
- [26] Diane Crichton, Simon Wilkinson, Jim O'Prey, Nelofer Syed, Paul Smith, Paul R Harrison, Milena Gasco, Ornella Garrone, Tim Crook, and Kevin M Ryan. Dram, a p53-induced modulator of autophagy, is critical for apoptosis. *Cell*, 126(1):121–134, Jul 2006.
- [27] Kurt Degenhardt, Robin Mathew, Brian Beaudoin, Kevin Bray, Diana Anderson, Guanghua Chen, Chandreyee Mukherjee, Yufang Shi, Céline Gélinas, Yongjun Fan, Deirdre A Nelson, Shengkan Jin, and Eileen White. Autophagy promotes tumor cell survival and restricts necrosis, inflammation, and tumorigenesis. *Cancer Cell*, 10(1):51–64, Jul 2006.
- [28] Biva M. Desai, Jennifer Oliver-Krasinski, Diva D. De Leon, Cyrus Farzad, Nankang Hong, Steven D. Leach, and Doris A. Stoffers. Preexisting pancreatic acinar cells contribute to acinar cell, but not islet beta cell, regeneration. *J Clin Invest*, 117(4):971–977, Apr 2007.
- [29] Marina Pasca di Magliano and Craig D. Logsdon. Roles for kras in pancreatic tumor development and progression. *Gastroenterology*, 144(6):1220–1229, Jun 2013.
- [30] Ivan Dikic, Terje Johansen, and Vladimir Kirkin. Selective autophagy in cancer development and therapy. *Cancer Res*, 70(9):3431–3434, May 2010.
- [31] Matthew Dodson, Victor Darley-USmar, and Jianhua Zhang. Cellular metabolic and autophagic pathways: Traffic control by redox signaling. *Free Radic Biol Med*, 63C:207–221, May 2013.
- [32] Elaine A. Dunlop and Andrew R. Tee. The kinase triad, ampk, mtorc1 and ulk1, maintains energy and nutrient homeostasis. *Biochem Soc Trans*, 41(4):939–943, Aug 2013.
- [33] Chie Ebato, Toyoyoshi Uchida, Masayuki Arakawa, Masaaki Komatsu, Takashi Ueno, Koji Komiya, Kosuke Azuma, Takahisa Hirose, Keiji Tanaka, Eiki Kominami, Ryuzo Kawamori, Yoshio Fujitani, and Hirotaka Watada. Autophagy is important in islet

homeostasis and compensatory increase of beta cell mass in response to high-fat diet. *Cell Metab*, 8(4):325–332, Oct 2008.

[34] Georg Feldmann, Robert Beaty, Ralph H Hruban, and Anirban Maitra. Molecular genetics of pancreatic intraepithelial neoplasia. *J Hepatobiliary Pancreat Surg*, 14(3):224–232, 2007.

[35] Volker Fendrich, Ralph Schneider, Anirban Maitra, Ilse D. Jacobsen, Thomas Opfermann, and Detlef K. Bartsch. Detection of precursor lesions of pancreatic adenocarcinoma in pet-ct in a genetically engineered mouse model of pancreatic cancer. *Neoplasia*, 13(2):180–186, Feb 2011.

[36] Elisabetta Ferraro, Angela Pulicati, Maria Teresa Cencioni, Mauro Cozzolino, Francesca Navoni, Simona di Martino, Roberta Nardacci, Maria Teresa Carrì, and Francesco Cecconi. Apoptosome-deficient cells lose cytochrome c through proteasomal degradation but survive by autophagy-dependent glycolysis. *Mol Biol Cell*, 19(8):3576–3588, Aug 2008.

[37] Gian Maria Fimia, Anastassia Stoykova, Alessandra Romagnoli, Luigi Giunta, Sabrina Di Bartolomeo, Roberta Nardacci, Marco Corazzari, Claudia Fuoco, Ahmet Ucar, Peter Schwartz, Peter Gruss, Mauro Piacentini, Kamal Chowdhury, and Francesco Cecconi. Ambra1 regulates autophagy and development of the nervous system. *Nature*, 447(7148):1121–1125, Jun 2007.

[38] Jens Füllgrabe, Melinda A. Lynch-Day, Nina Heldring, Wenbo Li, Robert B. Struijk, Qi Ma, Ola Hermanson, Michael G. Rosenfeld, Daniel J. Klionsky, and Bertrand Joseph. The histone h4 lysine 16 acetyltransferase hmo13 regulates the outcome of autophagy. *Nature*, Jul 2013.

[39] S. Fogarty and D. G. Hardie. Development of protein kinase activators: Ampk as a target in metabolic disorders and cancer. *Biochim Biophys Acta*, 1804(3):581–591, Mar 2010.

[40] Kei Fujimoto, Piia T Hanson, Hung Tran, Eric L Ford, Zhiqiang Han, James D Johnson, Robert E Schmidt, Karen G Green, Burton M Wice, and Kenneth S Polonsky.

Autophagy regulates pancreatic beta cell death in response to pdx1 deficiency and nutrient deprivation. *J Biol Chem*, Aug 2009.

[41] Naonobu Fujita, Takashi Itoh, Hiroko Omori, Mitsunori Fukuda, Takeshi Noda, and Tamotsu Yoshimori. The atg16l complex specifies the site of lc3 lipidation for membrane biogenesis in autophagy. *Mol Biol Cell*, 19(5):2092–2100, May 2008.

[42] Sarah F Funderburk, Qing Jun Wang, and Zhenyu Yue. The beclin 1-vps34 complex—at the crossroads of autophagy and beyond. *Trends Cell Biol*, 20(6):355–362, Jun 2010.

[43] Christopher Fung, Rebecca Lock, Sizhen Gao, Eduardo Salas, and Jayanta Debnath. Induction of autophagy during extracellular matrix detachment promotes cell survival. *Mol Biol Cell*, 19(3):797–806, Mar 2008.

[44] Ian G Ganley, Du H Lam, Junru Wang, Xiaojun Ding, She Chen, and Xuejun Jiang. Ulk1.atg13.fip200 complex mediates mtor signaling and is essential for autophagy. *J Biol Chem*, 284(18):12297–12305, May 2009.

[45] M. Gannon, P. L. Herrera, and C. V. Wright. Mosaic cre-mediated recombination in pancreas using the pdx-1 enhancer/promoter. *Genesis*, 26(2):143–144, Feb 2000.

[46] M. Gannon, C. Shiota, C. Postic, C. V. Wright, and M. Magnuson. Analysis of the cre-mediated recombination driven by rat insulin promoter in embryonic and adult mouse pancreas. *Genesis*, 26(2):139–142, Feb 2000.

[47] Robert A. Gatenby and Robert J. Gillies. Why do cancers have high aerobic glycolysis? *Nat Rev Cancer*, 4(11):891–899, Nov 2004.

[48] Eyal Gottlieb and Karen H Vousden. p53 regulation of metabolic pathways. *Cold Spring Harb Perspect Biol*, 2(4):a001040, Apr 2010.

[49] Carmen Guerra, Manuel Collado, Carolina Navas, Alberto J Schuhmacher, Isabel Hernández-Porras, Marta Cañamero, Manuel Rodríguez-Justo, Manuel Serrano, and Mariano Barbacid. Pancreatitis-induced inflammation contributes to pancreatic cancer by inhibiting oncogene-induced senescence. *Cancer Cell*, 19(6):728–739, Jun 2011.

- [50] Carmen Guerra, Nieves Mijimolle, Alma Dhawahir, Pierre Dubus, Marta Barradas, Manuel Serrano, Victoria Campuzano, and Mariano Barbacid. Tumor induction by an endogenous k-ras oncogene is highly dependent on cellular context. *Cancer Cell*, 4(2):111–120, Aug 2003.
- [51] Carmen Guerra, Alberto J. Schuhmacher, Marta Cañamero, Paul J. Grippo, Lena Verdaguer, Lucía Pérez-Gallego, Pierre Dubus, Eric P. Sandgren, and Mariano Barbacid. Chronic pancreatitis is essential for induction of pancreatic ductal adenocarcinoma by k-ras oncogenes in adult mice. *Cancer Cell*, 11(3):291–302, Mar 2007.
- [52] Ilya Gukovsky and Anna S Gukovskaya. Impaired autophagy underlies key pathological responses of acute pancreatitis. *Autophagy*, 6(3):428–429, Apr 2010.
- [53] Ilya Gukovsky, Ning Li, Jelena Todoric, Anna Gukovskaya, and Michael Karin. Inflammation, autophagy, and obesity: common features in the pathogenesis of pancreatitis and pancreatic cancer. *Gastroenterology*, 144(6):1199–209.e4, Jun 2013.
- [54] Jessie Yanxiang Guo, Hsin-Yi Chen, Robin Mathew, Jing Fan, Anne M Strohecker, Gizem Karsli-Uzunbas, Jurre J Kamphorst, Guanghua Chen, Johanna M S Lemons, Vassiliki Karantza, Hilary A Coller, Robert S Dipaola, Celine Gelinis, Joshua D Rabinowitz, and Eileen White. Activated ras requires autophagy to maintain oxidative metabolism and tumorigenesis. *Genes Dev*, 25(5):460–470, Mar 2011.
- [55] Jessie Yanxiang Guo, Gizem Karsli-Uzunbas, Robin Mathew, Seena C. Aisner, Jurre J. Kamphorst, Anne M. Strohecker, Guanghua Chen, Sandy Price, Wenyun Lu, Xin Teng, Eric Snyder, Urmila Santanam, Robert S. Dipaola, Tyler Jacks, Joshua D. Rabinowitz, and Eileen White. Autophagy suppresses progression of k-ras-induced lung tumors to oncocytomas and maintains lipid homeostasis. *Genes Dev*, 27(13):1447–1461, Jul 2013.
- [56] Dana M. Gwinn, David B. Shackelford, Daniel F. Egan, Maria M. Mihaylova, Annabelle Mery, Debbie S. Vasquez, Benjamin E. Turk, and Reuben J. Shaw. Ampk phosphorylation of raptor mediates a metabolic checkpoint. *Mol Cell*, 30(2):214–226, Apr 2008.

- [57] Dale W Hailey, Angelika S Rambold, Prasanna Satpute-Krishnan, Kasturi Mitra, Rachid Sougrat, Peter K Kim, and Jennifer Lippincott-Schwartz. Mitochondria supply membranes for autophagosome biogenesis during starvation. *Cell*, 141(4):656–667, May 2010.
- [58] P. Hainaut and M. Hollstein. p53 and human cancer: the first ten thousand mutations. *Adv Cancer Res*, 77:81–137, 2000.
- [59] Takao Hanada, Nobuo N. Noda, Yoshinori Satomi, Yoshinobu Ichimura, Yuko Fujioka, Toshifumi Takao, Fuyuhiko Inagaki, and Yoshinori Ohsumi. The atg12-atg5 conjugate has a novel e3-like activity for protein lipidation in autophagy. *J Biol Chem*, 282(52):37298–37302, Dec 2007.
- [60] D. Hanahan and R. A. Weinberg. The hallmarks of cancer. *Cell*, 100(1):57–70, Jan 2000.
- [61] Douglas Hanahan and Robert A. Weinberg. Hallmarks of cancer: the next generation. *Cell*, 144(5):646–674, Mar 2011.
- [62] Taichi Hara, Kenji Nakamura, Makoto Matsui, Akitsugu Yamamoto, Yohko Nakahara, Rika Suzuki-Migishima, Minesuke Yokoyama, Kenji Mishima, Ichiro Saito, Hideyuki Okano, and Noboru Mizushima. Suppression of basal autophagy in neural cells causes neurodegenerative disease in mice. *Nature*, 441(7095):885–889, Jun 2006.
- [63] Daisuke Hashimoto, Masaki Ohmuraya, Masahiko Hirota, Akitsugu Yamamoto, Koichi Suyama, Satoshi Ida, Yuushi Okumura, Etsuhisa Takahashi, Hiroshi Kido, Kimi Araki, Hideo Baba, Noboru Mizushima, and Ken ichi Yamamura. Involvement of autophagy in trypsinogen activation within the pancreatic acinar cells. *J Cell Biol*, 181(7):1065–1072, Jun 2008.
- [64] Mitsuko Hayashi-Nishino, Naonobu Fujita, Takeshi Noda, Akihito Yamaguchi, Tamotsu Yoshimori, and Akitsugu Yamamoto. A subdomain of the endoplasmic reticulum forms a cradle for autophagosome formation. *Nat Cell Biol*, 11(12):1433–1437, Dec 2009.
- [65] Marta Herreros-Villanueva, Elizabeth Hijona, Angel Cosme, and Luis Bujanda. Mouse models of pancreatic cancer. *World J Gastroenterol*, 18(12):1286–1294, Mar 2012.

- [66] Reginald Hill, Joseph Hargan Calvopina, Christine Kim, Ying Wang, David W. Dawson, Timothy R. Donahue, Sarah Dry, and Hong Wu. Pten loss accelerates krasg12d-induced pancreatic cancer development. *Cancer Res*, 70(18):7114–7124, Sep 2010.
- [67] Sunil R Hingorani, Emanuel F Petricoin, Anirban Maitra, Vinodh Rajapakse, Catrina King, Michael A Jacobetz, Sally Ross, Thomas P Conrads, Timothy D Veenstra, Ben A Hitt, Yoshiya Kawaguchi, Don Johann, Lance A Liotta, Howard C Crawford, Mary E Putt, Tyler Jacks, Christopher V E Wright, Ralph H Hruban, Andrew M Lowy, and David A Tuveson. Preinvasive and invasive ductal pancreatic cancer and its early detection in the mouse. *Cancer Cell*, 4(6):437–450, Dec 2003.
- [68] Sunil R Hingorani, Lifu Wang, Asha S Multani, Chelsea Combs, Therese B Deramaudt, Ralph H Hruban, Anil K Rustgi, Sandy Chang, and David A Tuveson. Trp53r172h and krasg12d cooperate to promote chromosomal instability and widely metastatic pancreatic ductal adenocarcinoma in mice. *Cancer Cell*, 7(5):469–483, May 2005.
- [69] Nao Hosokawa, Taichi Hara, Takeshi Kaizuka, Chieko Kishi, Akito Takamura, Yutaka Miura, Shun ichiro Iemura, Tohru Natsume, Kenji Takehana, Naoyuki Yamada, Jun-Lin Guan, Noriko Oshiro, and Noboru Mizushima. Nutrient-dependent mtorc1 association with the ulk1-atg13-fip200 complex required for autophagy. *Mol Biol Cell*, 20(7):1981–1991, Apr 2009.
- [70] Ralph H Hruban, Anirban Maitra, and Michael Goggins. Update on pancreatic intraepithelial neoplasia. *Int J Clin Exp Pathol*, 1(4):306–316, 2008.
- [71] Ya-Ching Hsieh, Mohammad Athar, and Irshad H Chaudry. When apoptosis meets autophagy: deciding cell fate after trauma and sepsis. *Trends Mol Med*, 15(3):129–138, Mar 2009.
- [72] Chun Huang, Wei-Min Wang, Jian-Ping Gong, and Kang Yang. Oncogenesis and the clinical significance of k-ras in pancreatic adenocarcinoma. *Asian Pac J Cancer Prev*, 14(5):2699–2701, 2013.
- [73] H. Huang, J. Daniluk, Y. Liu, J. Chu, Z. Li, B. Ji, and C. D. Logsdon. Oncogenic k-ras requires activation for enhanced activity. *Oncogene*, Jan 2013.

- [74] Ken Inoki, Joungmok Kim, and Kun-Liang Guan. Ampk and mtor in cellular energy homeostasis and drug targets. *Annu Rev Pharmacol Toxicol*, 52:381–400, 2012.
- [75] Ken Inoki, Hongjiao Ouyang, Tianqing Zhu, Charlotta Lindvall, Yian Wang, Xiaojie Zhang, Qian Yang, Christina Bennett, Yuko Harada, Kryn Stankunas, Cun-Yu Wang, Xi He, Ormond A. MacDougald, Ming You, Bart O. Williams, and Kun-Liang Guan. Tsc2 integrates wnt and energy signals via a coordinated phosphorylation by ampk and gsk3 to regulate cell growth. *Cell*, 126(5):955–968, Sep 2006.
- [76] Eisuke Itakura, Chieko Kishi, Kinji Inoue, and Noboru Mizushima. Beclin 1 forms two distinct phosphatidylinositol 3-kinase complexes with mammalian atg14 and uvrag. *Mol Biol Cell*, 19(12):5360–5372, Dec 2008.
- [77] E. L. Jackson, N. Willis, K. Mercer, R. T. Bronson, D. Crowley, R. Montoya, T. Jacks, and D. A. Tuveson. Analysis of lung tumor initiation and progression using conditional expression of oncogenic k-ras. *Genes Dev*, 15(24):3243–3248, Dec 2001.
- [78] J. Jonkers, R. Meuwissen, H. van der Gulden, H. Peterse, M. van der Valk, and A. Berns. Synergistic tumor suppressor activity of brca2 and p53 in a conditional mouse model for breast cancer. *Nat Genet*, 29(4):418–425, Dec 2001.
- [79] Caroline Jose, Nadège Bellance, and Rodrigue Rossignol. Choosing between glycolysis and oxidative phosphorylation: a tumor’s dilemma? *Biochim Biophys Acta*, 1807(6):552–561, Jun 2011.
- [80] Mette Christine Jørgensen, Jonas Ahnfelt-Rønne, Jacob Hald, Ole D. Madsen, Palle Serup, and Jacob Hecksher-Sørensen. An illustrated review of early pancreas development in the mouse. *Endocr Rev*, 28(6):685–705, Oct 2007.
- [81] Chang Hwa Jung, Chang Bong Jun, Seung-Hyun Ro, Young-Mi Kim, Neil Michael Otto, Jing Cao, Mondira Kundu, and Do-Hyung Kim. Ulk-atg13-fip200 complexes mediate mtor signaling to the autophagy machinery. *Mol Biol Cell*, 20(7):1992–2003, Apr 2009.
- [82] Hye Seung Jung, Kun Wook Chung, Jeong Won Kim, Jin Kim, Masaaki Komatsu, Keiji Tanaka, Yen Hoang Nguyen, Tong Mook Kang, Kun-Ho Yoon, Ji-Won Kim, Yeon Taek Jeong, Myoung Sook Han, Moon-Kyu Lee, Kwang-Won Kim, Jaekyoon Shin,

and Myung-Shik Lee. Loss of autophagy diminishes pancreatic beta cell mass and function with resultant hyperglycemia. *Cell Metab*, 8(4):318–324, Oct 2008.

[83] Y. Kabeya, N. Mizushima, T. Ueno, A. Yamamoto, T. Kirisako, T. Noda, E. Kominami, Y. Ohsumi, and T. Yoshimori. Lc3, a mammalian homologue of yeast apg8p, is localized in autophagosome membranes after processing. *EMBO J*, 19(21):5720–5728, Nov 2000.

[84] Yukiko Kabeya, Noboru Mizushima, Akitsugu Yamamoto, Satsuki Oshitani-Okamoto, Yoshinori Ohsumi, and Tamotsu Yoshimori. Lc3, gabarap and gate16 localize to autophagosomal membrane depending on form-ii formation. *J Cell Sci*, 117(Pt 13):2805–2812, Jun 2004.

[85] Mi Ran Kang, Min Sung Kim, Ji Eun Oh, Yoo Ri Kim, Sang Yong Song, Sung Soo Kim, Chang Hyeok Ahn, Nam Jin Yoo, and Sug Hyung Lee. Frameshift mutations of autophagy-related genes atg2b, atg5, atg9b and atg12 in gastric and colorectal cancers with microsatellite instability. *J Pathol*, 217(5):702–706, Apr 2009.

[86] Vassiliki Karantza-Wadsworth, Shyam Patel, Olga Kravchuk, Guanghua Chen, Robin Mathew, Shengkan Jin, and Eileen White. Autophagy mitigates metabolic stress and genome damage in mammary tumorigenesis. *Genes Dev*, 21(13):1621–1635, Jul 2007.

[87] Antoine E. Karnoub and Robert A. Weinberg. Ras oncogenes: split personalities. *Nat Rev Mol Cell Biol*, 9(7):517–531, Jul 2008.

[88] Keiko Kawauchi, Keigo Araki, Kei Tobiume, and Nobuyuki Tanaka. p53 regulates glucose metabolism through an ikk-nf-kappab pathway and inhibits cell transformation. *Nat Cell Biol*, 10(5):611–618, May 2008.

[89] Toshiki Kazama, Silvana C. Faria, Vithya Varavithya, Sith Phongkitkarun, Hisao Ito, and Homer A. Macapinlac. Fdg pet in the evaluation of treatment for lymphoma: clinical usefulness and pitfalls. *Radiographics*, 25(1):191–207, 2005.

[90] V. Keim, N. Teich, F. Fiedler, W. Hartig, G. Thiele, and J. Mössner. A comparison of lipase and amylase in the diagnosis of acute pancreatitis in patients with abdominal pain. *Pancreas*, 16(1):45–49, Jan 1998.

- [91] Joungmok Kim and Kun-Liang Guan. Ampk connects energy stress to pik3c3/vps34 regulation. *Autophagy*, 9(7), May 2013.
- [92] Joungmok Kim, Young Chul Kim, Chong Fang, Ryan C. Russell, Jeong Hee Kim, Weiliang Fan, Rong Liu, Qing Zhong, and Kun-Liang Guan. Differential regulation of distinct vps34 complexes by ampk in nutrient stress and autophagy. *Cell*, 152(1-2):290–303, Jan 2013.
- [93] Tomonori Kimura, Yoshitsugu Takabatake, Atsushi Takahashi, and Yoshitaka Isaka. Chloroquine in cancer therapy: a double-edged sword of autophagy. *Cancer Res*, 73(1):3–7, Jan 2013.
- [94] Daniel J Klionsky, Hagai Abeliovich, Patrizia Agostinis, Devendra K Agrawal, Gjumrakch Aliev, David S Askew, Misuzu Baba, Eric H Baehrecke, Ben A Bahr, Andrea Ballabio, Bruce A Bamber, Diane C Bassham, Ettore Bergamini, Xiaoning Bi, Martine Biard-Piechaczyk, Janice S Blum, Dale E Bredesen, Jeffrey L Brodsky, John H Brumell, Ulf T Brunk, Wilfried Bursch, Nadine Camougrand, Eduardo Cebollero, Francesco Cecconi, Yingyu Chen, Lih-Shen Chin, Augustine Choi, Charleen T Chu, Jongkyeong Chung, Peter G H Clarke, Robert S B Clark, Steven G Clarke, Corinne Clavé, John L Cleveland, Patrice Codogno, María I Colombo, Ana Coto-Montes, James M Cregg, Ana Maria Cuervo, Jayanta Debnath, Francesca Demarchi, Patrick B Dennis, Phillip A Dennis, Vojo Deretic, Rodney J Devenish, Federica Di Sano, J. Fred Dice, Marian Difulgia, Savithamma Dinesh-Kumar, Clark W Distelhorst, Mojgan Djavaheri-Mergny, Frank C Dorsey, Wulf Dröge, Michel Dron, William A Dunn, Michael Duszenko, N. Tony Eissa, Zvulun Elazar, Audrey Esclatine, Eeva-Liisa Eskelinen, László Fésüs, Kim D Finley, José M Fuentes, Juan Fueyo, Kozo Fujisaki, Brigitte Galliot, Fen-Biao Gao, David A Gewirtz, Spencer B Gibson, Antje Gohla, Alfred L Goldberg, Ramon Gonzalez, Cristina González-Estévez, Sharon Gorski, Roberta A Gottlieb, Dieter Häussinger, You-Wen He, Kim Heidenreich, Joseph A Hill, Maria Høyer-Hansen, Xun Hu, Wei-Pang Huang, Akiko Iwasaki, Marja Jäättelä, William T Jackson, Xuejun Jiang, Shengkan Jin, Terje Johansen, Jae U Jung, Motoni Kadowaki, Chanhee Kang, Ameeta Kelekar, David H Kessel, Jan A K W Kiel, Hong Pyo Kim, Adi Kimchi, Timothy J Kinsella, Kirill Kiselyov, Katsuhiko Kitamoto, Erwin Knecht, Masaaki Komatsu, Eiki Kominami, Seiji Kondo, Attila L Kovács, Guido Kroemer, Chia-Yi Kuan, Rakesh Kumar, Mondira Kundu, Jacques Landry, Marianne Laporte, Weidong Le, Huan-Yao Lei, Michael J Lenardo, Beth Levine, Andrew Lieberman, Kah-Leong Lim, Fu-Cheng Lin, Willisa Liou, Leroy F Liu, Gabriel Lopez-

Berestein, Carlos López-Otín, Bo Lu, Kay F Macleod, Walter Malorni, Wim Martinet, Ken Matsuoka, Josef Mautner, Alfred J Meijer, Alicia Meléndez, Paul Michels, Giovanni Miotto, Wilhelm P Mistiaen, Noboru Mizushima, Baharia Mograbi, Iryna Monastyrska, Michael N Moore, Paula I Moreira, Yuji Moriyasu, Tomasz Motyl, Christian Münz, Leon O Murphy, Naweed I Naqvi, Thomas P Neufeld, Ichizo Nishino, Ralph A Nixon, Takeshi Noda, Bernd Nürnberg, Michinaga Ogawa, Nancy L Oleinick, Laura J Olsen, Bulent Ozpolat, Shoshana Paglin, Glen E Palmer, Issidora Papassideri, Miles Parkes, David H Perlmutter, George Perry, Mauro Piacentini, Ronit Pinkas-Kramarski, Mark Prescott, Tassula Proikas-Cezanne, Nina Raben, Abdelhaq Rami, Fulvio Reggiori, Bärbel Rohrer, David C Rubinsztein, Kevin M Ryan, Junichi Sadoshima, Hiroshi Sakagami, Yasuyoshi Sakai, Marco Sandri, Chihiro Sasakawa, Miklós Sass, Claudio Schneider, Per O Seglen, Oleksandr Seleverstov, Jeffrey Settleman, John J Shacka, Irving M Shapiro, Andrei Sibirny, Elaine C M Silva-Zacarin, Hans-Uwe Simon, Cristiano Simone, Anne Simonsen, Mark A Smith, Katharina Spanel-Borowski, Vickram Srinivas, Meredith Steeves, Harald Stenmark, Per E Stromhaug, Carlos S Subauste, Seiichiro Sugimoto, David Sulzer, Toshihiko Suzuki, Michele S Swanson, Ira Tabas, Fumihiko Takeshita, Nicholas J Talbot, Zsolt Tallóczy, Keiji Tanaka, Kozo Tanaka, Isei Tanida, Graham S Taylor, J. Paul Taylor, Alexei Terman, Gianluca Tettamanti, Craig B Thompson, Michael Thumm, Aviva M Tolkovsky, Sharon A Tooze, Ray Truant, Lesya V Tumanovska, Yasuo Uchiyama, Takashi Ueno, Néstor L Uzcátegui, Ida van der Klei, Eva C Vaquero, Tibor Vellai, Michael W Vogel, Hong-Gang Wang, Paul Webster, John W Wiley, Zhijun Xi, Gutian Xiao, Joachim Yahalom, Jin-Ming Yang, George Yap, Xiao-Ming Yin, Tamotsu Yoshimori, Li Yu, Zhenyu Yue, Michisuke Yuzaki, Olga Zabirnyk, Xiaoxiang Zheng, Xiongwei Zhu, and Russell L Deter. Guidelines for the use and interpretation of assays for monitoring autophagy in higher eukaryotes. *Autophagy*, 4(2):151–175, Feb 2008.

[95] Daniel J Klionsky and Jon D Lane. Alternative macroautophagy. *Autophagy*, 6(2):201, Feb 2010.

[96] Masaaki Komatsu, Satoshi Waguri, Takashi Ueno, Junichi Iwata, Shigeo Murata, Isei Tanida, Junji Ezaki, Noboru Mizushima, Yoshinori Ohsumi, Yasuo Uchiyama, Eiki Kominami, Keiji Tanaka, and Tomoki Chiba. Impairment of starvation-induced and constitutive autophagy in atg7-deficient mice. *J Cell Biol*, 169(3):425–434, May 2005.

[97] O. B. Kotoulas, S. A. Kalamidas, and D. J. Kondomerkos. Glycogen autophagy in glucose homeostasis. *Pathol Res Pract*, 202(9):631–638, 2006.

- [98] G. Kroemer, L. Galluzzi, P. Vandenabeele, J. Abrams, E. S. Alnemri, E. H. Baehrecke, M. V. Blagosklonny, W. S. El-Deiry, P. Golstein, D. R. Green, M. Hengartner, R. A. Knight, S. Kumar, S. A. Lipton, W. Malorni, G. Nuñez, M. E. Peter, J. Tschopp, J. Yuan, M. Piacentini, B. Zhivotovsky, G. Melino, and Nomenclature Committee on Cell Death 2009. Classification of cell death: recommendations of the nomenclature committee on cell death 2009. *Cell Death Differ*, 16(1):3–11, Jan 2009.
- [99] Guido Kroemer and Beth Levine. Autophagic cell death: the story of a misnomer. *Nat Rev Mol Cell Biol*, 9(12):1004–1010, Dec 2008.
- [100] Mariola Kulawiec, Vanniarajan Ayyasamy, and Keshav K. Singh. p53 regulates mtDNA copy number and mitochekpoint pathway. *J Carcinog*, 8:8, 2009.
- [101] Akiko Kuma, Masahiko Hatano, Makoto Matsui, Akitsugu Yamamoto, Haruaki Nakaya, Tamotsu Yoshimori, Yoshinori Ohsumi, Takeshi Tokuhsa, and Noboru Mizushima. The role of autophagy during the early neonatal starvation period. *Nature*, 432(7020):1032–1036, Dec 2004.
- [102] Akiko Kuma, Makoto Matsui, and Noboru Mizushima. Lc3, an autophagosome marker, can be incorporated into protein aggregates independent of autophagy: caution in the interpretation of lc3 localization. *Autophagy*, 3(4):323–328, 2007.
- [103] Manabu Kurokawa and Sally Kornbluth. Caspases and kinases in a death grip. *Cell*, 138(5):838–854, Sep 2009.
- [104] Maria A. Lebedeva, Jana S. Eaton, and Gerald S. Shadel. Loss of p53 causes mitochondrial DNA depletion and altered mitochondrial reactive oxygen species homeostasis. *Biochim Biophys Acta*, 1787(5):328–334, May 2009.
- [105] In Hye Lee, Yoshichika Kawai, Maria M. Fergusson, Ilsa I. Rovira, Alexander J R. Bishop, Noboru Motoyama, Liu Cao, and Toren Finkel. Atg7 modulates p53 activity to regulate cell cycle and survival during metabolic stress. *Science*, 336(6078):225–228, Apr 2012.
- [106] Kyoung Eun Lee and Dafna Bar-Sagi. Oncogenic kras suppresses inflammation-associated senescence of pancreatic ductal cells. *Cancer Cell*, 18(5):448–458, Nov 2010.

- [107] Mi Nam Lee, Sang Hoon Ha, Jaeyoon Kim, Ara Koh, Chang Sup Lee, Jung Hwan Kim, Hyeona Jeon, Do-Hyung Kim, Pann-Ghill Suh, and Sung Ho Ryu. Glycolytic flux signals to mtor through glyceraldehyde-3-phosphate dehydrogenase-mediated regulation of rheb. *Mol Cell Biol*, 29(14):3991–4001, Jul 2009.
- [108] B. Levine and G. Kroemer. Autophagy in aging, disease and death: the true identity of a cell death impostor. *Cell Death Differ*, 16(1):1–2, Jan 2009.
- [109] Beth Levine and John Abrams. p53: The janus of autophagy? *Nat Cell Biol*, 10(6):637–639, Jun 2008.
- [110] Beth Levine and Guido Kroemer. Autophagy in the pathogenesis of disease. *Cell*, 132(1):27–42, Jan 2008.
- [111] Antje S. Löffler, Sebastian Alers, Alexandra M. Dieterle, Hildegard Keppeler, Mirita Franz-Wachtel, Mondira Kundu, David G. Campbell, Sebastian Wesselborg, Dario R. Alessi, and Björn Stork. Ulk1-mediated phosphorylation of ampk constitutes a negative regulatory feedback loop. *Autophagy*, 7(7):696–706, Jul 2011.
- [112] Matthias Löhr, Günter Klöppel, Patrick Maisonneuve, Albert B. Lowenfels, and Jutta Lüttges. Frequency of k-ras mutations in pancreatic intraductal neoplasias associated with pancreatic ductal adenocarcinoma and chronic pancreatitis: a meta-analysis. *Neoplasia*, 7(1):17–23, Jan 2005.
- [113] Yuhuan Li, Li-Xin Wang, Guojun Yang, Fang Hao, Walter J Urba, and Hong-Ming Hu. Efficient cross-presentation depends on autophagy in tumor cells. *Cancer Res*, 68(17):6889–6895, Sep 2008.
- [114] Chengyu Liang, Pinghui Feng, Bonsu Ku, Iris Dotan, Dan Canaani, Byung-Ha Oh, and Jae U Jung. Autophagic and tumour suppressor activity of a novel beclin1-binding protein uvrag. *Nat Cell Biol*, 8(7):688–699, Jul 2006.
- [115] Jiyong Liang, Shan H Shao, Zhi-Xiang Xu, Bryan Hennessy, Zhiyong Ding, Michelle Larrea, Seiji Kondo, Dan J Dumont, Jordan U Gutterman, Cheryl L Walker, Joyce M Slingerland, and Gordon B Mills. The energy sensing lkb1-ampk pathway regulates p27(kip1) phosphorylation mediating the decision to enter autophagy or apoptosis. *Nat Cell Biol*, 9(2):218–224, Feb 2007.

- [116] X. H. Liang, S. Jackson, M. Seaman, K. Brown, B. Kempkes, H. Hibshoosh, and B. Levine. Induction of autophagy and inhibition of tumorigenesis by beclin 1. *Nature*, 402(6762):672–676, Dec 1999.
- [117] Johan Van Limbergen, David C Wilson, and Jack Satsangi. The genetics of crohn’s disease. *Annu Rev Genomics Hum Genet*, May 2009.
- [118] Giuseppe Lippi, Massimo Valentino, and Gianfranco Cervellin. Laboratory diagnosis of acute pancreatitis: in search of the holy grail. *Crit Rev Clin Lab Sci*, 49(1):18–31, 2012.
- [119] Rebecca Lock, Srirupa Roy, Candia M Kenific, Judy S Su, Eduardo Salas, Sabrina M Ronen, and Jayanta Debnath. Autophagy facilitates glycolysis during ras-mediated oncogenic transformation. *Mol Biol Cell*, 22(2):165–178, Jan 2011.
- [120] J. S. Long and K. M. Ryan. New frontiers in promoting tumour cell death: targeting apoptosis, necroptosis and autophagy. *Oncogene*, 31(49):5045–5060, Dec 2012.
- [121] Xinghua Lu, Tong Xu, Jiaming Qian, Xiaoheng Wen, and Dongsheng Wu. Detecting k-ras and p53 gene mutation from stool and pancreatic juice for diagnosis of early pancreatic cancer. *Chin Med J (Engl)*, 115(11):1632–1636, Nov 2002.
- [122] Zhen Lu, Robert Z Luo, Yiling Lu, Xuhui Zhang, Qinghua Yu, Shilpi Khare, Seiji Kondo, Yasuko Kondo, Yinhua Yu, Gordon B Mills, Warren S-L Liao, and Robert C Bast. The tumor suppressor gene arhi regulates autophagy and tumor dormancy in human ovarian cancer cells. *J Clin Invest*, 118(12):3917–3929, Dec 2008.
- [123] Oliver D K Maddocks and Karen H Vousden. Metabolic regulation by p53. *J Mol Med (Berl)*, 89(3):237–245, Mar 2011.
- [124] Li Yen Mah, Jim O’Prey, Alice D. Baudot, Attje Hoekstra, and Kevin M. Ryan. Dram-1 encodes multiple isoforms that regulate autophagy. *Autophagy*, 8(1):18–28, Jan 2012.
- [125] Anirban Maitra, Noriyoshi Fukushima, Kyoichi Takaori, and Ralph H. Hruban. Precursors to invasive pancreatic cancer. *Adv Anat Pathol*, 12(2):81–91, Mar 2005.

- [126] M. C. Maiuri, E. Tasdemir, A. Criollo, E. Morselli, J. M. Vicencio, R. Carnuccio, and G. Kroemer. Control of autophagy by oncogenes and tumor suppressor genes. *Cell Death Differ*, 16(1):87–93, Jan 2009.
- [127] M. Chiara Maiuri, Einat Zalcikvar, Adi Kimchi, and Guido Kroemer. Self-eating and self-killing: crosstalk between autophagy and apoptosis. *Nat Rev Mol Cell Biol*, 8(9):741–752, Sep 2007.
- [128] Maria Chiara Maiuri, Shoaib Ahmad Malik, Eugenia Morselli, Oliver Kepp, Alfredo Criollo, Pierre-Luc Mouchel, Rosa Carnuccio, and Guido Kroemer. Stimulation of autophagy by the p53 target gene sestrin2. *Cell Cycle*, 8(10):1571–1576, May 2009.
- [129] Olga A Mareninova, Kip Hermann, Samuel W French, Mark S O’Konski, Stephen J Pandol, Paul Webster, Ann H Erickson, Nobuhiko Katunuma, Fred S Gorelick, Ilya Gukovsky, and Anna S Gukovskaya. Impaired autophagic flux mediates acinar cell vacuole formation and trypsinogen activation in rodent models of acute pancreatitis. *J Clin Invest*, 119(11):3340–3355, Nov 2009.
- [130] Olga A. Mareninova, Kai-Feng Sung, Peggy Hong, Aurelia Lugea, Stephen J. Pandol, Ilya Gukovsky, and Anna S. Gukovskaya. Cell death in pancreatitis: caspases protect from necrotizing pancreatitis. *J Biol Chem*, 281(6):3370–3381, Feb 2006.
- [131] Guillermo Mariño, Natalia Salvador-Montoliu, Antonio Fueyo, Erwin Knecht, Noboru Mizushima, and Carlos López-Otín. Tissue-specific autophagy alterations and increased tumorigenesis in mice deficient in atg4c/autophagin-3. *J Biol Chem*, 282(25):18573–18583, Jun 2007.
- [132] Wim Martinet, Patrizia Agostinis, Barbara Vanhooeke, Michael Dewaele, and Guido R Y De Meyer. Autophagy in disease: a double-edged sword with therapeutic potential. *Clin Sci (Lond)*, 116(9):697–712, May 2009.
- [133] M. Masini, M. Bugliani, R. Lupi, S. del Guerra, U. Boggi, F. Filipponi, L. Marselli, P. Masiello, and P. Marchetti. Autophagy in human type 2 diabetes pancreatic beta cells. *Diabetologia*, 52(6):1083–1086, Jun 2009.
- [134] Robin Mathew, Sameera Kongara, Brian Beaudoin, Cristina M Karp, Kevin Bray, Kurt Degenhardt, Guanghua Chen, Shengkan Jin, and Eileen White. Autophagy suppresses

tumor progression by limiting chromosomal instability. *Genes Dev*, 21(11):1367–1381, Jun 2007.

[135] S. P. Mathupala, C. Heese, and P. L. Pedersen. Glucose catabolism in cancer cells. the type ii hexokinase promoter contains functionally active response elements for the tumor suppressor p53. *J Biol Chem*, 272(36):22776–22780, Sep 1997.

[136] Satoaki Matoba, Ju-Gyeong Kang, Willmar D Patino, Andrew Wragg, Manfred Boehm, Oksana Gavrilova, Paula J Hurley, Fred Bunz, and Paul M Hwang. p53 regulates mitochondrial respiration. *Science*, 312(5780):1650–1653, Jun 2006.

[137] Kohichi Matsunaga, Eiji Morita, Tatsuya Saitoh, Shizuo Akira, Nicholas T Ktistakis, Tetsuro Izumi, Takeshi Noda, and Tamotsu Yoshimori. Autophagy requires endoplasmic reticulum targeting of the pi3-kinase complex via atg14l. *J Cell Biol*, 190(4):511–521, Aug 2010.

[138] Paola Maycotte, Suraj Aryal, Christopher T. Cummings, Jacqueline Thorburn, Michael J. Morgan, and Andrew Thorburn. Chloroquine sensitizes breast cancer cells to chemotherapy independent of autophagy. *Autophagy*, 8(2):200–212, Feb 2012.

[139] David G McEwan and Ivan Dikic. Not all autophagy membranes are created equal. *Cell*, 141(4):564–566, May 2010.

[140] Anna L Means, Ingrid M Meszoely, Kazufumi Suzuki, Yoshiharu Miyamoto, Anil K Rustgi, Robert J Coffey, Christopher V E Wright, Doris A Stoffers, and Steven D Leach. Pancreatic epithelial plasticity mediated by acinar cell transdifferentiation and generation of nestin-positive intermediates. *Development*, 132(16):3767–3776, Aug 2005.

[141] Maryam Mehrpour, Audrey Esclatine, Isabelle Beau, and Patrice Codogno. Overview of macroautophagy regulation in mammalian cells. *Cell Res*, 20(7):748–762, Jul 2010.

[142] Alfred J. Meijer. Autophagy research: lessons from metabolism. *Autophagy*, 5(1):3–5, Jan 2009.

- [143] Carol Mercer, Alagammai Kaliappan, and Patrick Dennis. A novel, human atg13 binding protein, atg101, interacts with ulk1 and is essential for macroautophagy. *Autophagy*, 5(5), Jul 2009.
- [144] Noboru Mizushima and Tamotsu Yoshimori. How to interpret lc3 immunoblotting. *Autophagy*, 3(6):542–545, 2007.
- [145] Jennifer P Morton, Paul Timpson, Saadia A Karim, Rachel A Ridgway, Dimitris Athineos, Brendan Doyle, Nigel B Jamieson, Karin A Oien, Andrew M Lowy, Valerie G Brunton, Margaret C Frame, T. R Jeffrey Evans, and Owen J Sansom. Mutant p53 drives metastasis and overcomes growth arrest/senescence in pancreatic cancer. *Proc Natl Acad Sci U S A*, 107(1):246–251, Jan 2010.
- [146] Valeri V. Mossine and Thomas P. Mawhinney. 1-amino-1-deoxy-d-fructose ("fructosamine") and its derivatives. *Adv Carbohydr Chem Biochem*, 64:291–402, 2010.
- [147] Usha Nair and Daniel J. Klionsky. Molecular mechanisms and regulation of specific and nonspecific autophagy pathways in yeast. *J Biol Chem*, 280(51):41785–41788, Dec 2005.
- [148] Yuya Nishida, Satoko Arakawa, Kenji Fujitani, Hirofumi Yamaguchi, Takeshi Mizuta, Toku Kanaseki, Masaaki Komatsu, Kinya Otsu, Yoshihide Tsujimoto, and Shigeomi Shimizu. Discovery of atg5/atg7-independent alternative macroautophagy. *Nature*, 461(7264):654–658, Oct 2009.
- [149] Barbara L. Parsons and Fanxue Meng. K-ras mutation in the screening, prognosis and treatment of cancer. *Biomark Med*, 3(6):757–769, Dec 2009.
- [150] Andrew Scott Paulson, Hop S. Tran Cao, Margaret A. Tempero, and Andrew M. Lowy. Therapeutic advances in pancreatic cancer. *Gastroenterology*, 144(6):1316–1326, Jun 2013.
- [151] Stephanos Pavlides, Diana Whitaker-Menezes, Remedios Castello-Cros, Neal Flomenberg, Agnieszka K. Witkiewicz, Philippe G. Frank, Mathew C. Casimiro, Chenguang Wang, Paolo Fortina, Sankar Addya, Richard G. Pestell, Ubaldo E. Martinez-Outschoorn, Federica Sotgia, and Michael P. Lisanti. The reverse warburg effect: aerobic

glycolysis in cancer associated fibroblasts and the tumor stroma. *Cell Cycle*, 8(23):3984–4001, Dec 2009.

[152] Gloria M. Petersen, Mariza de Andrade, Michael Goggins, Ralph H. Hruban, Melissa Bondy, Jeannette F. Korczak, Steven Gallinger, Henry T. Lynch, Sapna Syngal, Kari G. Rabe, Daniela Seminara, and Alison P. Klein. Pancreatic cancer genetic epidemiology consortium. *Cancer Epidemiol Biomarkers Prev*, 15(4):704–710, Apr 2006.

[153] Hannah E.J. Polson, Jane de Lartigue, Daniel J. Rigden, Marco Reedijk, Sylvie Urbé, Michael J. Clague, and Sharon A. Tooze. Mammalian atg18 (wipi2) localizes to omegasome-anchored phagophores and positively regulates lc3 lipidation. *Autophagy*, 6(4):506–522, May 2010.

[154] Heather H Pua, Ivan Dzhagalov, Mariana Chuck, Noboru Mizushima, and You-Wen He. A critical role for the autophagy gene atg5 in t cell survival and proliferation. *J Exp Med*, 204(1):25–31, Jan 2007.

[155] Xueping Qu, Jie Yu, Govind Bhagat, Norihiko Furuya, Hanina Hibshoosh, Andrea Troxel, Jeffrey Rosen, Eeva-Liisa Eskelinen, Noboru Mizushima, Yoshinori Ohsumi, Giorgio Cattoretti, and Beth Levine. Promotion of tumorigenesis by heterozygous disruption of the beclin 1 autophagy gene. *J Clin Invest*, 112(12):1809–1820, Dec 2003.

[156] Brinda Ravikumar, Sovan Sarkar, Janet E Davies, Marie Futter, Moises Garcia-Arencibia, Zeyn W Green-Thompson, Maria Jimenez-Sanchez, Viktor I Korolchuk, Maike Lichtenberg, Shouqing Luo, Dunecan C O Massey, Fiona M Menzies, Kevin Moreau, Usha Narayanan, Maurizio Renna, Farah H Siddiqi, Benjamin R Underwood, Ashley R Winslow, and David C Rubinsztein. Regulation of mammalian autophagy in physiology and pathophysiology. *Physiol Rev*, 90(4):1383–1435, Oct 2010.

[157] Fulvio Reggiori and Daniel J. Klionsky. Autophagosomes: biogenesis from scratch? *Curr Opin Cell Biol*, 17(4):415–422, Aug 2005.

[158] Andrew D. Rhim, Emily T. Mirek, Nicole M. Aiello, Anirban Maitra, Jennifer M. Bailey, Florencia McAllister, Maximilian Reichert, Gregory L. Beatty, Anil K. Rustgi, Robert H. Vonderheide, Steven D. Leach, and Ben Z. Stanger. Emt and dissemination precede pancreatic tumor formation. *Cell*, 148(1-2):349–361, Jan 2012.

- [159] Mathias Rosenfeldt, Colin Nixon, Emma Liu, Li Yen Mah, and Kevin M. Ryan. Analysis of macroautophagy by immunohistochemistry. *Autophagy*, 8(6), Jun 2012.
- [160] Mathias T Rosenfeldt and Kevin M Ryan. The role of autophagy in tumour development and cancer therapy. *Expert Rev Mol Med*, 11:e36, 2009.
- [161] Mathias T. Rosenfeldt and Kevin M. Ryan. The multiple roles of autophagy in cancer. *Carcinogenesis*, 32(7):955–963, Jul 2011.
- [162] Peter M. Rothwell, F Gerald R. Fowkes, Jill F F. Belch, Hisao Ogawa, Charles P. Warlow, and Tom W. Meade. Effect of daily aspirin on long-term risk of death due to cancer: analysis of individual patient data from randomised trials. *Lancet*, 377(9759):31–41, Jan 2011.
- [163] David C Rubinsztein, Jason E Gestwicki, Leon O Murphy, and Daniel J Klionsky. Potential therapeutic applications of autophagy. *Nat Rev Drug Discov*, 6(4):304–312, Apr 2007.
- [164] P. Ruiz-Lozano, M. L. Hixon, M. W. Wagner, A. I. Flores, S. Ikawa, AS Baldwin, Jr, K. R. Chien, and A. Gualberto. p53 is a transcriptional activator of the muscle-specific phosphoglycerate mutase gene and contributes in vivo to the control of its cardiac expression. *Cell Growth Differ*, 10(5):295–306, May 1999.
- [165] Tatsuya Saitoh, Naonobu Fujita, Myoung Ho Jang, Satoshi Uematsu, Bo-Gie Yang, Takashi Satoh, Hiroko Omori, Takeshi Noda, Naoki Yamamoto, Masaaki Komatsu, Keiji Tanaka, Taro Kawai, Tohru Tsujimura, Osamu Takeuchi, Tamotsu Yoshimori, and Shizuo Akira. Loss of the autophagy protein atg16l1 enhances endotoxin-induced il-1beta production. *Nature*, 456(7219):264–268, Nov 2008.
- [166] F. Scarlatti, R. Granata, A. J. Meijer, and P. Codogno. Does autophagy have a license to kill mammalian cells? *Cell Death Differ*, 16(1):12–20, Jan 2009.
- [167] Fabiana Schwartzenberg-Bar-Yoseph, Michal Armoni, and Eddy Karnieli. The tumor suppressor p53 down-regulates glucose transporters glut1 and glut4 gene expression. *Cancer Res*, 64(7):2627–2633, Apr 2004.

- [168] Ruizhe Shen, Qi Wang, Shidan Cheng, Tingting Liu, He Jiang, Jiaying Zhu, and Lifu Wang. The biological features of panin initiated from oncogenic kras mutation in genetically engineered mouse models. *Cancer Lett*, Jul 2013.
- [169] G. Shi, D. DiRenzo, C. Qu, D. Barney, D. Miley, and S. F. Konieczny. Maintenance of acinar cell organization is critical to preventing kras-induced acinar-ductal metaplasia. *Oncogene*, 32(15):1950–1958, Apr 2013.
- [170] Yu shin Sou, Satoshi Waguri, Jun ichi Iwata, Takashi Ueno, Tsutomu Fujimura, Taichi Hara, Naoki Sawada, Akane Yamada, Noboru Mizushima, Yasuo Uchiyama, Eiki Kominami, Keiji Tanaka, and Masaaki Komatsu. The atg8 conjugation system is indispensable for proper development of autophagic isolation membranes in mice. *Mol Biol Cell*, 19(11):4762–4775, Nov 2008.
- [171] Elena Shvets and Zvulun Elazar. Autophagy-independent incorporation of gfp-lc3 into protein aggregates is dependent on its interaction with p62/sqstm1. *Autophagy*, 4(8):1054–1056, Nov 2008.
- [172] Anne Simonsen and Sharon A Tooze. Coordination of membrane events during autophagy by multiple class iii pi3-kinase complexes. *J Cell Biol*, 186(6):773–782, Sep 2009.
- [173] Rajat Singh, Susmita Kaushik, Yongjun Wang, Youqing Xiang, Inna Novak, Masaaki Komatsu, Keiji Tanaka, Ana Maria Cuervo, and Mark J Czaja. Autophagy regulates lipid metabolism. *Nature*, 458(7242):1131–1135, Apr 2009.
- [174] Qiming Sun, Weiliang Fan, Keling Chen, Xiaojun Ding, She Chen, and Qing Zhong. Identification of barkor as a mammalian autophagy-specific factor for beclin 1 and class iii phosphatidylinositol 3-kinase. *Proc Natl Acad Sci U S A*, 105(49):19211–19216, Dec 2008.
- [175] Akito Takamura, Masaaki Komatsu, Taichi Hara, Ayako Sakamoto, Chieko Kishi, Satoshi Waguri, Yoshinobu Eishi, Okio Hino, Keiji Tanaka, and Noboru Mizushima. Autophagy-deficient mice develop multiple liver tumors. *Genes Dev*, 25(8):795–800, Apr 2011.

[176] Ezgi Tasdemir, M. Chiara Maiuri, Lorenzo Galluzzi, Ilio Vitale, Mojgan Djavaheri-Mergny, Marcello D'Amelio, Alfredo Criollo, Eugenia Morselli, Changlian Zhu, Francis Harper, Ulf Nannmark, Chrysanthi Samara, Paolo Pinton, José Miguel Vicencio, Rosa Carnuccio, Ute M Moll, Frank Madeo, Patrizia Paterlini-Brechot, Rosario Rizzuto, Gyorgy Szabadkai, Gérard Pierron, Klas Blomgren, Nektarios Tavernarakis, Patrice Codogno, Francesco Cecconi, and Guido Kroemer. Regulation of autophagy by cytoplasmic p53. *Nat Cell Biol*, 10(6):676–687, Jun 2008.

[177] P. G. Terhune, D. M. Phifer, T. D. Tosteson, and D. S. Longnecker. K-ras mutation in focal proliferative lesions of human pancreas. *Cancer Epidemiol Biomarkers Prev*, 7(6):515–521, Jun 1998.

[178] Sharon A Tooze and Tamotsu Yoshimori. The origin of the autophagosomal membrane. *Nat Cell Biol*, 12(9):831–835, Sep 2010.

[179] Mark W. True. Circulating biomarkers of glycemia in diabetes management and implications for personalized medicine. *J Diabetes Sci Technol*, 3(4):743–747, Jul 2009.

[180] David A. Tuveson, Alice T. Shaw, Nicholas A. Willis, Daniel P. Silver, Erica L. Jackson, Sandy Chang, Kim L. Mercer, Rebecca Grochow, Hanno Hock, Denise Crowley, Sunil R. Hingorani, Tal Zaks, Catrina King, Michael A. Jacobetz, Lifu Wang, Roderick T. Bronson, Stuart H. Orkin, Ronald A. DePinho, and Tyler Jacks. Endogenous oncogenic k-ras(g12d) stimulates proliferation and widespread neoplastic and developmental defects. *Cancer Cell*, 5(4):375–387, Apr 2004.

[181] Audrey Vincent, Joseph Herman, Rich Schulick, Ralph H Hruban, and Michael Goggins. Pancreatic cancer. *Lancet*, 378(9791):607–620, Aug 2011.

[182] Karen H Vousden and Carol Prives. Blinded by the light: The growing complexity of p53. *Cell*, 137(3):413–431, May 2009.

[183] Jaroslaw Walkowiak, Karl-Heinz Herzig, Krystyna Strzykala, Juliusz Przyslawski, and Marian Krawczynski. Fecal elastase-1 is superior to fecal chymotrypsin in the assessment of pancreatic involvement in cystic fibrosis. *Pediatrics*, 110(1 Pt 1):e7, Jul 2002.

- [184] Qilong Wang, Bin Liang, Najeeb A. Shirwany, and Ming-Hui Zou. 2-deoxy-d-glucose treatment of endothelial cells induces autophagy by reactive oxygen species-mediated activation of the amp-activated protein kinase. *PLoS One*, 6(2):e17234, 2011.
- [185] O. WARBURG. On the origin of cancer cells. *Science*, 123(3191):309–314, Feb 1956.
- [186] Jemma L Webber and Sharon A Tooze. New insights into the function of atg9. *FEBS Lett*, 584(7):1319–1326, Apr 2010.
- [187] Weihua Wu and Shimin Zhao. Metabolic changes in cancer: beyond the warburg effect. *Acta Biochim Biophys Sin (Shanghai)*, 45(1):18–26, Jan 2013.
- [188] Rui-Hua Xu, Helene Pelicano, Yan Zhou, Jennifer S. Carew, Li Feng, Kapil N. Bhalla, Michael J. Keating, and Peng Huang. Inhibition of glycolysis in cancer cells: a novel strategy to overcome drug resistance associated with mitochondrial respiratory defect and hypoxia. *Cancer Res*, 65(2):613–621, Jan 2005.
- [189] Shenghong Yang, Xiaoxu Wang, Gianmarco Contino, Marc Liesa, Ergun Sahin, Haoqiang Ying, Alexandra Bause, Yinghua Li, Jayne M Stommel, Giacomo Dell’antonio, Josef Mautner, Giovanni Tonon, Marcia Haigis, Orian S Shirihai, Claudio Doglioni, Nabeel Bardeesy, and Alec C Kimmelman. Pancreatic cancers require autophagy for tumor growth. *Genes Dev*, 25(7):717–729, Apr 2011.
- [190] Haoqiang Ying, Alec C. Kimmelman, Costas A. Lyssiotis, Sujun Hua, Gerald C. Chu, Eliot Fletcher-Sananikone, Jason W. Locasale, Jaekyoung Son, Hailei Zhang, Jonathan L. Coloff, Haiyan Yan, Wei Wang, Shujuan Chen, Andrea Viale, Hongwu Zheng, Ji-Hye Paik, Carol Lim, Alexander R. Guimaraes, Eric S. Martin, Jeffery Chang, Aram F. Hezel, Samuel R. Perry, Jian Hu, Boyi Gan, Yonghong Xiao, John M. Asara, Ralph Weissleder, Y Alan Wang, Lynda Chin, Lewis C. Cantley, and Ronald A. Depinho. Oncogenic kras maintains pancreatic tumors through regulation of anabolic glucose metabolism. *Cell*, 149(3):656–670, Apr 2012.
- [191] Päivi Ylä-Anttila, Helena Vihinen, Eija Jokitalo, and Eeva-Liisa Eskelinen. 3d tomography reveals connections between the phagophore and endoplasmic reticulum. *Autophagy*, 5(8):1180–1185, Nov 2009.

- [192] Andrew R J Young, Masako Narita, Manuela Ferreira, Kristina Kirschner, Mahito Sadaie, Jeremy F J Darot, Simon Tavaré, Satoko Arakawa, Shigeomi Shimizu, Fiona M Watt, and Masashi Narita. Autophagy mediates the mitotic senescence transition. *Genes Dev*, 23(7):798–803, Apr 2009.
- [193] Li Yu, Christina K McPhee, Lixin Zheng, Gonzalo A Mardones, Yueguang Rong, Junya Peng, Na Mi, Ying Zhao, Zhihua Liu, Fengyi Wan, Dale W Hailey, Viola Oorschot, Judith Klumperman, Eric H Baehrecke, and Michael J Lenardo. Termination of autophagy and reformation of lysosomes regulated by mtor. *Nature*, 465(7300):942–946, Jun 2010.
- [194] Li Yu, Lindsey Strandberg, and Michael J Lenardo. The selectivity of autophagy and its role in cell death and survival. *Autophagy*, 4(5):567–573, Jul 2008.
- [195] Zhenyu Yue, Shengkan Jin, Chingwen Yang, Arnold J Levine, and Nathaniel Heintz. Beclin 1, an autophagy gene essential for early embryonic development, is a haploinsufficient tumor suppressor. *Proc Natl Acad Sci U S A*, 100(25):15077–15082, Dec 2003.
- [196] Xuehuo Zeng and Timothy J Kinsella. Mammalian target of rapamycin and s6 kinase 1 positively regulate 6-thioguanine-induced autophagy. *Cancer Res*, 68(7):2384–2390, Apr 2008.
- [197] Martin Zenker, Julia Mayerle, Markus M. Lerch, Andreas Tagariello, Klaus Zerres, Peter R. Durie, Matthias Beier, Georg Hülkamp, Celina Guzman, Helga Rehder, Frits A. Beemer, Ben Hamel, Philippe Vanlieferinghen, Ruth Gershoni-Baruch, Marta W. Vieira, Miroslav Dumic, Ron Auslender, Vera L. Gil-da Silva-Lopes, Simone Steinlicht, Manfred Rauh, Stavit A. Shalev, Christian Thiel, Arif B. Ekici, Andreas Winterpacht, Yong Tae Kwon, Alexander Varshavsky, and André Reis. Deficiency of *ubr1*, a ubiquitin ligase of the n-end rule pathway, causes pancreatic dysfunction, malformations and mental retardation (johanson-blizzard syndrome). *Nat Genet*, 37(12):1345–1350, Dec 2005.
- [198] Jianliang Zhang, Rony Francois, Renuka Iyer, Mukund Seshadri, Maria Zajack-Kaye, and Steven N. Hochwald. Current understanding of the molecular biology of pancreatic neuroendocrine tumors. *J Natl Cancer Inst*, 105(14):1005–1017, Jul 2013.

- [199] Xing Zhang, Jie Tian, Jinchao Feng, Shouping Zhu, and Guorui Yan. An anatomical mouse model for multimodal molecular imaging. *Conf Proc IEEE Eng Med Biol Soc*, 2009:5817–5820, 2009.
- [200] Yun Zhong, Qing Jun Wang, Xianting Li, Ying Yan, Jonathan M Backer, Brian T Chait, Nathaniel Heintz, and Zhenyu Yue. Distinct regulation of autophagic activity by atg14l and rubicon associated with beclin 1-phosphatidylinositol-3-kinase complex. *Nat Cell Biol*, 11(4):468–476, Apr 2009.
- [201] Oren Ziv, Benjamin Glaser, and Yuval Dor. The plastic pancreas. *Dev Cell*, 26(1):3–7, Jul 2013.